Comparative Electron Impact and Fast Atom Bombardment Mass Spectrometric Studies of Some HMPA Adducts of Phenyltin and Phenyllead Halides and Studies of Strong Hydrogen Bonding by FAB-MS

by

Humayun Mondal, B.Sc. (Hons.), M.Sc. (Alig.)

A Thesis

submitted to the Department of Chemistry

in partial fulfilment of the requirements

for the degree of

Master of Science

October 1984

Brock University

St. Catharines, Ontario

To my parents

for their affection, endurance and inspiration

Abstract

The fragmentation patterns and mass spectra of some phenyltin and -lead halide adducts with hexamethylphosphoramide are compared by subjecting them to electron impact and fast atom bombardment ionization in a mass spectrometer. This comparison is restricted to the metal-containing ions. Ligand-exchange mechanisms of some of the metal-containing species are explored by FAB-MS. Several moisture-sensitive organo-metallics and H-bonded systems have been examined by FAB for attempted characterization, but without any success. Scavenging and trapping of water molecules by complex aggregates in solutions of quaternary ammonium fluorides and hydroxides are investigated by FAB to complement previous NMR-studies.

Acknowledgements

The author would like to express his immense gratitude and admiration to Professor J. M. Miller for his suggestion to undertake this project, his patience, help and constant guidance throughout the course of this work.

It is a pleasure to thank Dr. J. H. Clark for his boundless encouragement to carry out research on H-bonded systems and the provision of some of the samples used.

Special thanks should go to Mr. T. R. B. Jones for many helpful discussions and his unforgettable effort to acquaint the author with the mass spectrometer.

He would also like to thank Professor I. Wharf for the provision of the organometallics used in this study, to Dr. J. K. Puri for various helpful suggestions and to the Faculty and Staff of the Department of Chemistry for their assistance.

Thanks are still due to his friends Saeed, Shaheer, Cindy, Naresh, Roger, Jeff and Adrian for their help and support in different phases of this work and to Donna, Afzal and Jahangir for verbal encouragement.

Finally great appreciation is expressed to Janet Hastie for her patience and care in typing out this thesis.

Financial assistance from Brock University and Imperial Oil Company are gratefully acknowledged.

TABLE OF CONTENTS

LIST OF TABLES

LIST OF FIGURES

INTRODUCTION

(1) Fundamentals of Mass Spectrometry

For the last two decades mass spectrometry has been one of the most important analytical tools used to reveal the molecular weight and structure of compounds. The process by which the mass spectrum, i.e. , mass-to-charge ratio versus abundance of ions, is obtained, involves the following steps:

(i) Introduction of the sample into the ion source by an appropriate inlet system.

(ii) Vaporization of the sample into a high vacuum (ca. 10^{-6} Torr).

(iii) Ionization of the vaporized sample followed by the formation of a radical or quasi molecular ion and successive fragmentations to yield structurally significant ions.

(iv) Extraction of ions in the form of well-defined ion beam.

(v) Separation of the ions by the mass analyzer.

(vi) Recording of the ion-current of different ions corresponding to their mass/charge ratios.

Examination of the spectrum with the application of different empirical rules or library search procedures (not always) helps us elucidate the structure of the sample under investigation and determine the presence of contaminants (if any).

(2) Different Ionization Techniques

Electron Impact : This is the most common technique to produce ions and it involves the interaction of the molecule (in gas phase) with a beam of electrons having an energy of ca. 70 eV. As a matter of fact, this energy is more than what a molecule needs for ionization. Some of this extra energy may be stored in the molecular ions, making them very unstable and they soon get rid of this energy by a process of bond cleavage which results in various fragmentation products, depending on the energy content of the molecular ion. Generally, the degree of fragmentation is large, which tells us about the structure of the molecule. One serious drawback associated with this technique is that sometimes the molecular ions undergo extremely facile fragmentation and it becomes impossible to detect them.

Chemical Ionization : This is one of the "soft" ionization techniques. In this case, the sample is ionized by an ion-molecule reaction and a "pseudomolecular" ion is formed by the gain or loss of a proton. The internal energy content of the pseudomolecular ion is much less than that formed in EI ionization [1]. Hence, the degree of fragmentation is low and there is a greater probability of detecting the molecular ion.

Field Ionization : In this case the molecules are ionized by a high electric field produced generally from a metal blade edge or fine wire [2]. The quantity of surplus energy stored in the molecular ion is small which gives rise to its higher abundance. However, owing to the low degree of fragmentation, less structural information is obtained in this technique, and thermally unstable compounds must still be volatilized.

All these three methods of ionization need the sample to be presented in the gas phase. This is done generally by heating the sample which hinders the detection of non-volatile, relatively polar compounds of high molecular weight. The only other alternative adopted was to chemically derivatize the substance to increase its volatility and thermal stability, but that too was not very promising. Therefore, extensive research has been pursued for the last 15 years to develop "solid state" ion sources that do not necessarily need sample volatility and thermal stability for mass spectrometric analysis. Some of the important ones are discussed briefly below.

Field Desorption : This is essentially a modification of field ionization technique [3]. The sample is deposited in a thin film on microdendrites, usually carbon, grown on fine metal wire and the loaded emitter is then subjected to a very high electric field and the wire heated, if necessary, to desorb ions from the sample. This technique is useful for yielding molecular weight information, but the ion currents are transient and not intense.

Plasma Desorption : Samples are deposited on a thin metal foil and energized by the passage of high-energy fission fragments from ^{252}Cf nuclei or ions from a particle accelerator. Both positive and negative ions are produced in this case. Mass analysis in the apparatus used to date [4] is done by time-of-flight measurements. It is potentially capable of producing molecular ions of large biomolecules, but the mass limit has not yet been reached [5]. Also, no commercial system is available.

Secondary Ion Mass Spectrometry (SIMS): In this case, the ionization of solids is induced by bombardment of the solid surface by Ar^+ or Xe^+ having 2-5 keV energy. It is capable of producing both positive and negative ions for small molecules, but there are a few main drawbacks associated with this method as below:

(1) The bombardment of the sample surface with fast and highly energetic ions imparts an electric charge to sample surfaces [6] (if the sample is non-conducting), which hinders the incoming ion beam and tends to block the emission of secondary ions.

(2) Large kinetic energy distribution [7] that occurs when the sputtered ions leave the sample surface, decreases the resolution.

(3) Spectra obtained are very transient, except for refractory materials.

(4) The mass range is limited [8-10], if quadrupole mass analysis is used.

Fast Atom Bombardment (FAB) : Michael Barber and his co-workers [11,12] made a spectacular development in the field of mass spectrometry in the beginning of the 80's by designing a source free from almost all the problems encountered in SIMS. They bombarded the sample surface with fast atoms (Ar or Xe) instead of fast ions and hence the name "Fast Atom Bombardment" was given to this unique source. The major drawback associated with this source at first was caused by the extremely short life-time of the sample. However, this was surmounted very soon by dissolving the sample in a non-volatile liquid such as glycerol which keeps renewing the surface for a long time. This liquid is termed the "matrix" in FAB-MS. Since its birth, works in this area in four years have been very rapid and progressive.

(3) Application of FAB-MS to Organometallics and Co-ordination Compounds :

The compound which initiated the study of organometallics in FAB-MS and has been described as a "milestone" [13] in the history of mass spectrometry, is vitamin B_{12}. However, Barber et al. succeeded in crossing this barrier and obtained mass spectra not only of cyanocobalamine, but from the corresponding methyl and hydroxy derivatives [14]. Figure 1 represents the basic structure of cobalamine. The molecular weight of cyano, methyl, hydroxy derivatives

Figure 1

Basic molecular structure of Cobalamine

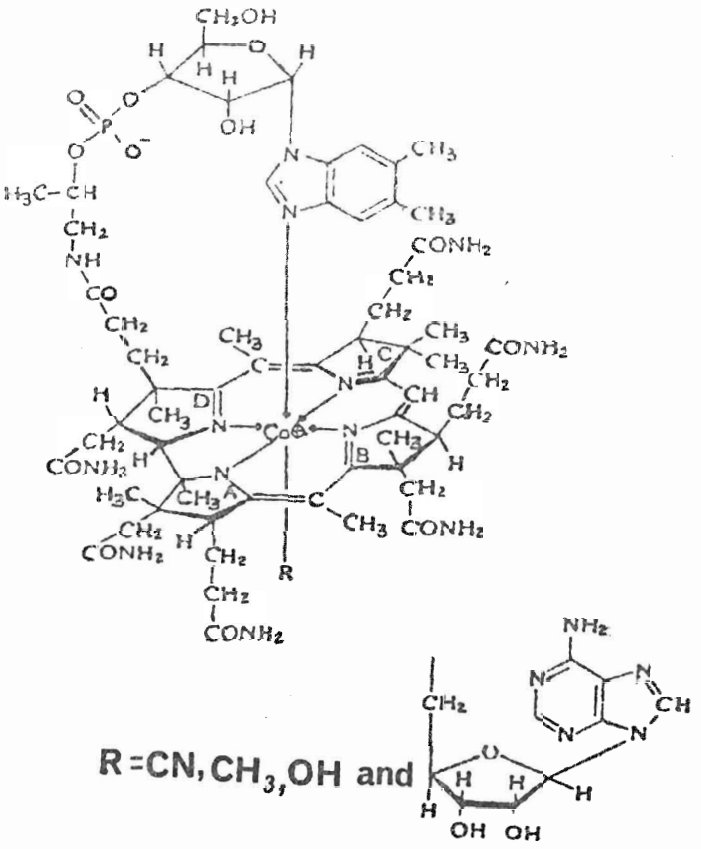
R=CN, CH3, OH and

of cobalamine and of coenzyme B_{12} are 1354, 1343, 1345 and 1578, respectively. In each case an intense pseudomolecular ion ($M + H^+$) is obtained and the relative intensities of the parent ions *versus* the fragments obtained by the loss of various axial ligands are CN > CH_3 > adenosine > OH. The other important fragmentations include the loss of the second axial ligand, dimethyl benzimidazole, phosphate linkage, water *etc.* Negative ion spectra were also obtained for these compounds with $(M-H)^-$ ions but with fewer fragmentation products and the peaks were two mass units lower than in the positive ion spectra [15]. Barber *et al.* had also been able to obtain the positive ion FAB mass spectrum of a relatively non-polar, thermally labile, water sensitive, oily liquid compound of rhodium (the structure being given below) without using any matrix liquid [14,16].

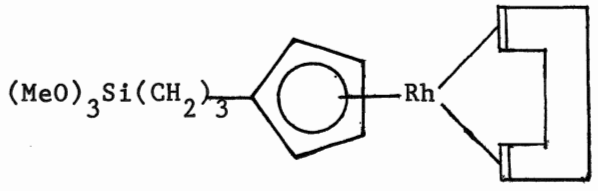

A very intense parent ion was observed at m/z 438 without any quasi-molecular ion. This may be due to the absence of any source of protonation. Loss of neutral C_8H_4, $(MeO)_3SiH$ and $(MeO)_3SiCH{=}CH$ resulted in the formation of other important ions in the high mass region. Si-containing ions such as $SiH(MeO)_2^+$ and $Si(MeO)_3^+$ appeared as strong ions at m/z 91 and 121, respectively. Bare Rh^+ at m/z 103 and $RhC_5H_5^+$ at m/z 168 were also observed, whereas Rh-cyclooctadiene proved to be very unstable. In the same year, the ionic complex of gold

$(Ph_3P)_4Au^+ClO_4^-$, was studied by Barber's group in FAB-MS. The FAB-MS of positive ions constituted the cation parent ion and the subsequent losses of ligands and that of negative ions was dominated by perchlorate anion.

They also used FAB to investigate the structure of the antibiotics, bleomycin A_2, B_2 and their metal complexes [17]. Two important peaks were obtained by the FAB-MS of bleomycin A_2. First was that of the salt $(A_2\text{-}H^+ + FeSO_4)$, observed as a "pseudomolecular" ion at m/z 1566, due to the loss of amide hydrogen of the histidine residue on complexation and the second prominent ion was observed at m/z 472 corresponding to Fe^{2+} ion complexed to the surrounding ligands but lacking the disaccharide groups and the peptide chain.

Schwarz and co-workers [18] were able to obtain good results in both positive and negative FAB for corrins, molecular weight information being more evident in negative ion mode. The basic structure of the corrin is given in Figure 2. The stable ion formed by the loss of two CN ligands reflected the valence change of Co from (III) to (I). Dell et al. compared the FAB and FD spectra for hydroxamate containing siderophores [19]. Siderophores are low molecular weight chelating agents secreted by a wide range of micro-organisms and having a very high affinity for Fe(III). Molecular weight information which is a very valuable step in the structure determination of the siderophores, is

Figure 2

Basic molecular structure of Corrin

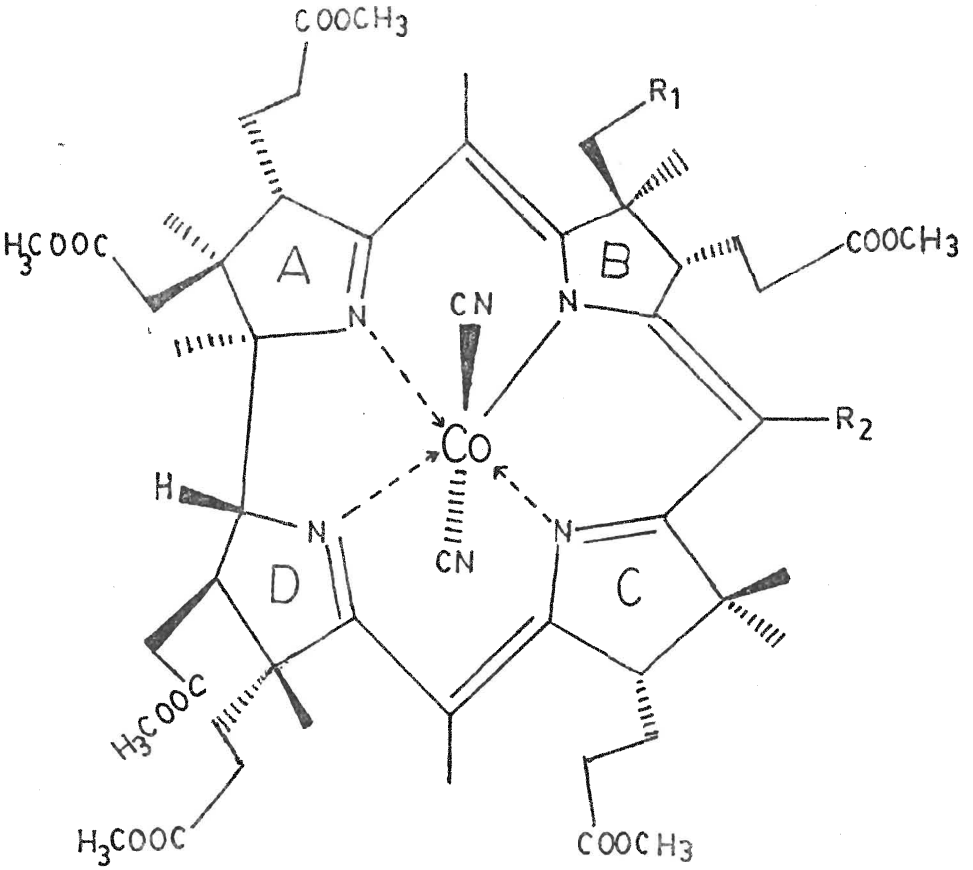

R_1	R_2
$COOCH_3$	H
$COOCH_3$	Br
$COOCH_3$	NO_2
COOH	H
CH_2Cl	H
CH_2I	H
$CH_2OSO_2CH_3$	H
CH_3	H

obtained in both FAB and FD, but the former gave very stable and reliable spectra and used as an initial experiment for the potentially novel siderophores.

FAB was used by Puzo and co-workers [20] to study cisplatin, cis-$Pt(NH_3)_2Cl_2$, applied as an anticancer drug. Structural investigation was carried out mainly on the 1:2 complex of cisplatin and guanosine, the structure being given in Figure 3. In the high mass region of positive ion FAB, important clusters were detected due to the loss of Cl^- from the molecular ion and the loss of HCl from the resultant ion whereas in the negative ion FAB, loss of two water molecules from the molecular ion gave a prominent cluster.

Minard and Geoffroy [21] used FAB to study relatively non-volatile compounds of rhodium and cobalt as $(Ph_3P)_3RhCl$ (Wilkinson's catalyst), $C_8H_{12}Rh(PPh_2)(Cl)RhC_8H_{12}$ and $(Ph_2P)_3Co_3(CO)_6$ in a 9:1 mixture of 18-crown-6 and tetraglyme. Good stable spectra having structurally significant fragmentations by the stepwise loss of carabonyls, chloro, phenyl *etc.* along with weak molecular ions were obtained. Schiebel and Schulten [22] compared the FD and FAB spectra of various cobalamin derivatives and commented that FD is more suitable for mixture analysis.

FAB (both positive and negative ion mode) and FD of arsenobetaine ($(CH_3)_3As^+CH_2COO^-$) isolated from plaice were compared by van der Greef *et al.* [23] and they found FAB to be much more informative about the structure and the exact mass measurement of $[M+H]^+$ ion was also possible by a multichannel analyzer.

Figure 3

Structural representation of the 1:2 complex of cisplatin and guanosine

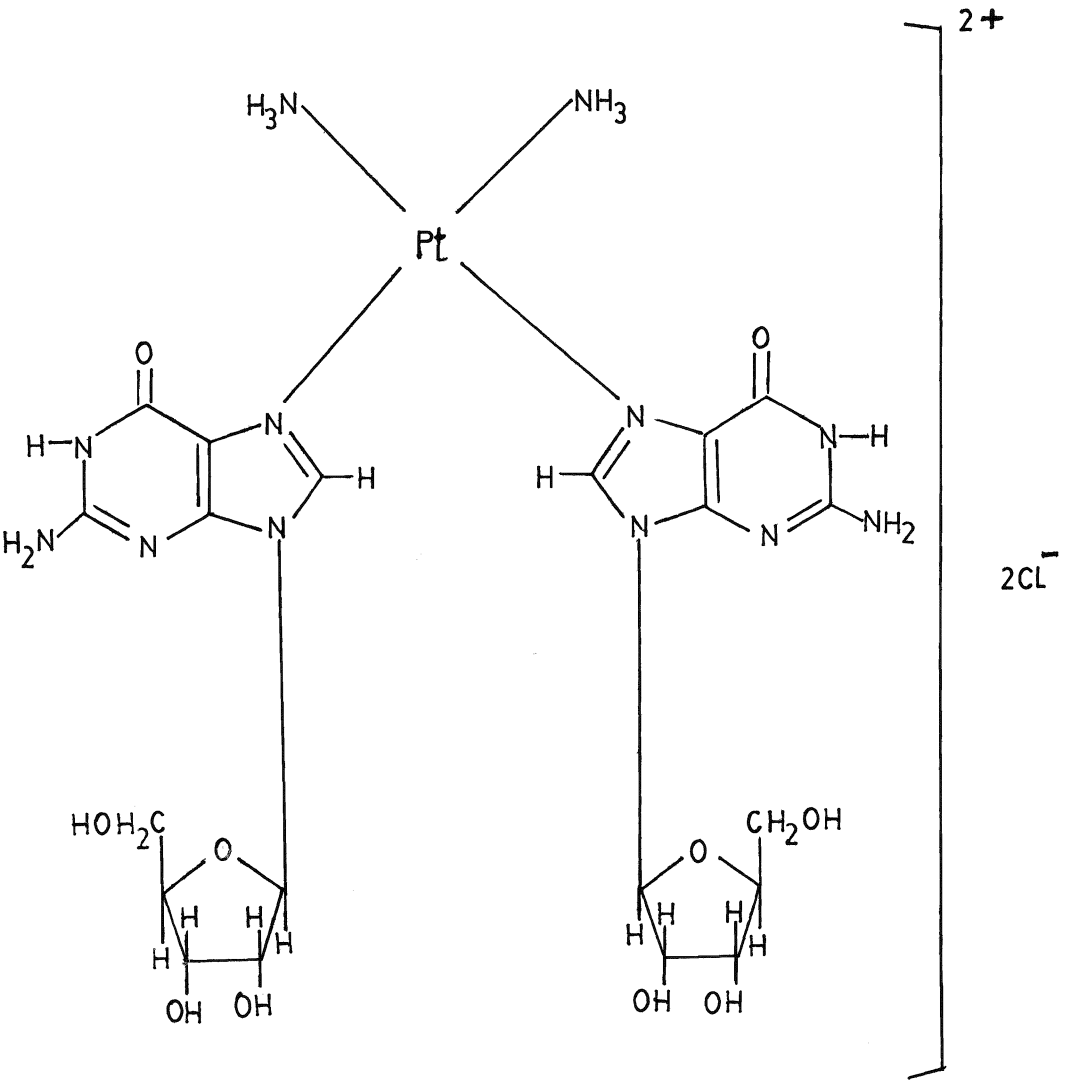
2+
H3N
NH3
Pt
O
H–N
N
H
H2N
N
N
O
N
H
N
N–H
N
NH2
2CL⁻
HOH2C
O
H
H
H
H
OH
OH
CH2OH
O
H
H
H
H
OH
OH

Thatchenko and co-workers [24] for the first time compared FAB and FD spectra of a number of cationic η^3-allylic complexes of nickel and palladium. They found FD to be relatively easy for the characterization of the molecular weight of the cation of these complexes. The difficulty in obtaining FAB spectra of these compounds may be attributed to the use of DMF and glycerol as matrix liquids that do not yield very good spectra for this type of co-ordination compound. Johnstone and co-workers [25,26] used FAB to study a series of crown ether complexes of metallic cations, the molecular ion in each case being of the type $[\text{crown} + M^{n+} + A^{(n-1)-}]^+$, where A is the anion. The metallic salts studied included the chlorides, acetates and nitrates of Li, Na, K, Rb, Cs, Mg, Ca, Ba, Cu, Hg, La, Ce, Th and Co. The order of complexation for this particular crown was K > Cs > Na.

They also studied the mechanism of energy transfer for these complexes and found that the observed mass spectral peak heights were proportional to the concentration of these species in solution that helped them in determining quantitatively the stability constants of crown ether-metal salts.

Davis and co-workers [27] applied FAB to a series of mono- and poly-nuclear transition metal complexes of rhodium, ruthenium, rhenium, palladium, platinum and some metal clusters of iron and osmium by using different matrices such as glycerol, diamylphenol (DAP) and Carbowax 200. The complexes investigated are listed below:

(I) $RhCl(PPh_3)_3$

(II) $RhBr(PPh_3)_3$

(III) $RuCl_2(PPh_3)_3$

(IV) $ReCl(CO)_3[P(C_6H_4F\text{-}p)_3]_2$

(V) $Re(ONO_2)(CO)_3[P(C_6H_4Me\text{-}p)_3]_2$

(VI) $Pd(PPh_3)_4$

(VII) $Pt(PPh_3)_4$

(VIII) $Fe_4(H)C(CO)_{12}AuPPh_3$

(IX) $Os_4H_3(CO)_{12}(CH_3CN)_2(PF_6)$

Molecular ions are observed for both compounds I and II.

Compound III gives $(M+H\text{-}PPh_3)$ as the highest mass ion which is quite consistent with the solution behaviour of the molecule [28]. This may be because solubility plays a major role in the fragmentation process in FAB.

$[M+H\text{-}Cl]^+$ and $[M+H\text{-}NO_3]^+$ are observed as the ions of highest mass and intensity for compounds IV and V, respectively and this extremely easy cleavage of the Re-X (X = Cl, NO_3) bond most probably results in the disappearence of the molecular ion. The spectra of VI and VII are dominated by the ions formed by the successive loss of PPh_3 from the molecular ions. No negative ion spectrum is obtained for compounds I-VII. Quasi molecular ions $[M+H]^+$ and $[M+H]^-$ (although unexpected) are observed in positive and negative ion FAB for the cluster compound VIII.

The positive ion spectrum of the salt IX gives $[Os_4H_3(CO)_{12}(CH_3CN)_2]^+$ as the highest mass ion. On the contrary, the highest mass ion is obtained by the loss of $2CH_3CN$ from the salt in the negative ion mode, followed by ions obtained due to the loss of CO and H ligands. Cerny *et al.* [29] compared FAB and FD of neutral 1+ and 2+ cationic transition metal complexes of Re(III), Re(I), Ag(I), Rh(I), Os(II), Os(III), Os(VI) and Mo(VI). They suggested that FAB is a better method for detecting 1+ complexes that yield both a molecular ion and structurally significant fragments. For neutral species, FD was considered in preference to FAB as the latter does not give molecular weight information in most compounds with thermally labile ligands. However, for dicationic complexes, neither of them proved fruitful. They found that loss of monodentate ligands is preferable to that of bidentates. Redox processes (*i.e.* , the reduction of higher oxidation state metal centre to a lower one) were found responsible for a number of fragment peaks. They remarked that the FAB fragmentation pattern can well be used in illustrating the solution chemistry of complex ions. They also studied the copper (both Cu(I) and Cu(II)) complexes of biological interest [30] by FAB. Interestingly, a number of rearrangement fragment ions were observed in the FAB spectra of these complexes, probably originating from protonated species in the glycerol matrix.

Costello and co-workers [31] used FAB to study water soluble Tc(III) complexes separated from radiopharmaceutical preparations. In

another study, the same group [32] did a FD and FAB study of a series of Tc(III) and Tc(V) complexes that are known as important clinical diagnostic agents by using DMSO/glycerol (1:1) and water/glycerol (1:1) as matrix liquids.

Cohen et al. [33] also studied a series of Tc(III) cation complexes by FAB in positive ion mode and obtained sufficient structural information in a monothioglycerol matrix.

Hansen and co-workers [34] described the superiority of FD over FAB by taking FD-MS of a Tc(V) complex.

Meili and Seibl [35] obtained spectacular results of cobalamines in FAB when the matrix liquid glycerol was replaced by ethyl and butyl esters of citric acid (TEC, TBC), benzoic acid benzyl ester (BzBz) and 2-nitrophenyloctyl ether (NPOE). In benzoic acid benzyl ester, the relative intensities of the ions are of the order of $[M\text{-}CN\text{-}CN]^+ > [M\text{-}CN]^+ > [M]^{+\cdot}$. $[M\text{-}CN]^+$ appears as the most intense ion followed by either M^+ or $[M\text{-}CN\text{-}CN]^+$ when NPOE is being used as a matrix. They also found out that by using a slightly oxidizing matrix, the metal valence change from Co(III) to Co(II) can be largely prevented, and in some cases the intensity of the ions is directly proportional to the time the sample was subjected to atom bombardment.

Group IV organometallic halides have been found by Miller's group [36] to be strong Lewis acids that complex with the glycerol or sulfolane matrix. They also investigated ligand exchange reactions in solution to complement the NMR study of the aforementioned phenomenon. Another

compound whose quasimolecular ion was first observed by Miller [36] before confirmation by elemental analysis and x-ray crystallography, was a purported pyridoxamine-palladium chloride complex, $[(\text{pyridoxamine-H}_2)^{++}(PdCl_4)^{--}(H_2O)]$, the most interesting aspect being the presence of water of hydration that was not found earlier in EI mass spectra.

Miller et al. also compared EI and FAB spectra of some phenyl derivatives of main group elements as $((C_6H_5)_3SnEC_6F_5$, E = O, S [37] in a glycerol matrix. The intensity of the molecular ion in FAB was found to be lower than that in EI which was attributed to the inherent characteristics of group IV organometallics. The complexation with glycerol was also barely noticed for these compounds. Triphenyl-metal halides of germanium, tin and lead were studied by FAB in glycerol and sulfolane matrices and the co-ordination of sulfolane sometimes with organometallic halides were also evidenced.

Hartman and Farquharson [38] applied FAB-MS to study some main group Lewis acid co-ordination compounds. The co-ordination compound, bis(quinuclidine)boron difluoride cation gave $D_2BF_2^+$ as the base peak in glycerol, the next important peak being obtained by the loss of quinuclidine from it.

Sharp et al. [39] studied a series of rhodium, iridium and platinum organometallic complexes, comprising of either σ - or π -bonding cumulene ligands by FAB-MS using 18-crown-6/tetraglyme (9:1) as a matrix liquid, suggested earlier by Minerd and Geoffroy [21].

Rhodium and platinum series gave metal-bis(triphenylphosphine) as the most intense ion whereas iridium series gave $Ir(PPh_3)_2CO^+$ as the most intense ion. Metal-ligand bonds were easier to break than cumulene ligands that were always lost as intact units. Molecular weight information was quite evident in the platinum complexes (molecular ion peak gave up to 35% relative intensity), whereas rhodium complexes gave very little information about it. They also included the comparison of FAB mass spectra of $R(PPh_3)_3Cl$ (Wilkinson's catalyst), $Ir(PPh_3)_2COCl$ (Vaska's compound), $Rh(PPh_3)COCl$ and $Pt(C_6H_5)_3)_2(C_2H_4)$. They found FAB to be sufficient to provide structural information of all those non-volatile organometallics intractible to conventional mass spectrometry. The data were also consistent with the solution properties of this class of compound. A look at the isotopic clusters, especially for those complexes containing tin (with 10 istopes), germanium (6 isotopes) and platinum (5 isotopes), readily gives an insight into the structure and rules out the necessity of doing any exact mass measurement for such type of compounds. Sharp also commented that Minard and Geoffroy's [21] liquid system would serve as an ideal matrix for organometallics. Jablonski et al. [40] used FAB to study an isostrucural series of organo-metallic cations of the form cis-, trans-$[(diars)Fe(CO)_2(C(O)Me)L]^+BF_4^-$ (L = $P(OMe)_3$, $PhP(OMe)_3$, Ph_2POMe, PMe_3, $PhPMe_2$, Ph_2Me etc.). The structure is in Figure 4. Characterization of these complexes with conventional mass spectrometric techniques was complicated by the problems of low volatility and thermal

Figure 4

Molecular structure of organo-metallic cations of the form cis-, trans-$[(diars)Fe(CO)_2(C(O)Me)L]^+ BF_4^-$; L = phosphorus donor

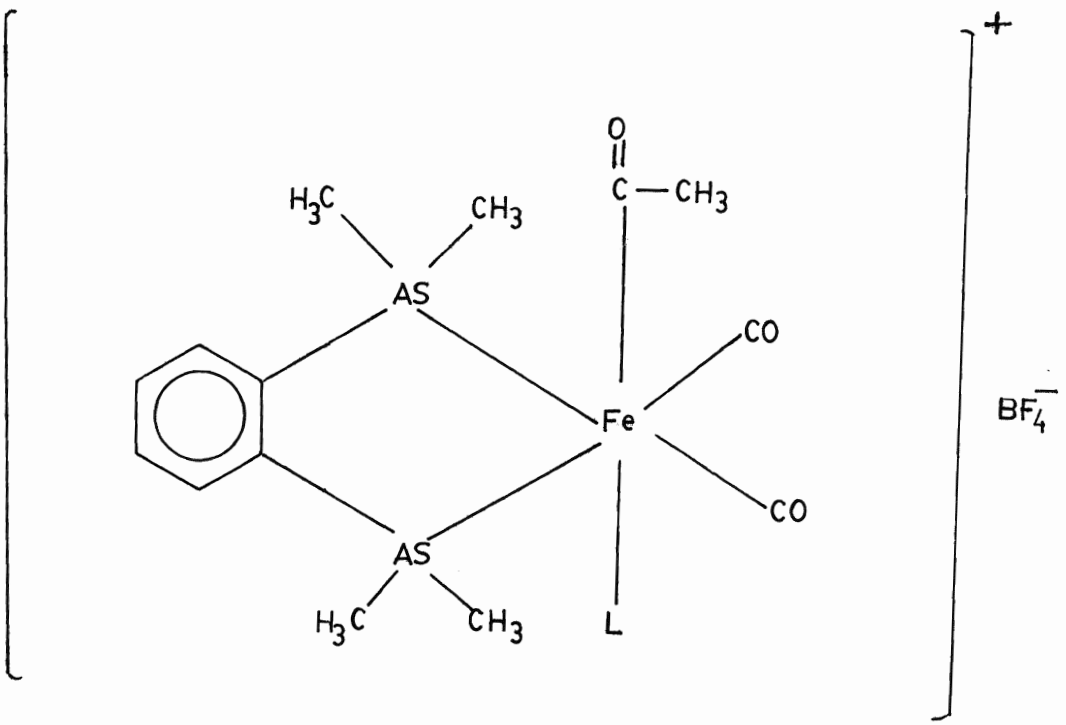
O
C — CH3
H3C
CH3
AS
CO
Fe
CO
AS
H3C
CH3
L
+
BF4−

instability. In FAB-MS, prominent peaks are observed for the cationic portion of the complex (C^+ and C^++1, respectively). The base peak at m/z 357 in each case corresponds to the fragment $[(diars)FeMe]^+$. The fragmentation patterns are dominated by successive CO loss, competing phosphine ligand cleavage and ligand decomposition. Formation of the rearrangement product via

$$[Fe\text{-}(C(O)Me)]^+ \longrightarrow [Fe\text{-}Me]^+ + CO$$

has also been asserted. Glycerol successfully served as the matrix liquid in each case.

Unger applied combined FAB-MS/MS [41] to elucidate the structures of Tc and Fe cationic transition-metal complexes, used as organ imaging agents. Loss of ligands was traced by metastable fragmentation while complete characterization of the complex was done by collisional activation. Complex ion stabilities were assessed by the transition metal centre (Tc versus Fe) and the size of the alkyl substituent attached to the equatorial chelating ligand.

(4) Area of Interest

The major part of my research is devoted to the comparative study of EI and FAB mass spectra of various phenyl-tin and -lead halide adducts with hexamethylphosphoramide whose spectroscopic studies have been done earlier [42,43]. FAB-MS has been found to be analogous to the solution chemistry because of its need to suspend the sample in solution, and

this has motivated us to explore the possibility of ligand exchange in these compounds by mixing them in a suitable matrix. We have been able to characterize these group IV organometallics by the relatively high abundance of the adduct ions in the high mass region of positive ion FAB that were quite obscure in earlier EI studies [42,43] although parent ion intensities are low enough to be detected in FAB.

We have attempted to study the characteristic behaviours of moisture sensitive, thermally unstable organometallics like Grignard reagent, butyllithium etc. in FAB, but without any success.

Another area of interest to us was the investigation of the presence of strong hydrogen bonds by FAB of various oxime complexes [44] that exist at room temperature to complement NMR and IR studies of these systems.

The last, and very exciting, part of our work was to probe the trapping of large amounts of water molecules by quaternary ammonium fluorides by FAB-MS, a complementary study to the ^{19}F NMR work of Clark and Miller [45].

Investigation of this ion-aggregation phenomenon in tetraalkyl- and trialkylaryl ammonium hydroxides has also been attempted by FAB.

This thesis aims to

1. study the applicability of FAB to HMPA adducts of phenyltin and lead halides,
2. differentiate between EI and FAB for both tin and lead compounds,
3. study the applicability of FAB to hydrogen-bonded systems.

Experimental

(1) Instrumentation:

Mass Spectrometer:

Mass spectra of all the compounds of interest were taken using a Kratos MS-30 double beam, double focussing mass spectrometer (Fig. 5) [46]. The samples were introduced by a heated solid probe for EI and an unheated probe for FAB. A resolution of 1000 and an accelerating voltage of 4 kV were used for both EI and FAB with a scan rate of 10 sec/decade. In addition, for EI, an ionization voltage of 70 eV at source temperature of ca. 100^{o} C was used, while for FAB an ion gun voltage of 8 keV at source pressure of 10^{-5} torr was used. The FAB source was always maintained at room temperature. Data were collected and all computations were carried out using a Kratos DS-55 data system, interfaced with the mass spectrometer as shown in Figure 6.

The FORTRAN program BMASROS was used to calculate the isotopic patterns of specific ions. The programs PKAVG, PLOT and QUAN were used to obtain qualitative and quantitative mass spectral data.

The FAB assembly is schematically represented in Figure 7.

Atom Gun:

The atom gun was designated as the heart of FAB equipment by Rinehart [47]. In our mass spectrometer, an Ion Tech saddle field source [48] is used to generate the fast atom beam. A schematic diagram

Figure 5

Schematic diagram of AEI MS-30 mass spectrometer

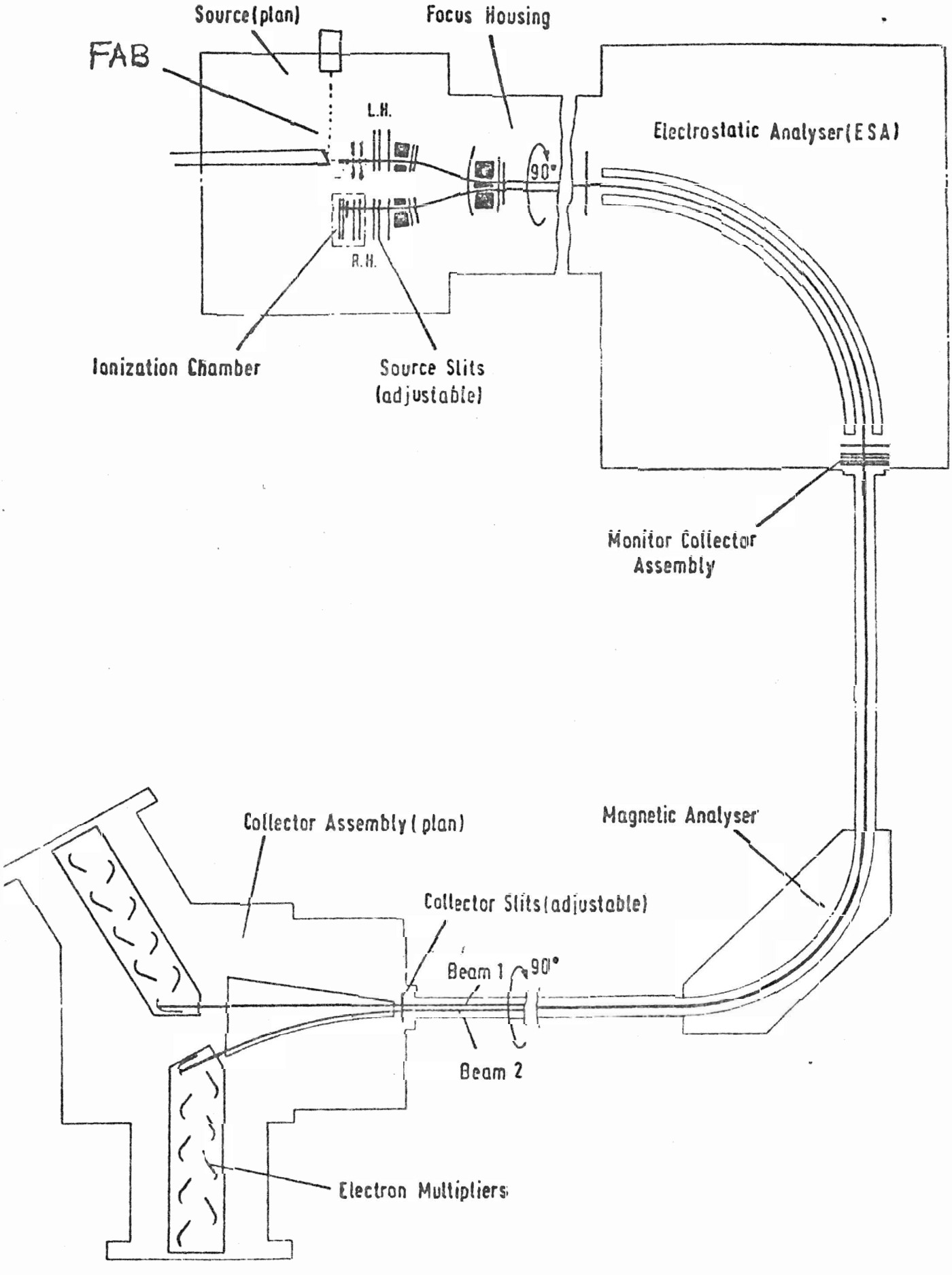
Source(plan)
Focus Housing
FAB
L.H.
Electrostatic Analyser(ESA)
90°
R.H.
Ionization Chamber
Source Slits
(adjustable)
Monitor Collector
Assembly
Collector Assembly (plan)
Magnetic Analyser
Collector Slits(adjustable)
Beam 1
90°
Beam 2
Electron Multipliers

Figure 6

DS-55 data system schematic

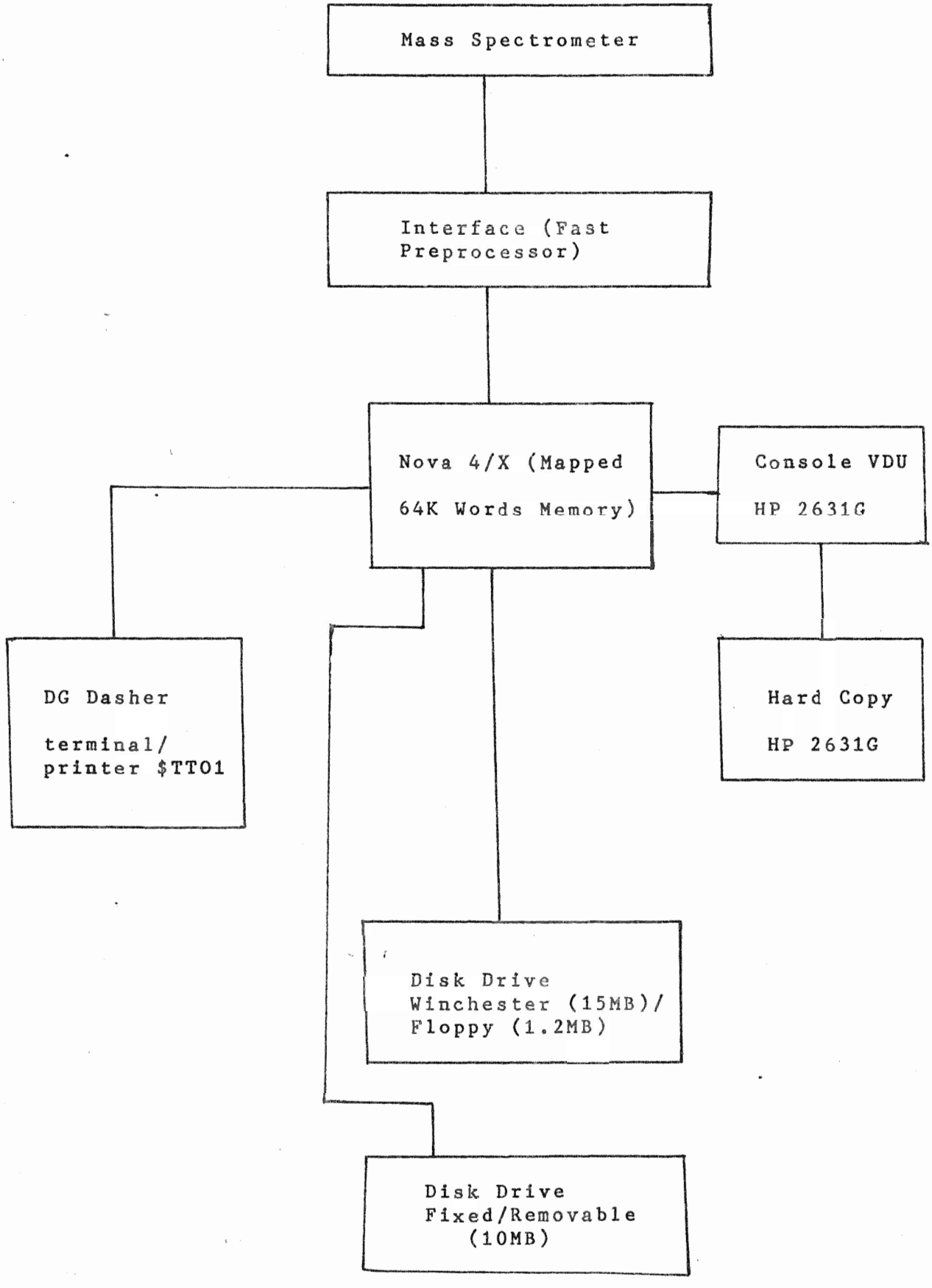
Mass Spectrometer
Interface (Fast Preprocessor)
Nova 4/X (Mapped 64K Words Memory)
Console VDU HP 2631G
DG Dasher terminal/ printer $TTO1
Hard Copy HP 2631G
Disk Drive Winchester (15MB)/ Floppy (1.2MB)
Disk Drive Fixed/Removable (10MB)

Figure 7

Schematic representation of FAB assembly

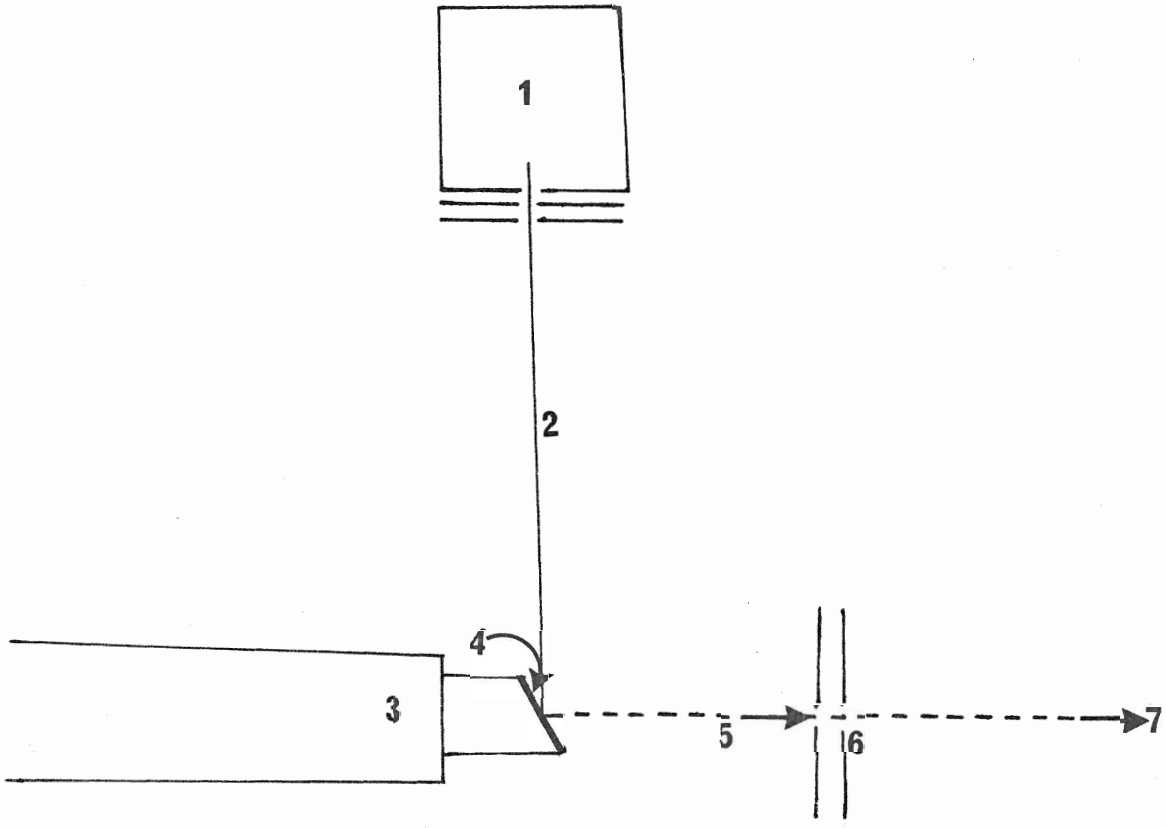

Reproduced with permission [53]

1. Atom gun
2. Fast atom beam
3. FAB probe
4. Sample film
5. Secondary ion beam
6. Extraction electrodes
7. Mass analyser

Figure 8

Schematic diagram of the FAB ion source

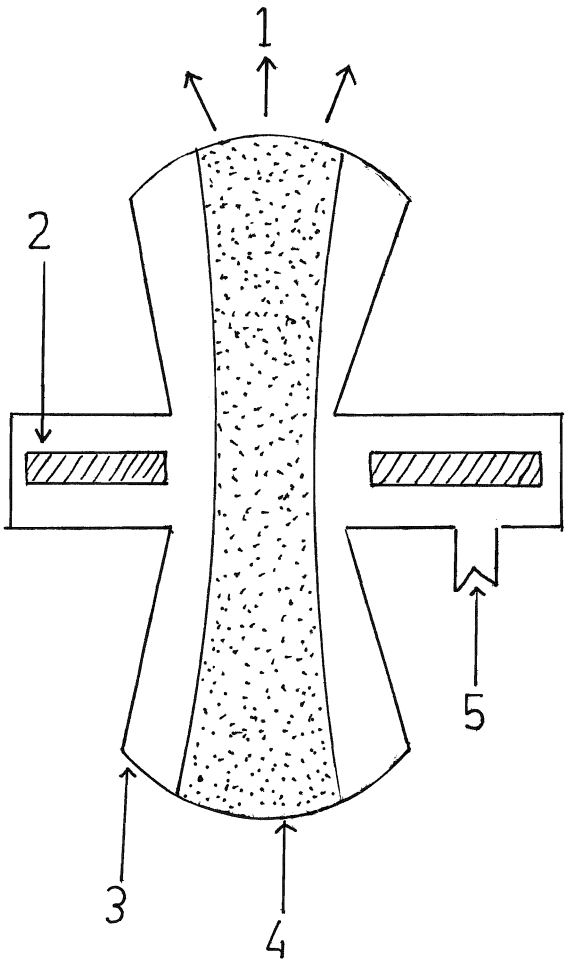

1. Ion beam
2. Anode
3. Cathode
4. Plasma
5. Gas

of this source [49] is represented in Figure 8.

The gases argon and xenon are generally used in our atom gun but it has been observed that the spectrum intensity is maximized in the case of xenon due to greater momentum transfer in the sputtering process. The atom gun is connected to a B-50 power supply which provides 6-8 keV energy to accelerate the rare gas ions before they are neutralized.

FAB Probe:

This is a solid polished shaft, electrically insulated from the high voltage of the source. The removable probe tip, made of stainless steel, is mounted on the shaft by two pins. We do not use copper probe tips any more as they have been observed to form cluster ions with the sample or matrix [50]. They are also eroded gradually by dilute nitric acid used for cleaning.

The angle of incidence of the beam with the probe tip is ca. 60^{o} in our instrument, which has been found to yield maximum ion abundance by Martin and co-workers [50].

FAB Source:

The FAB source replaces the standard EI source of beam 1 in our existing AEI-MS-30 mass spectrometer. It consists of a field plate and two beam centering plates. The probe tip is maintained at the accelerating potential and the ion repeller voltage is applied to the ion exit slit, the opposite to the EI arrangement.

The source is pumped rapidly, both to extract the inert gas used for bombarding the sample and to maintain adequate vacuum in the presence of evaporating matrix liquids. FAB-MS is simple in nature. New ion sources can be bought for old mass spectrometers, or a FAB ion gun can be linked to the FD, EI or CI ion source with little alteration in source components [51].

The complete FAB upgrade kit was supplied by Kratos.

Matrix Liquid:

The use of matrix liquid is one of the main features in FAB-MS that makes it distinguishable from other soft ionization techniques. Although it is not essential to use the liquid dispersant with each sample, it does help in maintaining the sample ion intensity by continuously renewing the sample surface.

In the FAB-MS analysis of HMPA adducts of phenyltin and -lead halides, HMPA with a trace of glycerol successfully served as a matrix.

The HMPA matrix was also used with success in obtaining the FAB mass spectra of tetraalkylammonium fluorides with added numbers of H_2O molecules. The use of glycerol proved fruitful in the mass spectral analysis of the tetraalkyl- and trialkyl-arylammonium hydroxides by FAB.

Calibration:

Manual calibration of the data system was done by assigning the masses 69, 119 and 131 from an acquired time file in both EI and FAB. Tris-perfluoroheptyltriazine was used as reference compound in FAB and perfluoroalkane in EI to give calibration ranges up to m/z 1017 and m/z 967, respectively. In FAB spectra, off-line time to mass conversion was used since a lock mass was lacking.

(2) Materials:

Tables I, II and III list the names of the suppliers and the names and formulae of the chemicals used and the compounds analysed.

(3) Preparation of the Hydroxide and Fluoride Samples for FAB Analysis

Aqueous solutions of tetraalkylammonium hydroxides were dried overnight under vacuum and then they were mixed with glycerol in 1:1 ratio before the addition of appropriate numbers of water molecules. Trialkyl-arylammonium hydroxides were treated in the same way after methanol was evaporated under reduced pressure at 50-60^{o}C from the solutions. No test was carried out to check the complete dryness of these samples. Tetrabutylammonium fluoride was a commercial sample. It was used as a trihydrate and was dissolved in HMPA in 1:10 ratio prior to the addition of H_2O molecules.

Table I

Chemical	Formula	Supplier
1. tris(perfluoroheptyl)--s-triazine	$C_{24}F_{45}N$	PCR Inc., Gainesville, Florida
2. perfluoroalkane	C_nF_{2n+2}	Pierce Chemical Co., Gainesville, Florida
3. glycerol	$C_3H_8O_3$	Aldrich Chemical Co., Inc., Milwaukee, Wisconsin
4. hexamethyl-phosphoramide	$C_6H_{18}N_3PO$	Aldrich Chemical Co., Inc., Milwaukee, Wisconsin
5. sulfolane	$C_4H_8SO_2$	BDH Chemicals Toronto, Ontario
6. argon (Ar)	--	Air Products
7. xenon (Xe)	--	Matheson Gas Products Canada

Table II

Compound	Source
Group A	
$Ph_3SnCl.HMPA$	I. Wharf,
$Ph_3SnBr.HMPA$	Department of Chemistry,
$Ph_3SnI.HMPA$	McGill University
$Ph_2SnCl_2.HMPA$	Montreal, Quebec
$Ph_2SnBr_2.HMPA$	see ref. 42 for preparation
$Ph_2SnBr_2.2HMPA$	
$Ph_2SnI_2.2HMPA$	
Group B	
$Ph_3PbCl.HMPA$	same as above
$Ph_3PbBr.HMPA$	see ref. 43 for preparation
$Ph_3PbI.HMPA$	
$Ph_2PbBr_2.HMPA$	
$Ph_2PbI_2.HMPA$	
$Ph_2PbCl_2.2HMPA$	
$Ph_2PbBr_2.2HMPA$	
$Ph_2PbI_2.2HMPA$	
Group C	
C_6H_5MgBr	Prepared from the standard procedure given in ref. 52
C_4H_9Li	Aldrich Chemical Co., Inc., Milwaukee, Wisconsin

Table III

Compound	Formula	Supplier
tetrabutylammonium fluoride, trihydrate	$(C_4H_9)_4NF.3H_2O$	Aldrich Chemical Co., Inc., Milwaukee, Wisconsin
trimethylphenylammonium hydroxide in methanol	$(CH_3)_3.C_6H_5NOH$	Eastman Kodak Company, Rochester, New York
benzyltrimethylammonium hydroxide in methanol	$C_6H_5CH_2(CH_3)_3NOH$	Eastman Kodak Company, Rochester, New York
tetrabutylammonium hydroxide in water	$(C_4H_9)_4NOH$	Aldrich Chemical Co., Inc., Milwaukee, Wisconsin
tetramethylammonium hydroxide in water	$(CH_3)_4NOH$	Matheson, Coleman and Bell, Norwood, Ohio
tetraethylammonium hydroxide in water	$(C_2H_5)_4NOH$	Aldrich Chemical Co., Inc., Milwaukee, Wisconsin
tetra-n-butylammonium fluoride-acetophenoxime disolvate	$C_8H_8NOH...F^-N^+(n\text{-}C_4H_9)_4$	J. H. Clark Department of Chemistry University of York Heslington, York, England see ref. 44 for preparation
tetra-n-butylammonium fluoride-dl-camphoroxime disolvate	$C_{10}H_{16}NOH...F^-N^+(n\text{-}C_4H_9)_4$	J. H. Clark University of York see ref. 44 for preparation

III. Results and Discussion

1. Role of HMPA and glycerol as matrix

HMPA, as a matrix, plays a major role by dissolving the organo-metallics easily while remaining unreactive to the samples. However, excess HMPA drives the ionic equilibrium towards the HMPA (complex) side and to this may be attributed the observation of stable HMPA-containing metal ions in FAB. Excess HMPA also raises the pressure inside the source due to its volatile nature. To reduce this extra pressure and to increase run stability and longevity, a trace amount of glycerol is added to the HMPA matrix before the analysis of each sample. Glycerol in these concentrations does not form any complex with the samples. In addition, HMPA helps us explore the ligand-exchange phenomenon for these organo-metallics.

2. Comparison of the EI and positive FAB mass spectra of some phenyltin halide adducts with hexamethylphosphoramide

The EI study of these compounds had already been done earlier [42]. The positive ion FAB mass spectra illustrated in this section are shown in Figures 9-11, 13-14 and 16-17. The following compounds were studied:

(i) $(C_6H_5)_3SnX.HMPA$ (X = Cl, Br, I)

(ii) $(C_6H_5)_2SnX_2.HMPA$ (X = Cl, Br)

(iii) $(C_6H_5)_2SnX_2.2HMPA$ (X = Br, I)

Partial EI and positive FAB mass spectra of the tin-containing ions of groups (i), (ii) and (iii) are given in Tables IV, V and VI, respectively.

(i) $Ph_3SnX.HMPA$ (X = Cl, Br, I): In both EI and FAB over fifty percent of the ion current is carried by HMPA and its fragmentation products. The only difference in FAB is that quasimolecular ions are observed instead of molecular ions for the ligand and even the dimers of HMPA give prominent peaks in most of the spectra taken. For the $Ph_3Sn.HMPA^+$ ion, the intensity decreases from X = Cl to X = Br and then increases for X = I in both EI and FAB. The EI spectra show a decrease in intensity for the $Ph_2SnX.HMPA^+$ in the order of I < Br < Cl whereas in FAB, only the $Ph_2SnBr.HMPA^+$ cluster is observed. The same trend is repeated for the $SnX.HMPA^+$ species. For $PhSn.HMPA^+$, while the stability of the ion decreases in EI, it increases in FAB as the halide changes from Cl to I.

$Sn.HMPA^+$ ion clusters are observed in almost all EI and FAB spectra. Tin bonds strongly to HMPA even after the subsequent loss of all phenyls and halogens from the parent ion. According to Wharf and co-workers [42], the probability of formation of this ion by recombination in the mass spectrometer cannot be ruled out in the EI spectrum, and recombination ions should be even more commmon in FAB. Most of the high mass ions observed in both EI and FAB have one HMPA co-ordinated. This may be due to the loss of phenyl or halogen from the

Table IV.

Comparison of EI and +FAB Data

(tin-containing ions)*

	EI ($Ph_3SnX.HMPA$)			FAB		
ION^+	X = Cl	X = Br	X = I	X = Cl	X = Br	X = I
$Ph_3Sn.2HMPA$	--	--	--	2.7	0.8	--
$Ph_3Sn.HMPA$	0.2	0.1	0.3	24.8	17.4	31.0
$Ph_2SnX.HMPA$	2.9	1.0	0.4	--	16.0	--
PhSn.HMPA	0.9	0.2	--	5.0	7.1	13.2
SnX.HMPA	6.8	1.7	0.8	--	4.4	--
$Ph_2Sn.HMPA$	--	--	--	--	--	2.7
Sn.HMPA	2.1	0.4	--	4.3	2.9	--
Ph_3SnX	2.3	1.3	--	--	--	--
Ph_2SnX	--	52.1	--	--	9.0	1.7
Ph_3Sn	33.7	--	39.5	26.7	11.6	25.2
PhSnX	27.8	6.1	--	--	2.3	--
Ph_2Sn	--	1.4	--	--	1.4	--
SnX	13.0	24.8	8.2	--	5.5	--
PhSn	6.1	6.2	25.4	23.0	10.5	14.3
Sn	4.2	4.5	21.0	13.6	10.8	11.8

* percentage of the total absolute intensity of the metal-containing ions.

parent ions $Ph_3SnX.HMPA^+$ being favoured over HMPA loss. It is not due to the HMPA matrix since it is observed in the EI spectra. It has been documented that the mass spectra of alkyls and aryls of Group IV elements are dominated by even electron ions [54,56]. We could also see the dominance of even electron ions such as Ph_3Sn^+, Ph_2SnX^+, $PhSn^+$ and SnX^+ over the odd electron ions such as $PhSnX^+$ and Sn^+ in both EI and FAB, although in FAB, Sn^+ ion intensities are much more prominent. Parent Lewis acids, Ph_3SnX^+ are found in EI, but not in FAB. Surprisingly, Ph_2Sn^+, probably formed by the loss of Br from Ph_2SnBr^+, carries the same amount of ion current in EI as it does in FAB.

The fragmentation patterns of $Ph_3SnX.HMPA$ are almost the same as those of Ph_3SnX^+. In the latter, the fragment ions are much more intense in both EI and FAB. Species with HMPA bonded to Sn(II) and Sn(IV) are found to be more stable in FAB.

Peaks corresponding to free phenyls and halogens are frequently observed in EI, but not in FAB. No parent ion is observed for these penta-co-ordinate tin species in EI and in FAB also, these are too weak to be detected.

The probable fragmentation pathways are presented in Figure 12.

Figure 9

Positive ion FAB mass spectrum of $(C_6H_5)_3SnCl.HMPA$

N.B. All the spectra and quan reports included in this thesis belong to FAB ionization although the computer printout in each case shows EI instead of FAB. Please ignore that as this is an artifact of our data system.

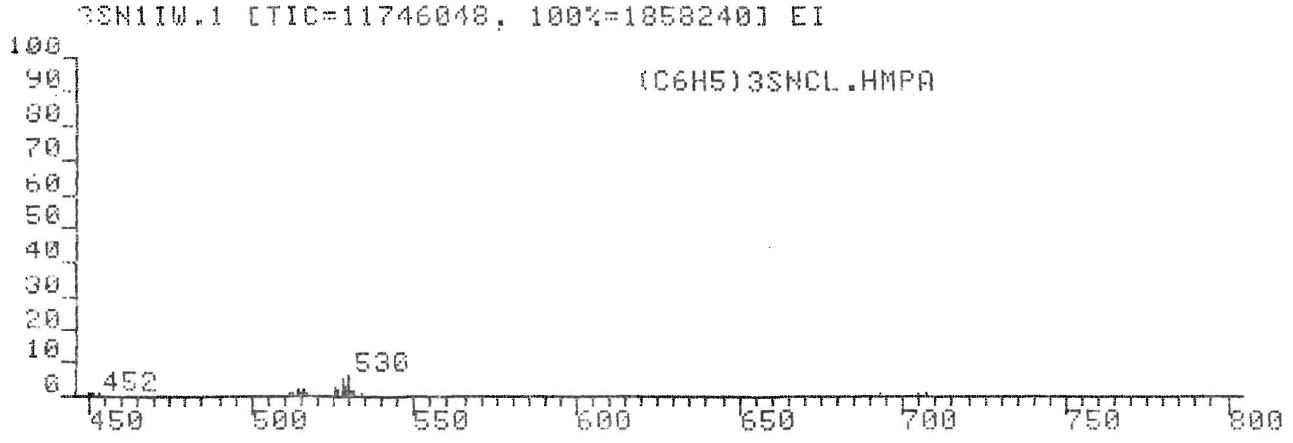
3SN1IW.1 [TIC=11746048, 100%=1858240] EI
(C6H5)3SNCL.HMPA
452
530

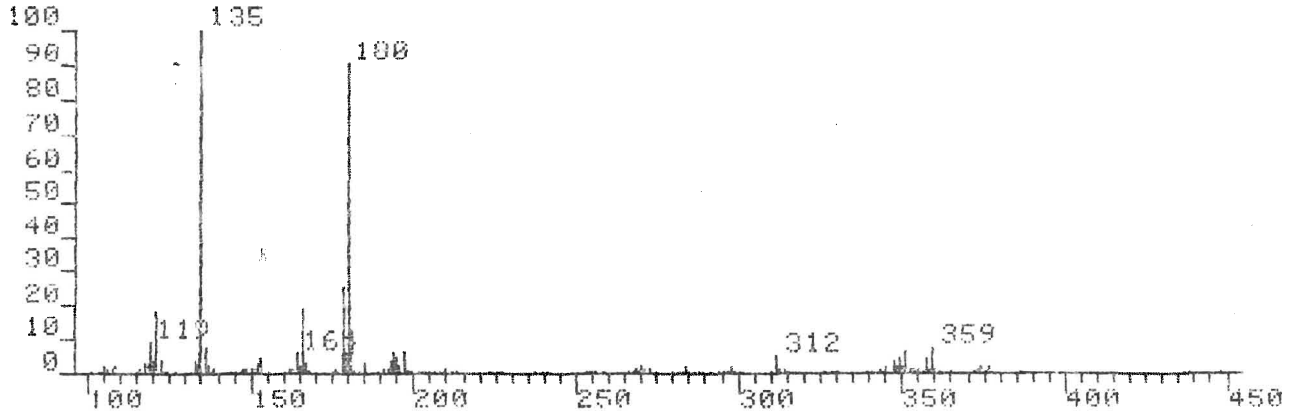
135
100
119
165
312
359

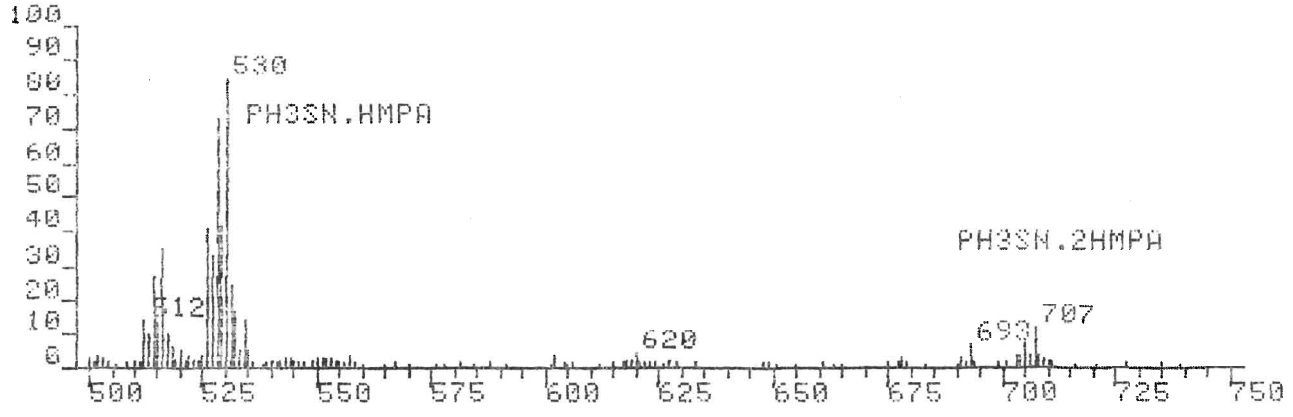
3SN1IW.1 [TIC=11746048, 100%=136944] EI
530
PH3SN.HMPA
PH3SN.2HMPA
512
620
693
707

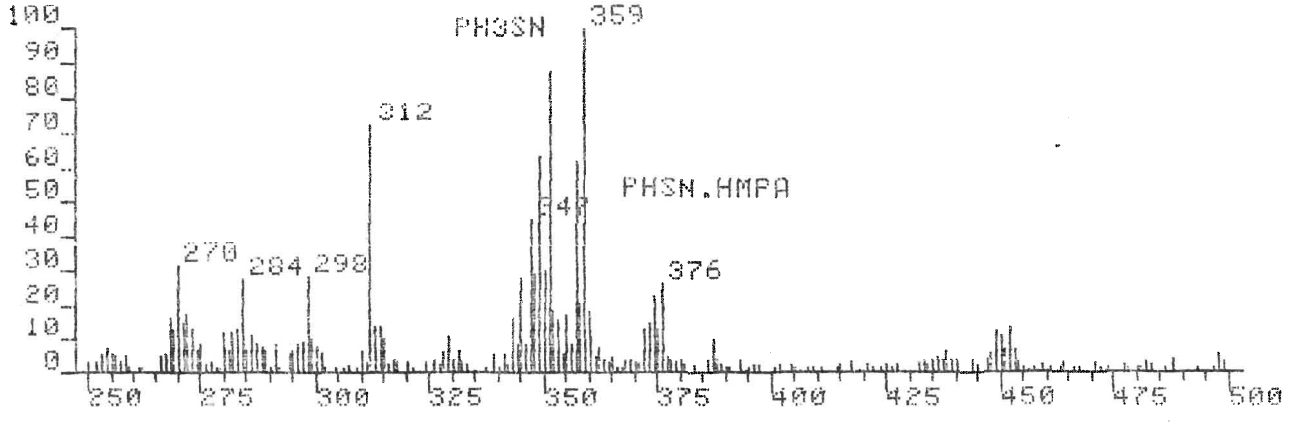
PH3SN
359
312
PHSN.HMPA
348
270
284
298
376

Figure 10

Positive ion FAB mass spectrum of $(C_6H_5)_3SnBr.HMPA$

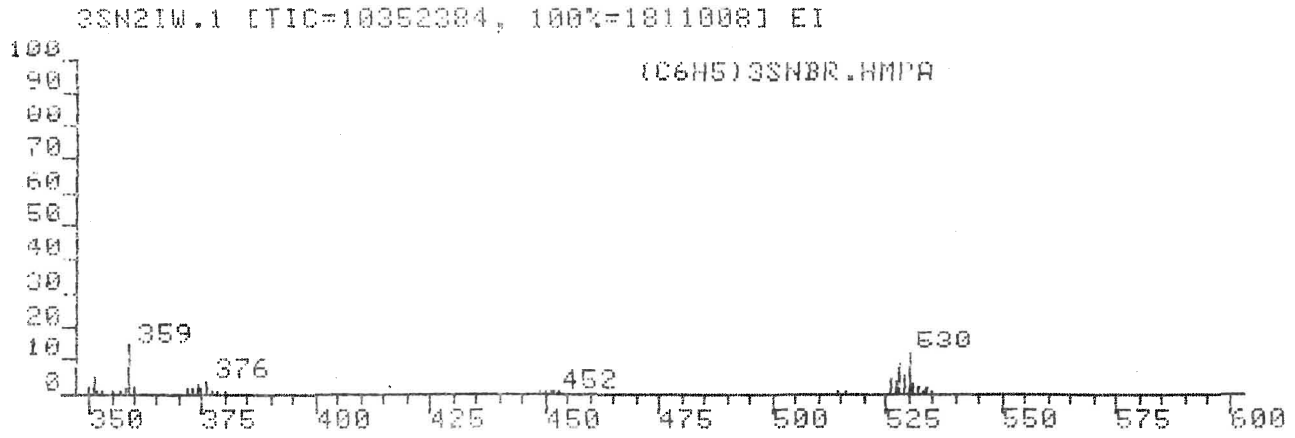
3SN2IW.1 [TIC=10352384, 100%=18110008] EI
(C6H5)3SNBR.HMPA
359
376
452
530

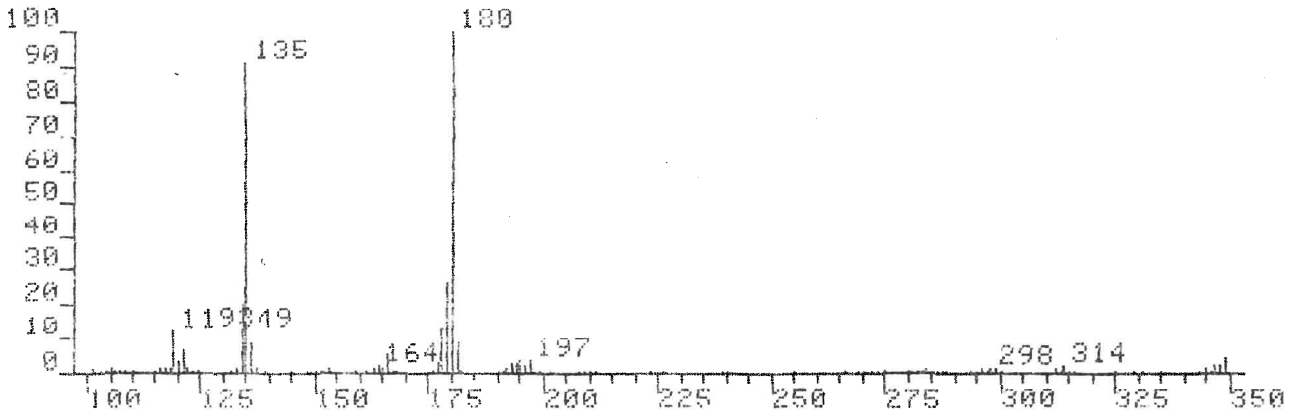
135
180
119
149
164
197
298
314

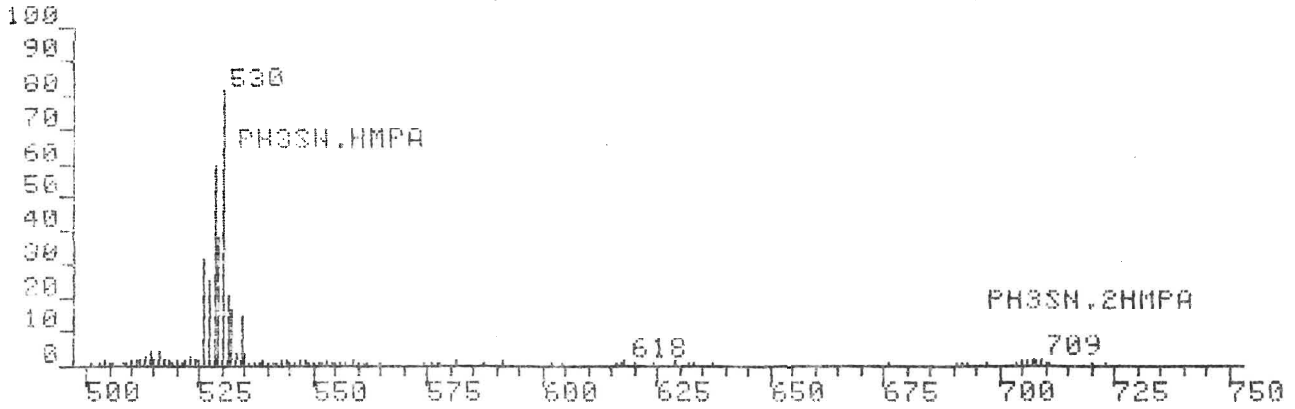
3SN2IW.1 [TIC=10352384, 100%=261172] EI
530
PH3SN.HMPA
PH3SN.2HMPA
618
709

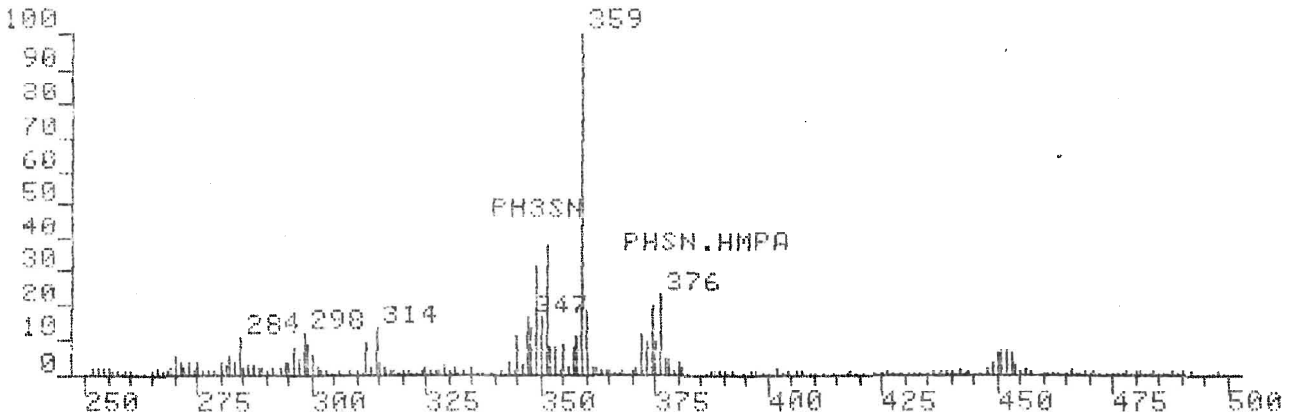
359
PH3SN
PHSN.HMPA
376
284
290
314
347

Figure 11

Positive ion FAB mass spectrum of $(C_6H_5)_3SnI.HMPA$

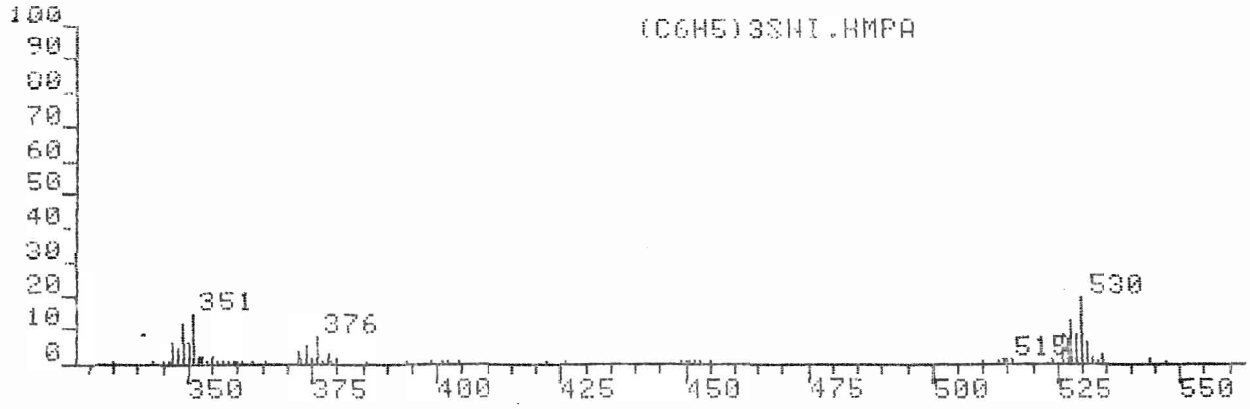
3SN3IW.1 [TIC=1807872, 100%=3194561 EI
(C6H5)3SNI.HMPA
351
376
519
530

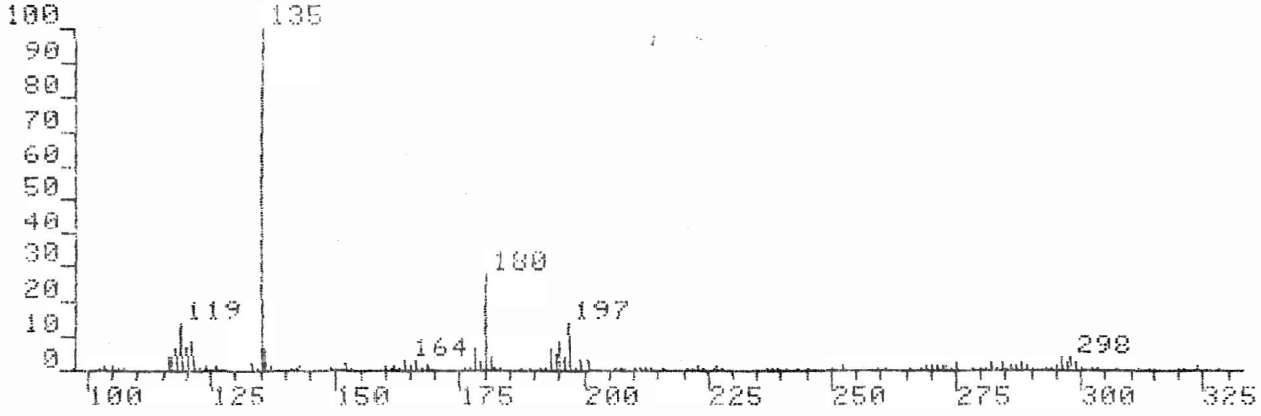
135
119
164
180
197
298

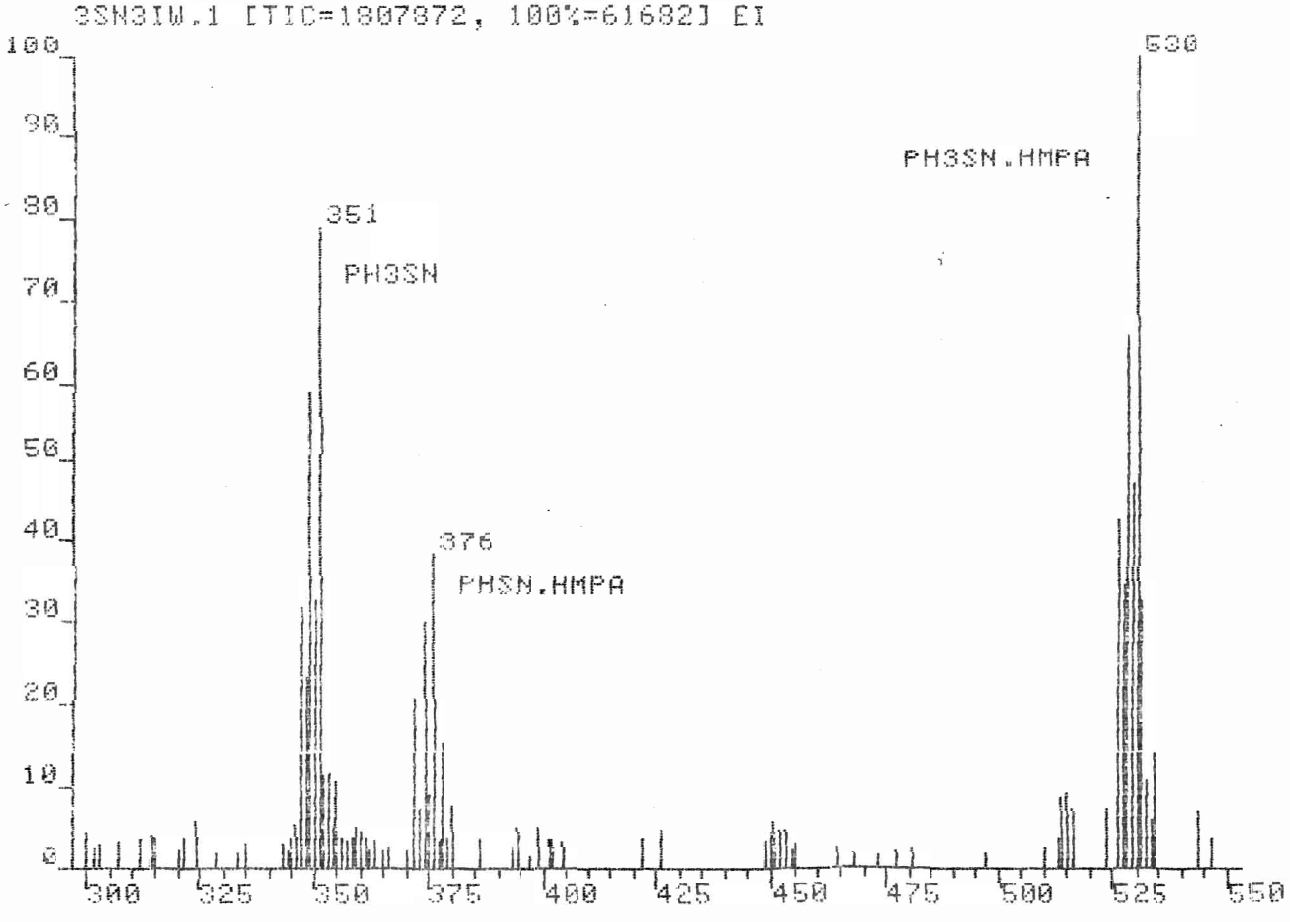
3SN3IW.1 [TIC=1807872, 100%=61682] EI
530
PH3SN.HMPA
351
PH3SN
376
PHSN.HMPA

Figure 12

Probable Fragmentation Schemes for the series $Ph_3SnX.HMPA$

(A) $Ph_3SnX.HMPA$ (EI)

(B) $Ph_3SnX.HMPA$ (FAB)

(A)

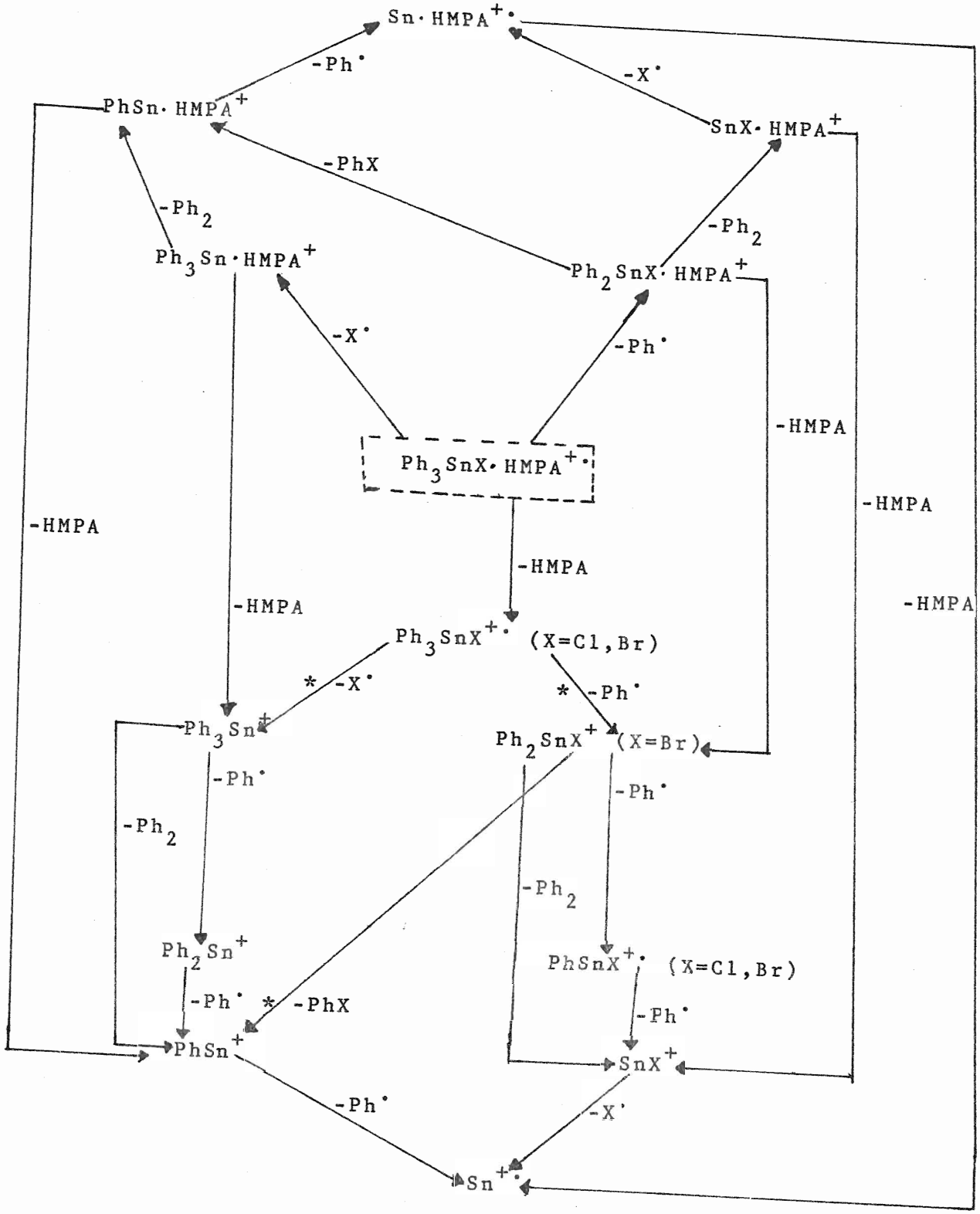

*metastable-confirmed transitions [55]

(B)

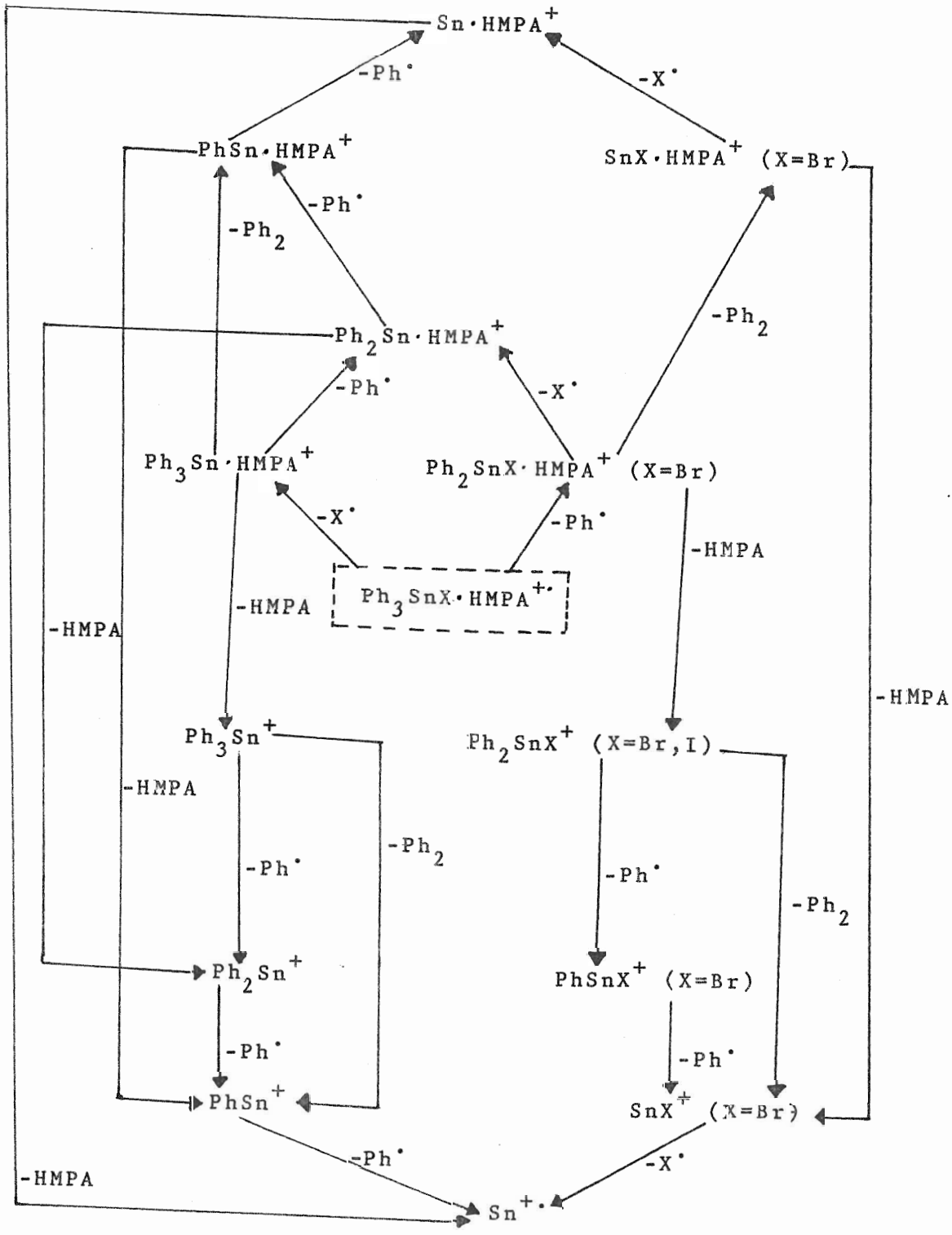
Sn·HMPA+
-Ph·
-X·
PhSn·HMPA+
SnX·HMPA+ (X=Br)
-Ph·
-Ph2
-Ph2
Ph2Sn·HMPA+
-Ph·
-X·
Ph3Sn·HMPA+
Ph2SnX·HMPA+ (X=Br)
-X·
-Ph·
-HMPA
-HMPA
Ph3SnX·HMPA+·
-HMPA
-HMPA
Ph3Sn+
Ph2SnX+ (X=Br,I)
-HMPA
-Ph·
-Ph2
-Ph·
-Ph2
Ph2Sn+
PhSnX+ (X=Br)
-Ph·
-Ph·
PhSn+
SnX+ (X=Br)
-Ph·
-X·
-HMPA
Sn+·

Figure 12a

Comparison of EI and FAB data

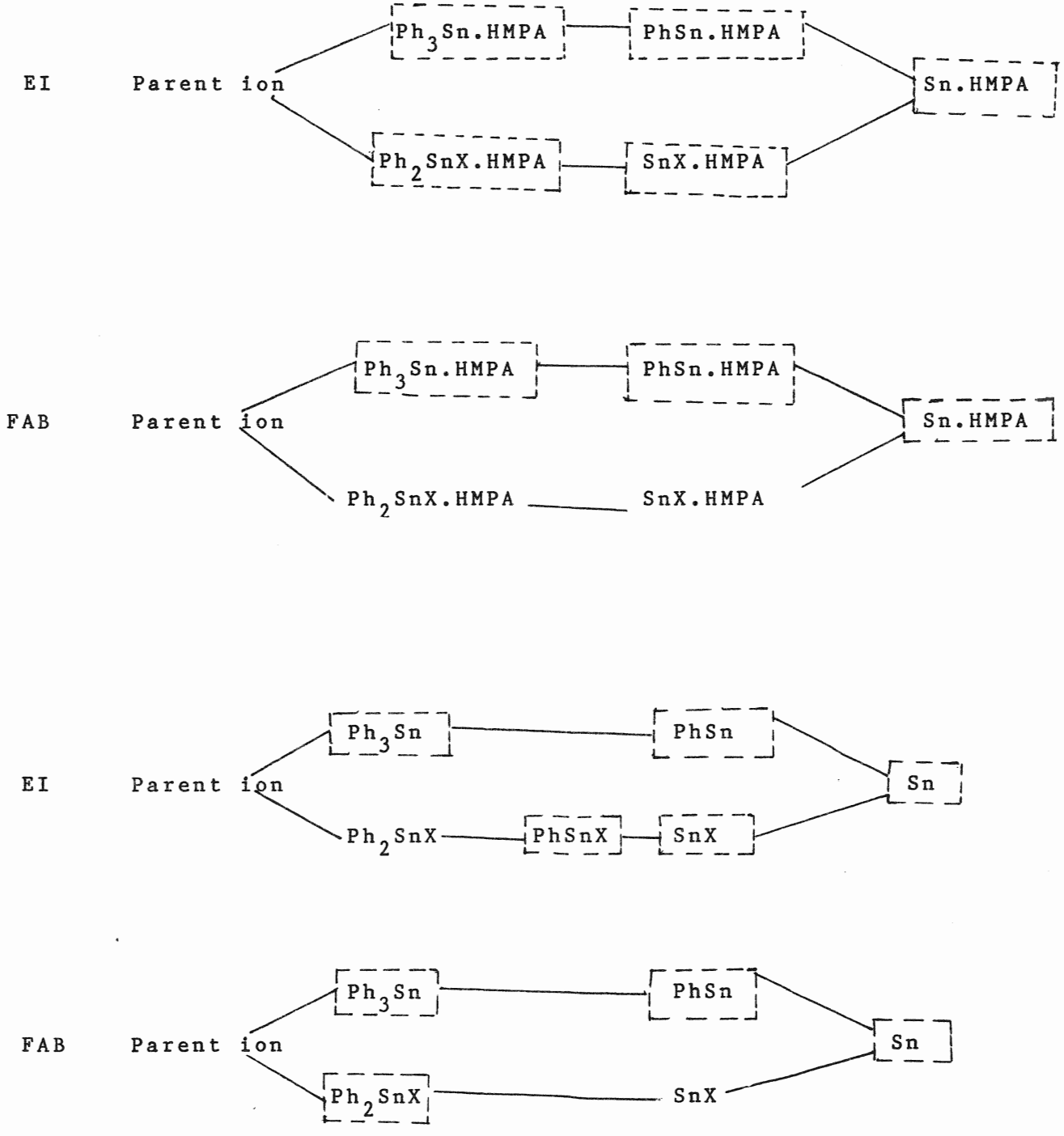

Dotted boxes indicate that the ion is present

Table V.

Comparison of EI and +FAB Data

(tin-containing ions)*

	EI (Ph_2SnX_2.HMPA)		FAB	
Ion^+	X = Cl	X = Br	X = Cl	X = Br
Ph_2SnX.HMPA	--	--	7.0	16.6
Ph_3Sn.HMPA	--	--	34.5	11.1
$PhSnX_2$.HMPA	--	--	--	--
PhSn.HMPA	--	--	12.7	11.2
SnX.HMPA	--	--	--	13.0
Sn.HMPA	--	--	--	4.9
Ph_2SnX_2.2HMPA	--	--	1.0	--
Ph_2Sn.2HMPA	--	--	1.0	--
Ph_2SnX_2	6.9	21.7	--	--
$PhSnX_2$	10.4	11.9	--	--
Ph_2SnX	19.5	25.9	2.6	3.9
PhSnX	28.3	4.1	--	1.2
Ph_2Sn	--	1.7	--	2.5
SnX_2	--	2.1	--	--
SnX	22.1	20.6	--	6.9
PhSn	6.4	7.9	19.2	17.3
Ph_3Sn	--	--	12.1	1.4
Sn	6.3	4.0	9.8	9.8

* percentage of the total absolute intensity of metal-containing ions.

(ii) Ph_2SnX_2.HMPA (X = Cl, Br)

In this class of compounds, HMPA-containing tin ions are not observed in EI in contrast to FAB in which these are of significant intensities. The stability of $Ph_2SnX.HMPA^+$ in FAB is a clear indication of the preferential loss of halogen from the parent ion. The bonding of tin to HMPA is relatively stable as observed for both chlorinated and brominated species in FAB. The mechanism of the formation of Ph_2SnCl_2.2HMPA in FAB is ambiguous in nature. Ions corresponding to parent Lewis acids are very intense in EI but are absent in FAB. Tin-containing fragments are dominated by even electron species such as $PhSnX_2^+$, Ph_2SnX^+, $PhSn^+$ and SnX^+ in both EI and FAB. The most abundant odd electron species are $PhSnX^+$ and Sn^+ itself. Ph_3Sn^+ follows the intensity pattern of $Ph_3Sn.HMPA^+$ (i.e., the intensity decreases as halides change from Cl to Br) in FAB but the mechanism of their formation is not yet clearly understood. Ph_2Sn^+ ions are observed for X = Br in both EI and FAB. FAB does not provide any dihalogenated tin species which contradicts the formation of SnX_2^+ ions in EI.

Probable fragmentation schemes for this series are presented in Figure 15.

Figure 13

Positive ion FAB mass spectrum of $(C_6H_5)_2SnCl_2$.HMPA

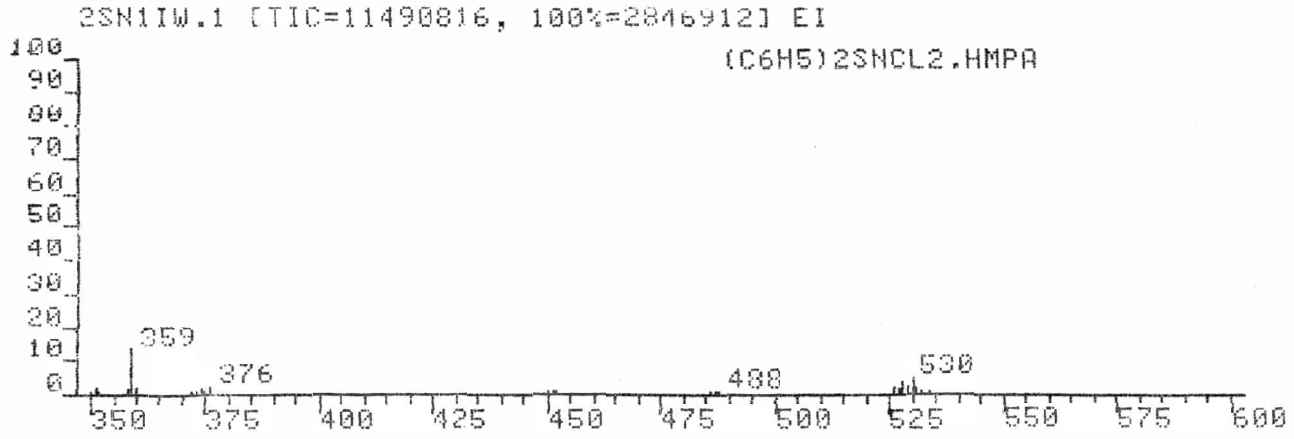
2SN1IW.1 [TIC=11490816, 100%=2846912] EI
(C6H5)2SNCL2.HMPA
359
376
480
530

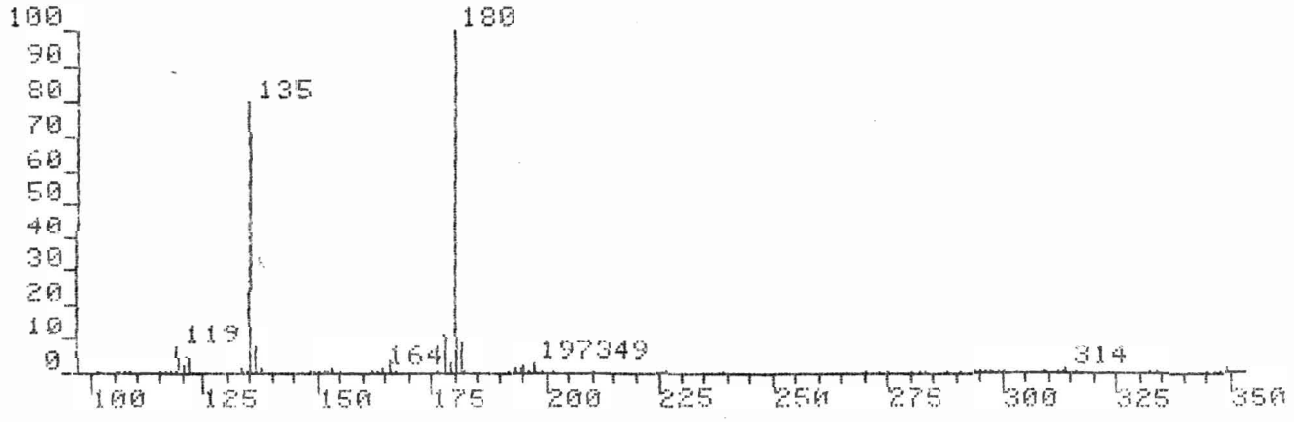
180
135
119
164
197349
314

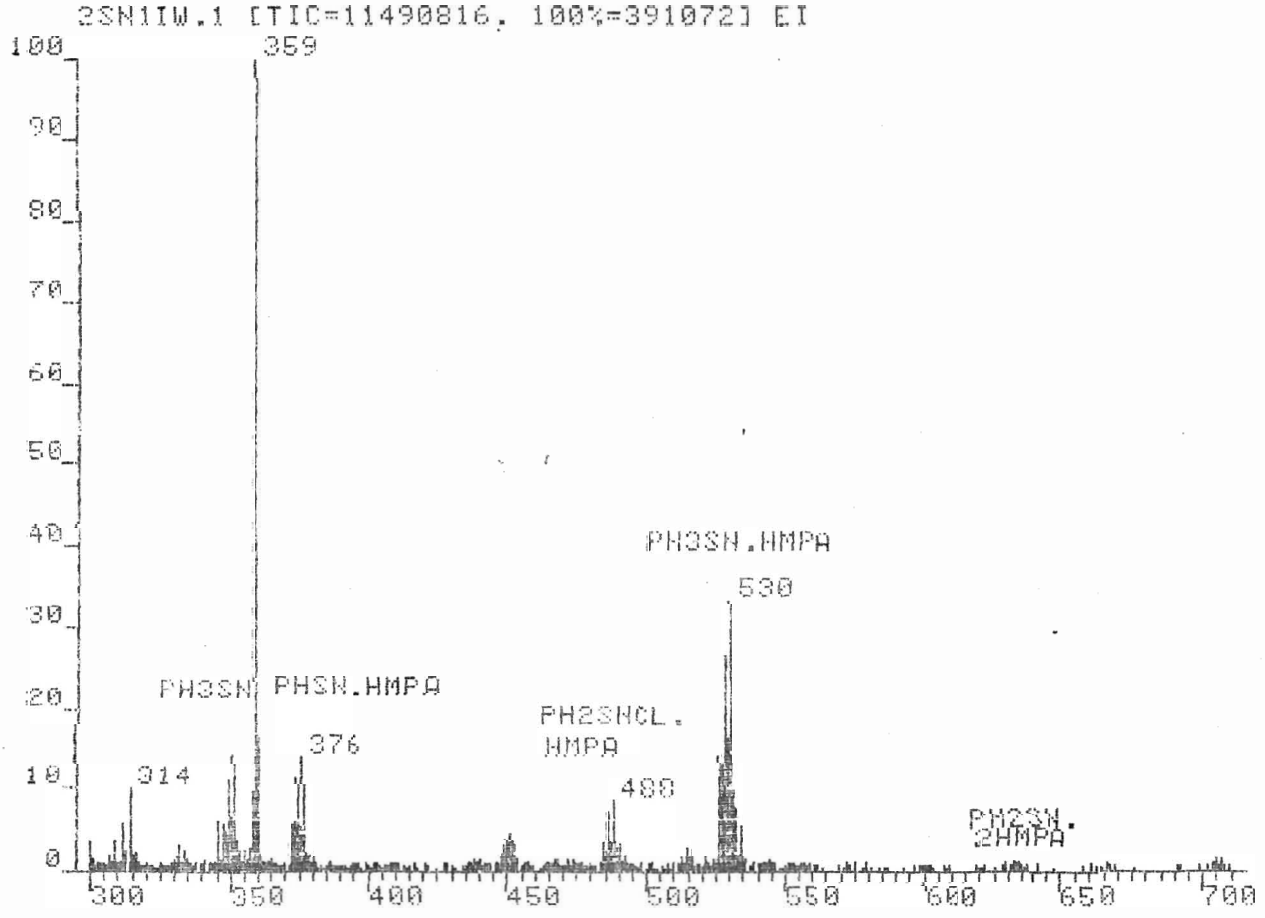
2SN1IW.1 [TIC=11490816, 100%=391072] EI
359
PH3SN.HMPA
530
PH3SN
PH3SN.HMPA
376
PH2SNCL.
HMPA
314
480
PH2SN.
2HMPA

Figure 14

Positive ion FAB mass spectrum of $(C_6H_5)_2SnBr_2$.HMPA

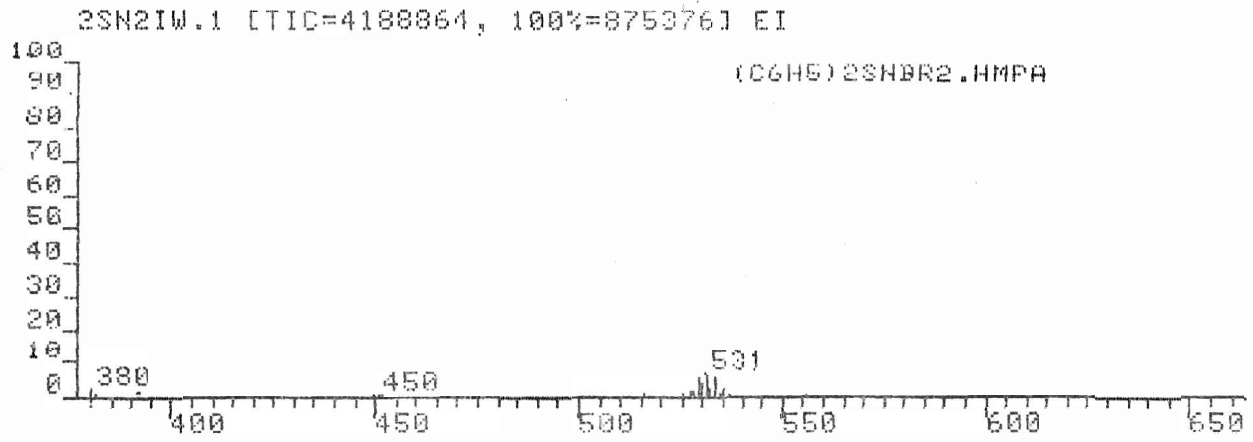
2SN2IW.1 [TIC=4188864, 100%=8753761 EI
(C6H5)2SNBR2.HMPA
531
380
450

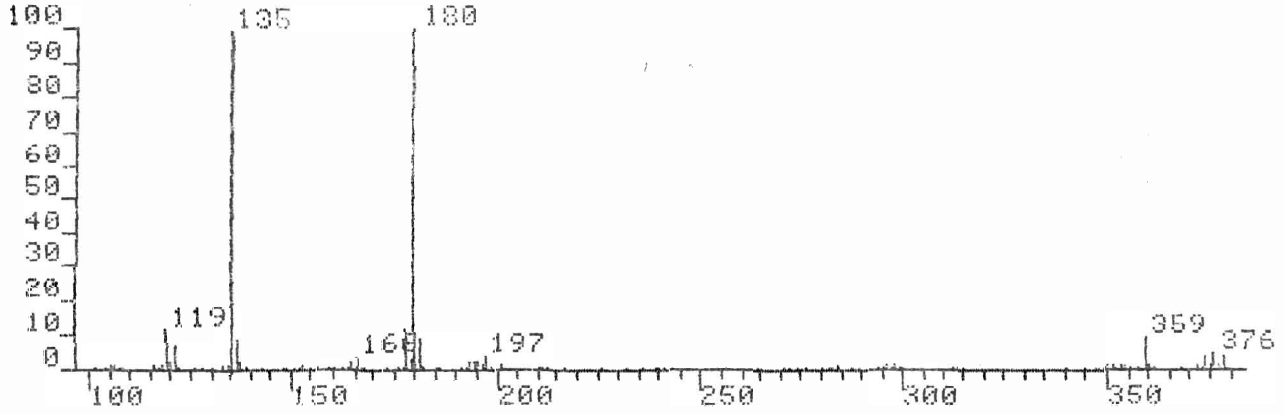
135
180
119
168
197
359
376

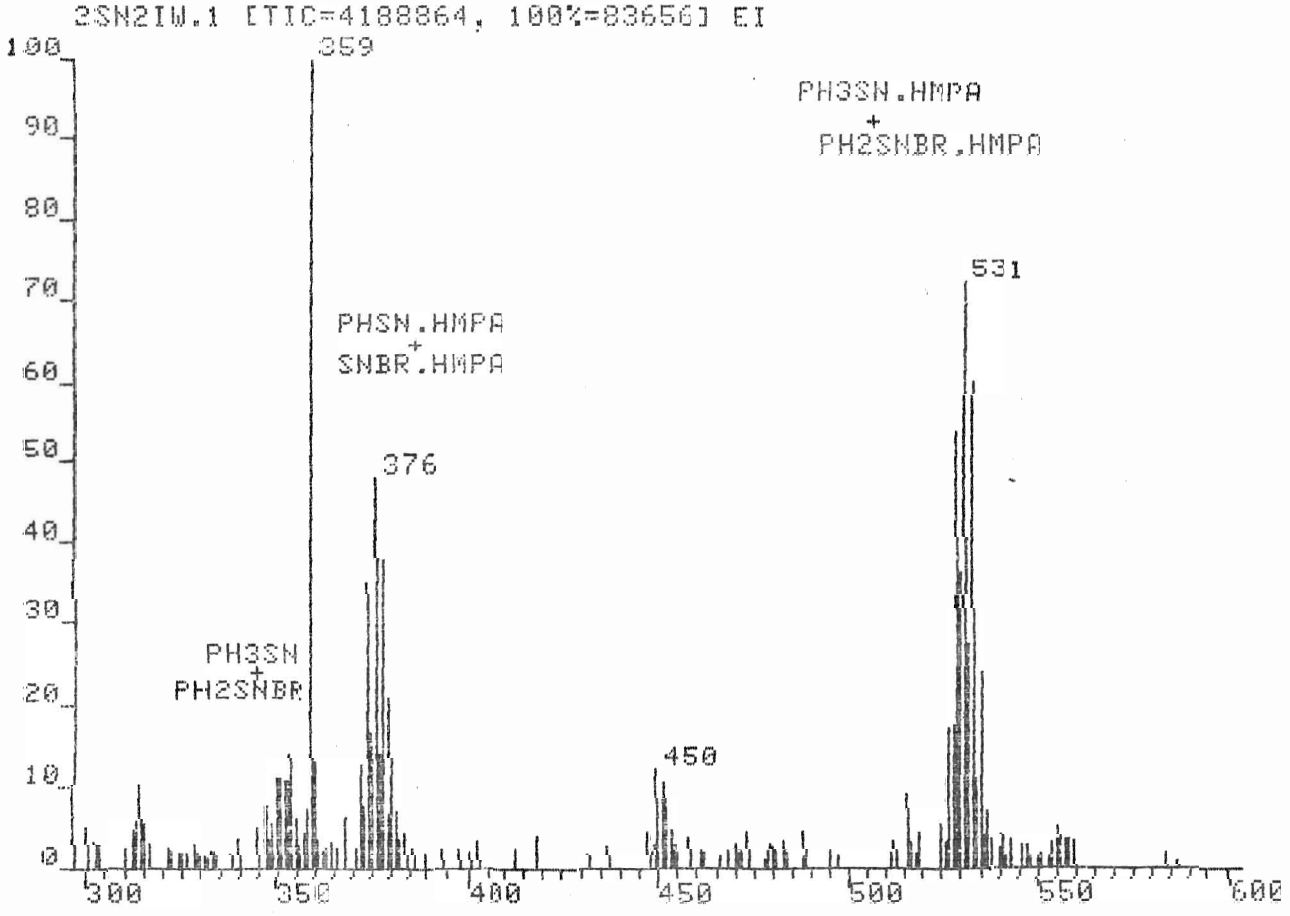
2SN2IW.1 [TIC=4188864, 100%=83656] EI
359
PH3SN.HMPA
+
PH2SNBR.HMPA
531
PHSN.HMPA
SNBR+.HMPA
376
PH3SN+
PH2SNBR
450

Figure 15

Probable fragmentation schemes for the series Ph_2SnX_2.HMPA

(A) Ph_2SnX_2.HMPA (EI)

(B) Ph_2SnX_2.HMPA (FAB)

(A)

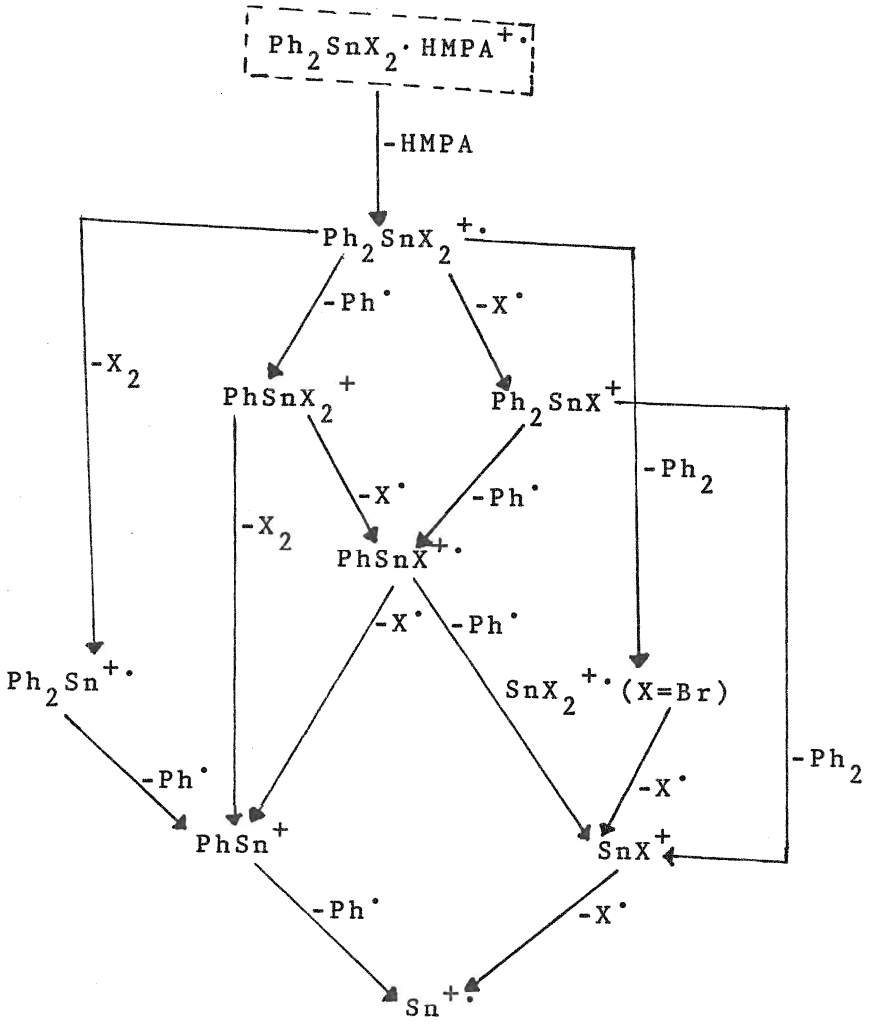
Ph2SnX2·HMPA+·
-HMPA
Ph2SnX2+·
-Ph·
-X·
-X2
PhSnX2+
Ph2SnX+
-Ph2
-X·
-Ph·
-X2
PhSnX+·
-X·
-Ph·
Ph2Sn+·
SnX2+· (X=Br)
-Ph2
-Ph·
-X·
PhSn+
SnX+
-Ph·
-X·
Sn+·

(B)

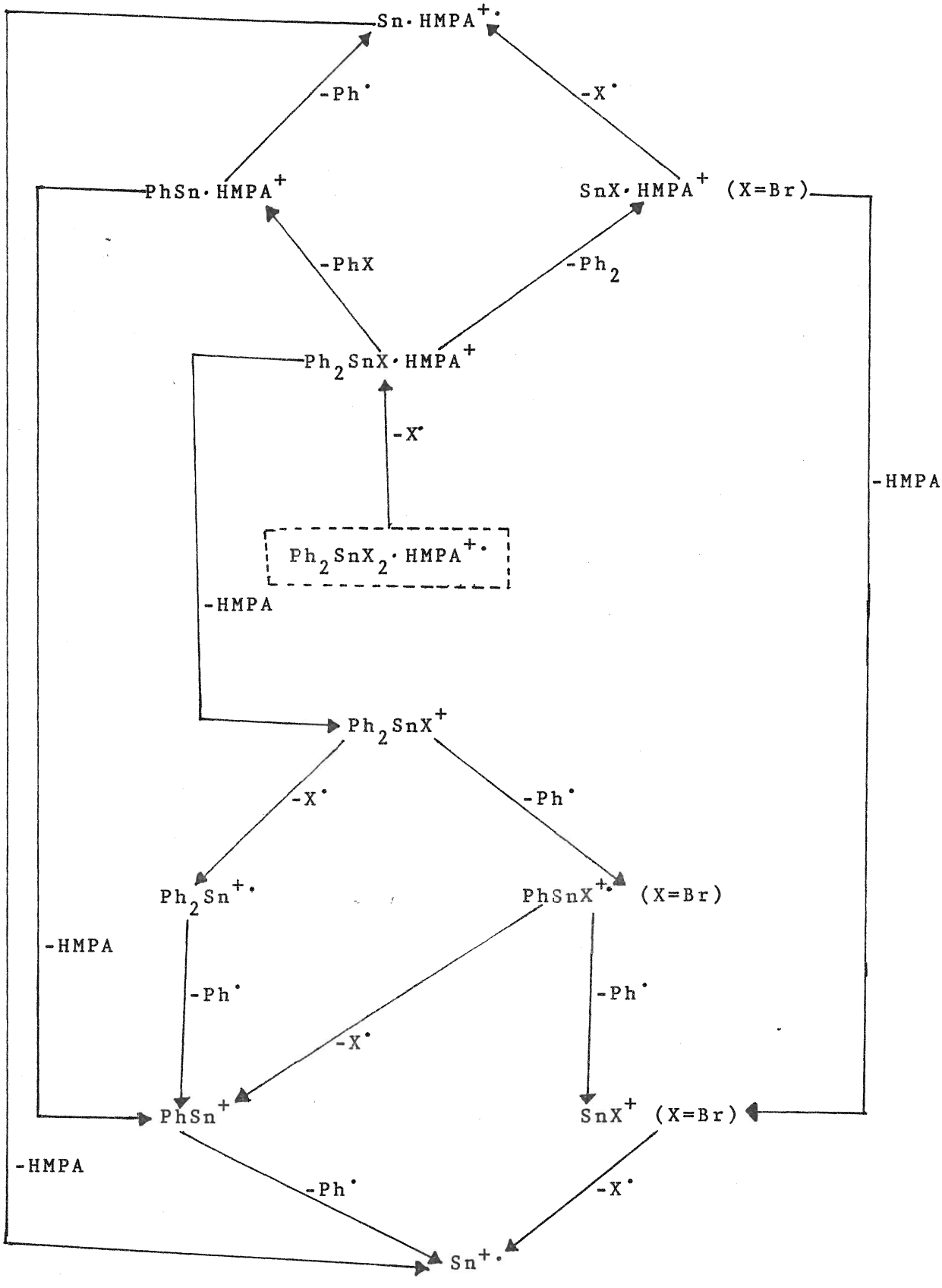
Sn·HMPA+·
-Ph·
-X·
PhSn·HMPA+
SnX·HMPA+ (X=Br)
-PhX
-Ph2
Ph2SnX·HMPA+
-X·
-HMPA
Ph2SnX2·HMPA+·
-HMPA
Ph2SnX+
-X·
-Ph·
Ph2Sn+·
PhSnX+· (X=Br)
-HMPA
-Ph·
-Ph·
-X·
PhSn+
SnX+ (X=Br)
-HMPA
-Ph·
-X·
Sn+·

Figure 15a

Comparison of EI and FAB data

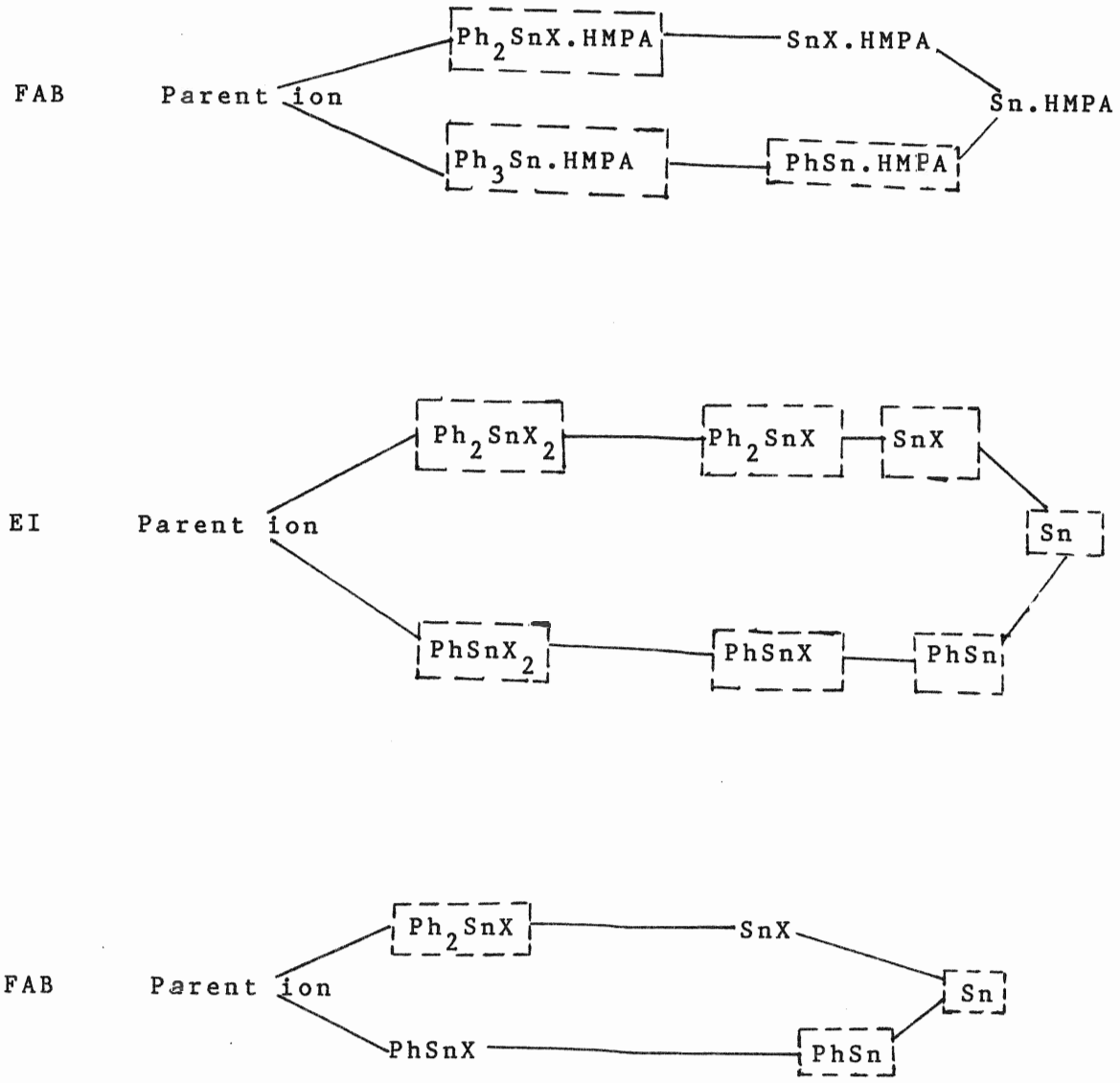

Table VI.

Comparison of EI and +FAB Data

(tin-containing ions)*

	EI (Ph_2SnX_2.2HMPA)		FAB	
Ion^+	X = Br	X = I	X = Br	X = I
Ph_2SnX.HMPA	0.5	2.9	12.6	32.5
$PhSnX_2$.HMPA	0.1	0.1	9.6	--
PhSn.HMPA	0.7	--	10.9	11.3
SnX.HMPA	0.1	1.8	7.7	6.0
Sn.HMPA	--	1.1	3.4	3.3
Ph_2SnX_2	2.6	--	--	9.1
$PhSnX_2$	1.4	1.5	2.0	--
Ph_2SnX	28.3	26.0	6.1	2.4
PhSnX	6.2	0.8	--	--
Ph_2Sn	0.6	--	--	--
SnX_2	0.3	2.2	--	10.0
SnX	42.7	19.2	9.2	--
PhSn	3.6	25.9	17.0	11.0
Sn	12.9	18.3	21.4	14.2

* percentage of the total absolute intensity of metal-containing ion.

(iii) $Ph_2SnX_2.2HMPA$ (X = Br, I)

This series of compounds shows HMPA-containing tin ions in both EI (comparatively low intensities) and FAB. This probably demonstrates the greater stabilities of hexa-co-ordinate tin species. Even electron ions $PhSnX_2^+$, Ph_2SnX^+, SnX^+ and $PhSn^+$ dominate the EI spectra as usual, but FAB shows lower intensities except for the $PhSn^+$ cluster. The odd electron ions $PhSnX^+$ (in EI) and Sn^+ (in both EI and FAB) appear at high intensity like those observed for the $Ph_2SnX_2.HMPA$ series. However, in this case bare tin ion intensities are increased to some extent. $Ph_2SnI_2^+$ (as a parent Lewis acid ion in FAB) and SnI_2^+ are more intense than their brominated counterparts, thus contradicting the general trend observed in mass spectrometry.

Possible fragmentation schemes for this series are given in Figure 18.

Figure 16

Positive ion FAB mass spectrum of $(C_6H_5)_2SnBr_2.2HMPA$

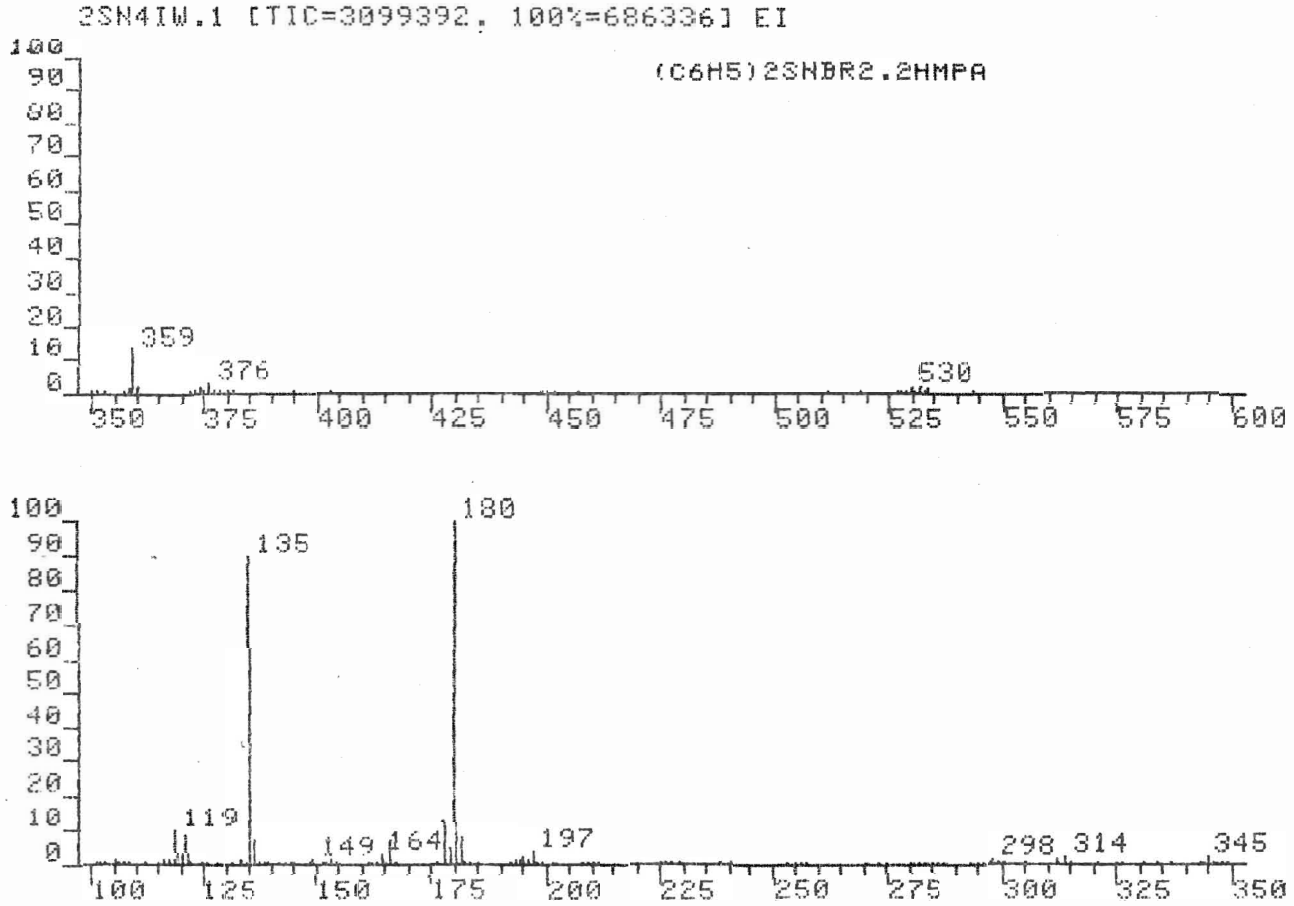
2SN4IW.1 [TIC=3099392, 100%=686336] EI
(C6H5)2SNBR2.2HMPA
359
376
530

180
135
119
149
164
197
298
314
345

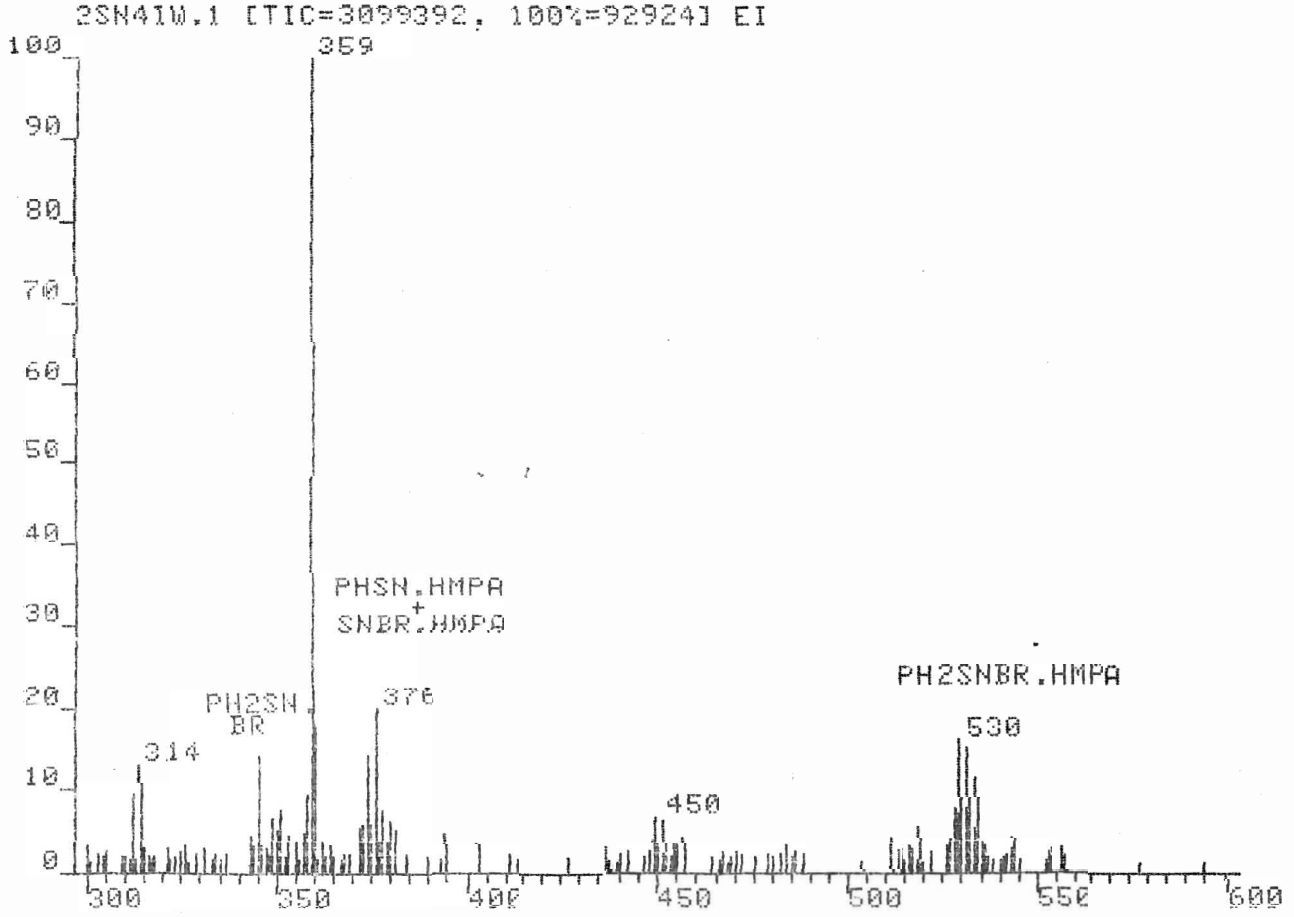
2SN41W.1 [TIC=3099392, 100%=92924] EI
359
PHSN.HMPA
SNBR+.HMPA
PH2SN
BR
376
314
450
PH2SNBR.HMPA
530

Figure 17

Positive ion FAB mass spectrum of $(C_6H_5)_2SnI_2.2HMPA$

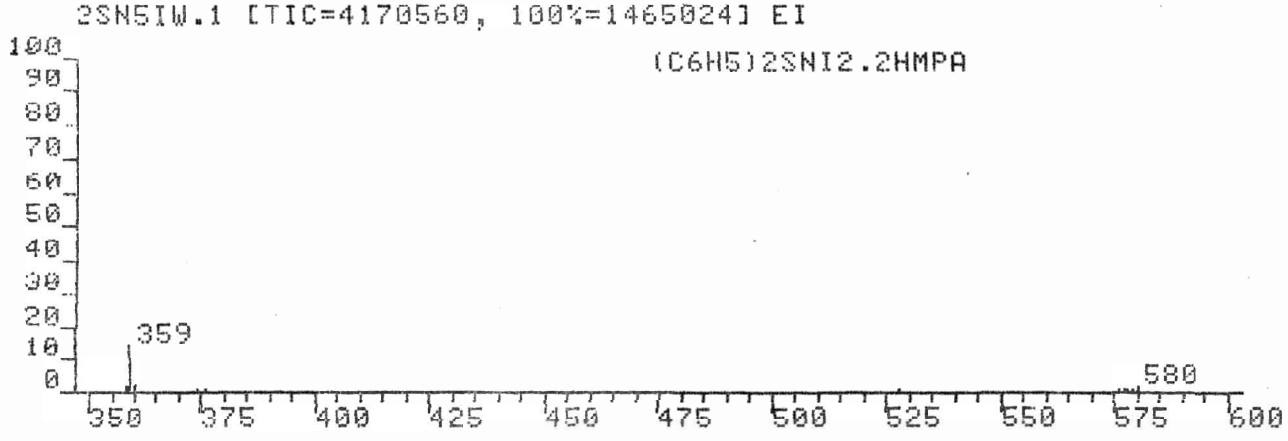
2SN5IW.1 [TIC=4170560, 100%=1465024] EI
(C6H5)2SNI2.2HMPA
359
580

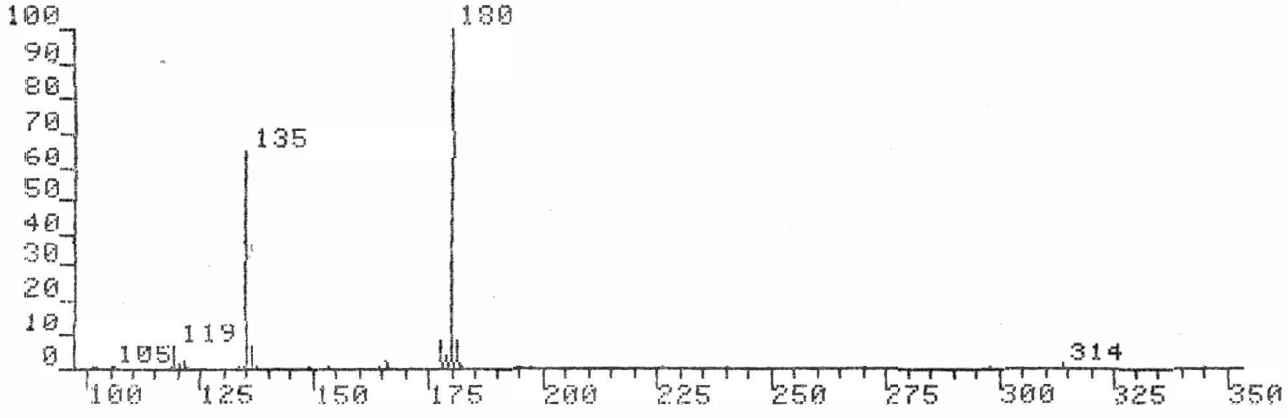
180
135
119
105
314

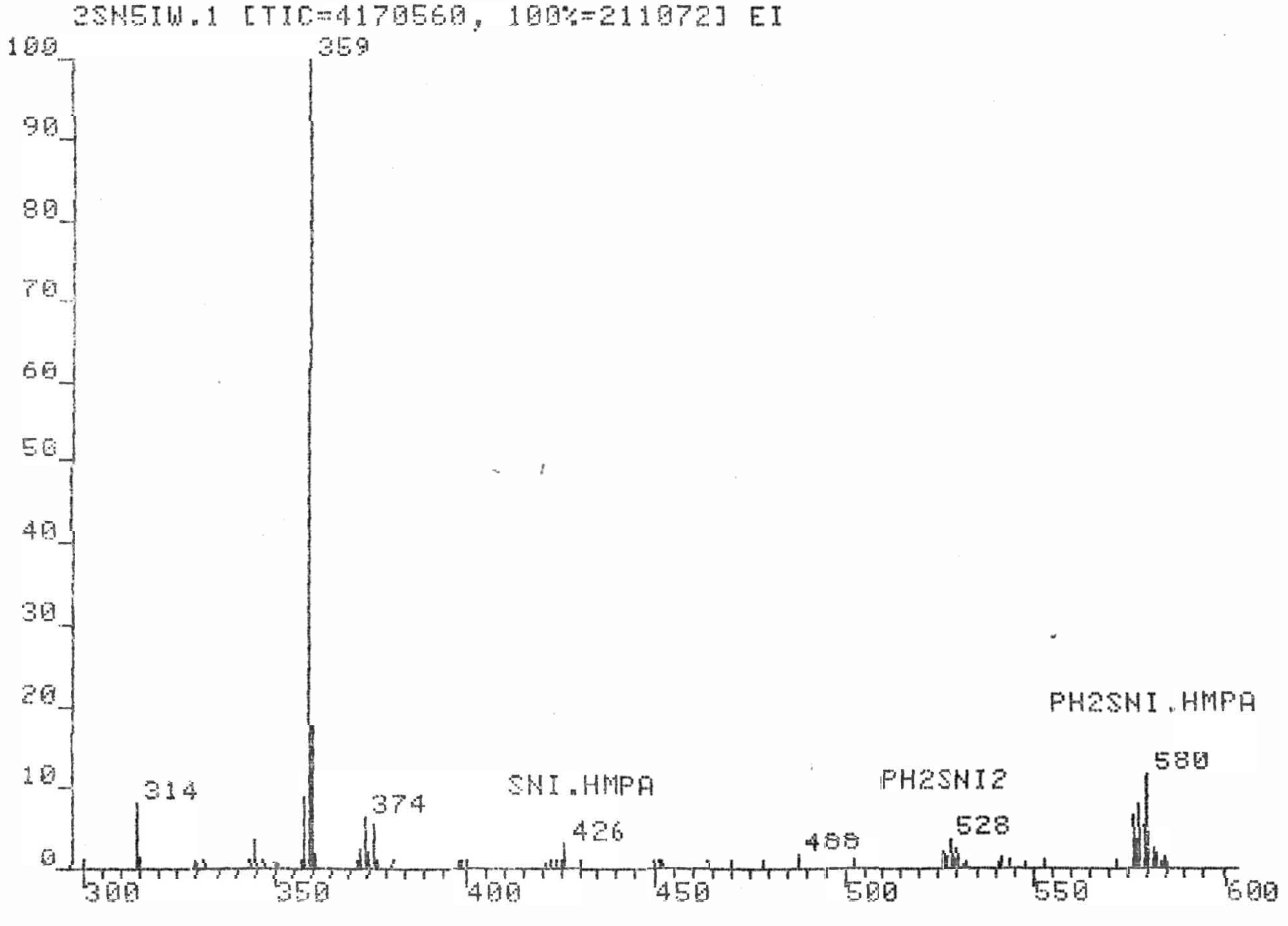
2SN5IW.1 [TIC=4170560, 100%=211072] EI
359
PH2SNI.HMPA
580
314
SNI.HMPA
374
PH2SNI2
426
528

Figure 18

Possible fragmentation schemes for the series $Ph_2SnX_2.2HMPA$

(A) $Ph_2SnX_2.2HMPA$ (EI)

(B) $Ph_2SnX_2.2HMPA$ (FAB)

(A)

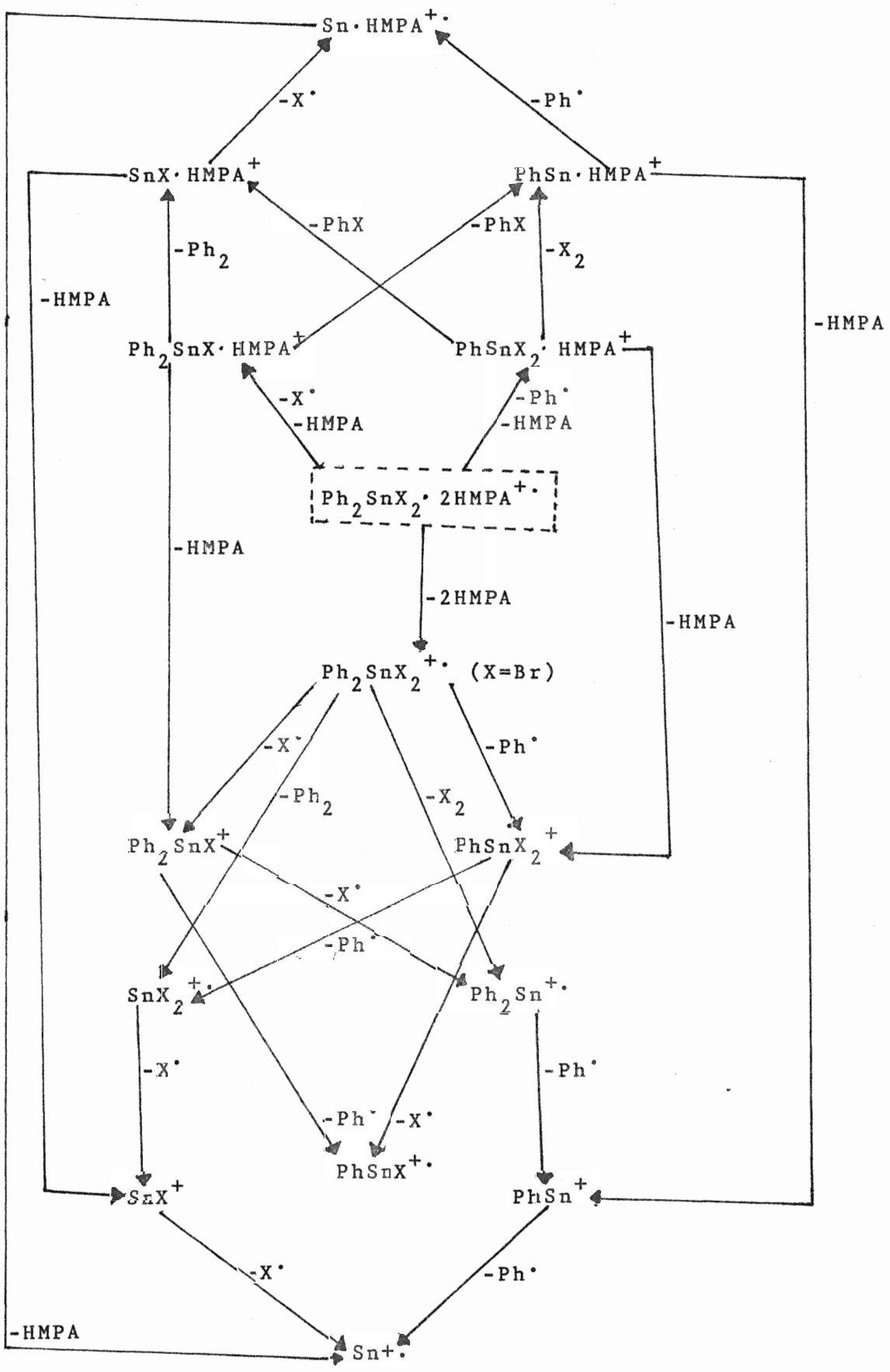
Sn·HMPA+·
-X·
-Ph·
SnX·HMPA+
PhSn·HMPA+
-PhX
-PhX
-Ph2
-X2
-HMPA
-HMPA
Ph2SnX·HMPA+
PhSnX2·HMPA+
-X·
-HMPA
-Ph·
-HMPA
Ph2SnX2·2HMPA+·
-HMPA
-2HMPA
-HMPA
Ph2SnX2+· (X=Br)
-X·
-Ph·
-Ph2
-X2
Ph2SnX+
PhSnX2+
-X·
-Ph·
SnX2+·
Ph2Sn+·
-X·
-Ph·
-Ph·
-X·
PhSnX+·
SnX+
PhSn+
-X·
-Ph·
-HMPA
Sn+·

(B)

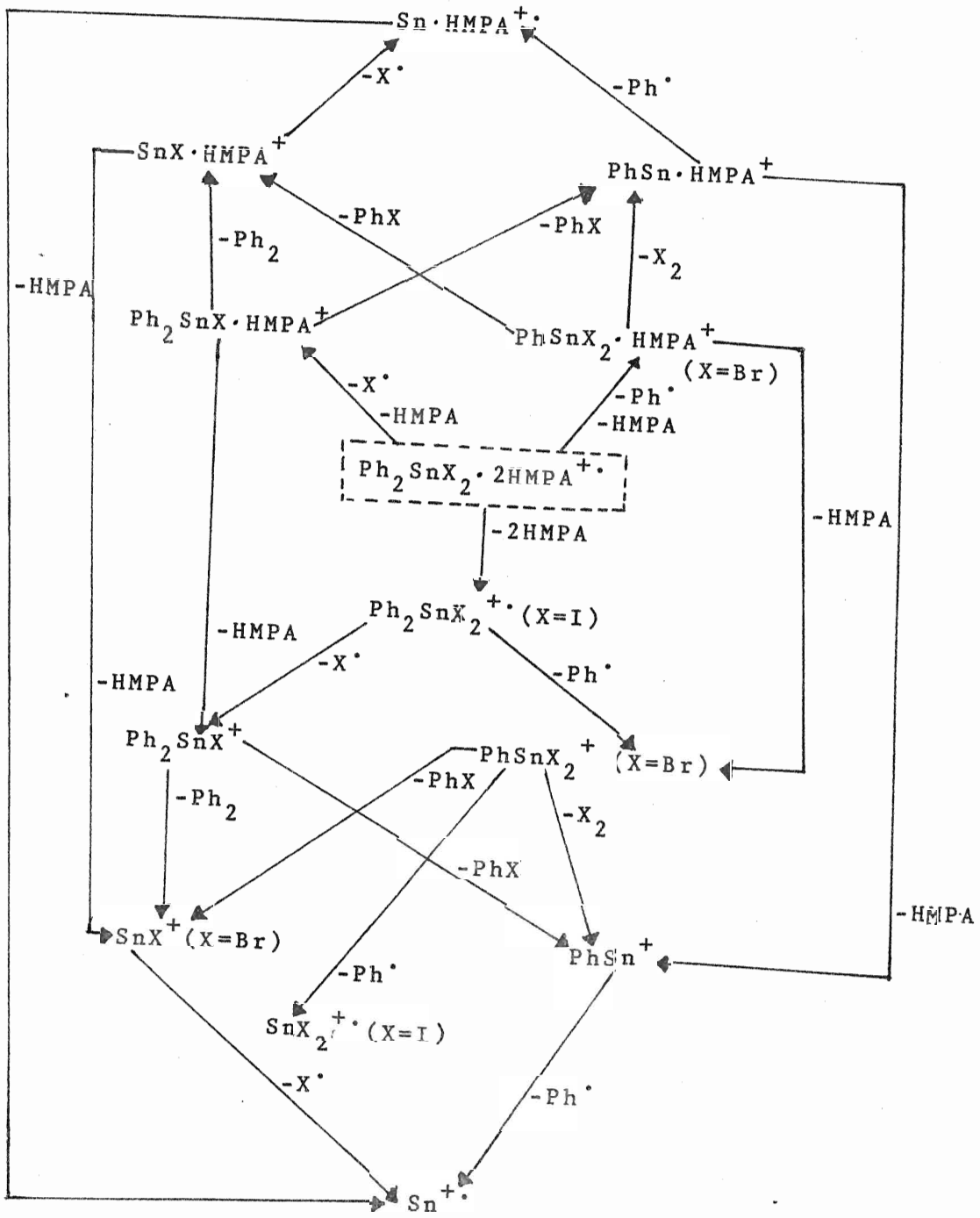
Sn·HMPA+·
-X·
-Ph·
SnX·HMPA+
PhSn·HMPA+
-PhX
-PhX
-Ph2
-X2
-HMPA
Ph2SnX·HMPA+
PhSnX2·HMPA+
(X=Br)
-X·
-HMPA
-Ph·
-HMPA
Ph2SnX2·2HMPA+·
-2HMPA
-HMPA
Ph2SnX2+· (X=I)
-HMPA
-X·
-Ph·
-HMPA
Ph2SnX+
PhSnX2+ (X=Br)
-PhX
-Ph2
-X2
-PhX
-HMPA
SnX+ (X=Br)
PhSn+
-Ph·
SnX2+· (X=I)
-X·
-Ph·
Sn+·

Figure 18a

Comparison of EI and FAB data

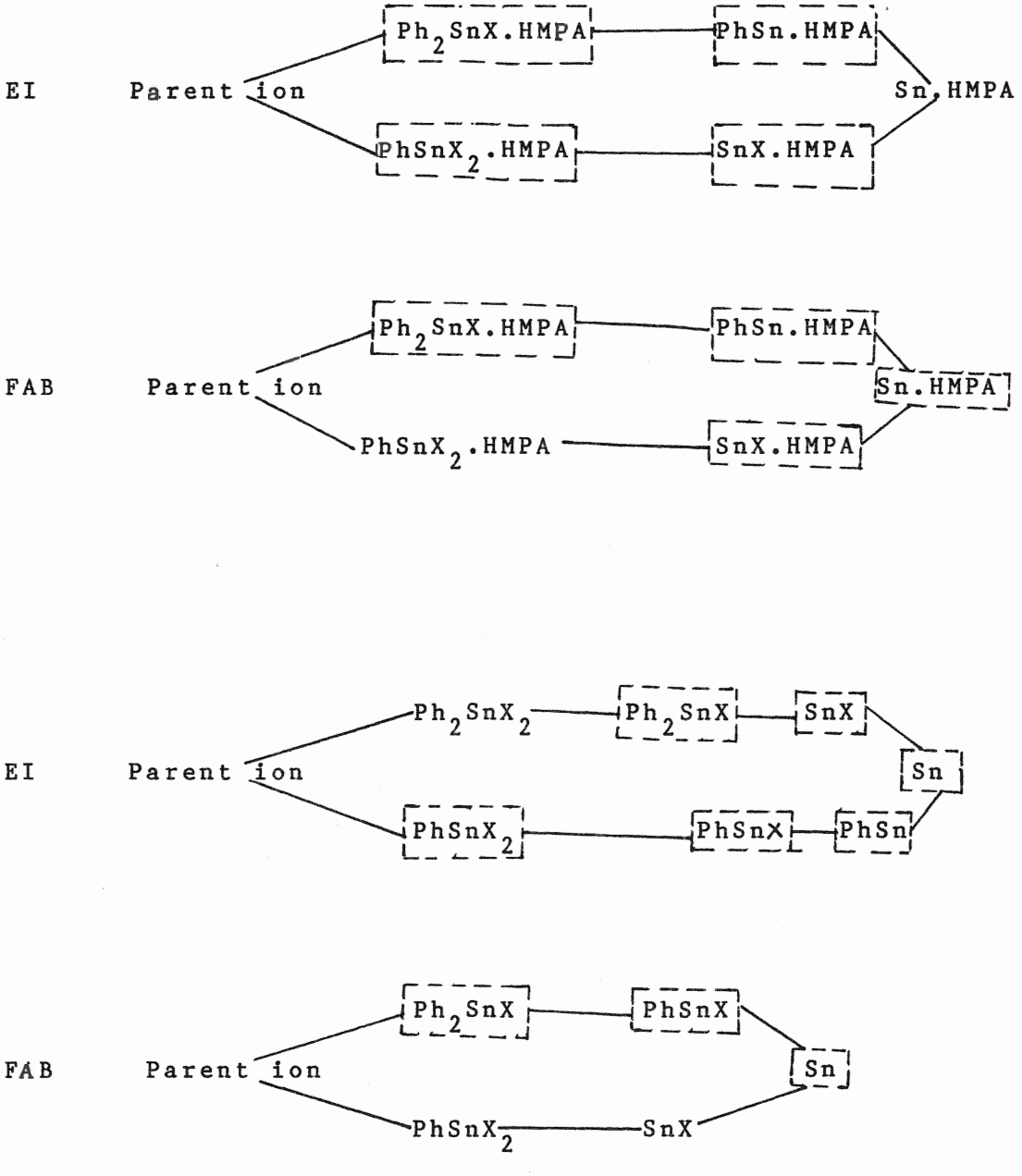

(3) FAB-MS of $(C_6H_5)_4Sn$

When Ph_4Sn was analysed by FAB in HMPA matrix, neither tin-containing organic fragments nor bare tin clusters were detected and there was no evidence of co-ordination of tin with HMPA. This proves that the addition of an extra HMPA to Ph_3Sn and Ph_2Sn species in the FAB mass spectra of Ph_3SnX.HMPA (X = Cl, Br) and Ph_2SnCl_2HMPA is not an artifact of FAB technique. On the other hand, the same type of fragmentation pattern was observed for the non-Lewis acid Ph_4Sn in a non-protonating, non-ionizing matrix like sulfolane or NPOE, as was seen in the EI spectra reported earlier [55]. Sulfolane behaved as the better matrix in this case. The spectra showed Ph_3Sn co-ordinated to sulfolane to give a stable ion cluster of Ph_3Sn.sulfolane.

Partial positive ion FAB mass spectrum of this compound is presented in Figure 19.

(4) <u>Comparison of the EI and positive ion FAB mass spectra of some phenyllead halide adducts with hexamethylphosphoramide</u>

The different series of compounds that were studied are listed below:

(i) Ph_3PbX.HMPA (X = Cl, Br, I)

(ii) Ph_2PbX_2.HMPA (X = Br, I)

(iii) Ph_2PbX_2.2HMPA X = Cl, Br, I)

These compounds have previously been the subject of EI studies by Wharf et al. [43] using the same MS-30 mass spectrometer as we are using.

Figure 19

Positive ion FAB mass spectrum of $(C_6H_5)_4Sn$

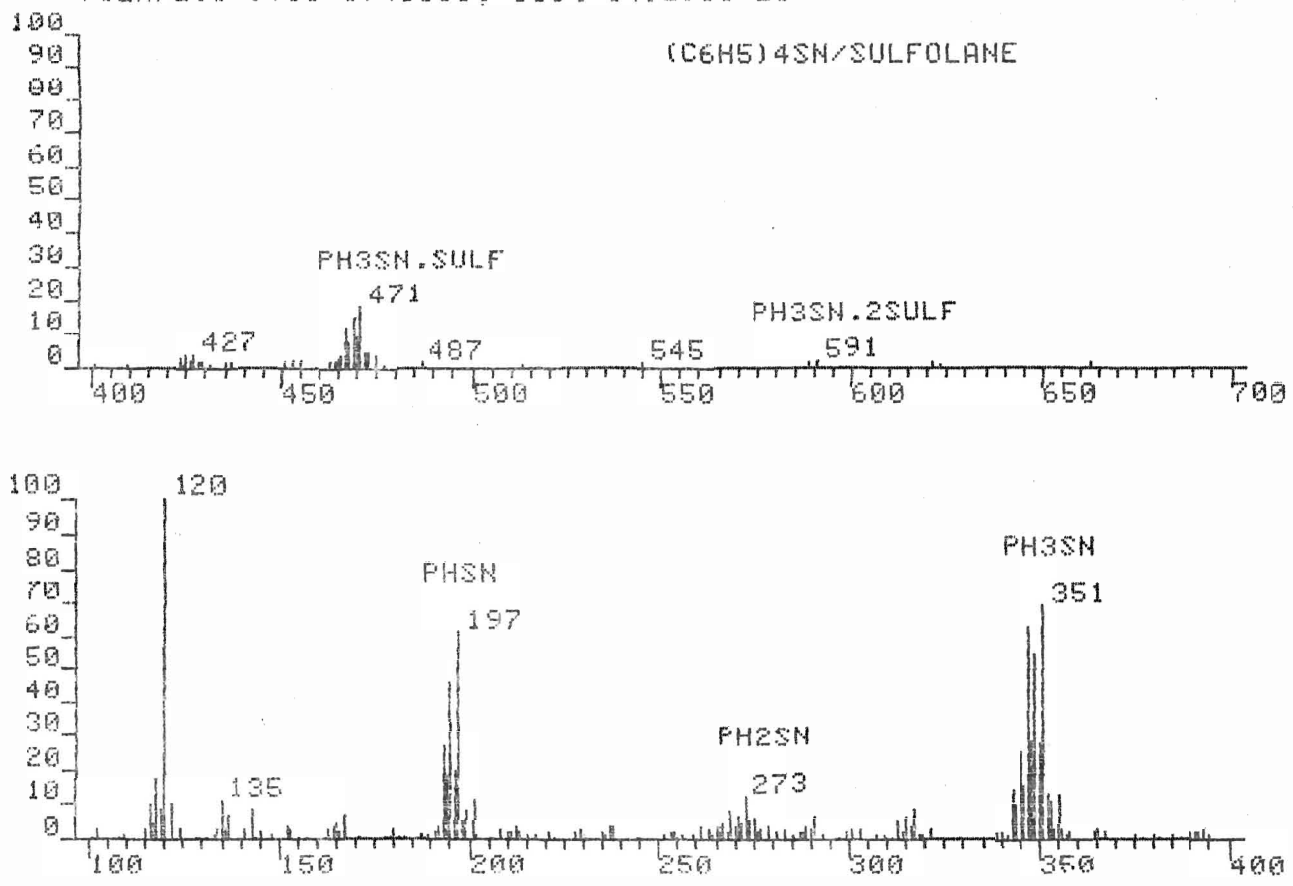
712AF2.1 [TIC=1740160, 100%=149296] EI
(C6H5)4SN/SULFOLANE
PH3SN.SULF
471
427
487
545
PH3SN.2SULF
591
120
PHSN
197
135
PH2SN
273
PH3SN
351

Partial EI and FAB mass spectra of the lead-containing ions of series (i), (ii) and (iii) are given in Tables VII, VIII and IX, respectively.

(i) $Ph_3PbX.HMPA$ (X = Cl, Br, I)

More than fifty percent of the ion current is carried by $HMPA^+$ and its fragments, analogous to those of the tin-containing compounds in both EI and FAB. The protonated dimers of $HMPA^+$ carry over twenty percent of the ion current in most of the FAB spectra of these compounds. $HMPA^+$ containing lead fragments (without the halogens) are comparatively more intense in the high mass end of the FAB spectra. A survey of the intensity patterns of tin- and lead-containing ions tells us that lead bonds more strongly with HMPA than tin in the FAB spectra. However, the probability of formation of this bond by recombination in the mass spectrometer was also predicted for these lead-containing compounds [43]. All the singly co-ordinated $Pb.HMPA^+$ species are possibly formed by the loss of halogens or phenyls from the parent molecular ions. The fragmentation patterns of lead-containing ions follow the general trend observed in the mass spectra of the organo-metallics of Group (IV) elements [54] by yielding highly abundant even electron ions such as Ph_2PbX^+, Ph_3Pb^+, PbX^+ and $PhPb^+$. Although Ph_3Pb^+ and $PhPb^+$ appear as prominent species, the halogenated lead-containing ions are not visible in FAB spectra. It is interesting to note that this agrees with the order of decrease of the M-X bond energies: Si-X > Ge-X > Sn-X > Pb-X [57]. The only abundant

Table VII.

Comparison of EI and +FAB Data

(lead-containing ions)*

	EI ($Ph_3PbX.HMPA$)			FAB		
ION^+	X = Cl	X = Br	X = I	X = Cl	X = Br	X = I
$Ph_2PbX.HMPA$	1.4	0.3	--	--	--	--
$Ph_3Pb.HMPA$	0.5	0.1	0.2	6.0	13.0	2.0
PhPb.HMPA	0.5	0.1	--	6.4	10.6	5.8
PbX.HMPA	1.4	0.4	--	--	--	2.5
Pb.HMPA	1.4	0.5	--	18.4	14.9	32.5
Ph_2PbX	16.6	22.9	0.9	--	--	--
Ph_3Pb	11.4	6.0	28.0	9.3	19.4	5.6
PhPbX	--	0.9	--	--	--	--
Ph_2Pb	--	0.9	--	--	--	--
PbX	23.7	22.0	9.9	--	--	--
PhPb	14.2	17.9	32.0	9.9	17.8	--
Pb	28.9	28.0	29.0	49.9	24.2	51.4

* percentage of the total absolute intensity of the metal-containing ions.

odd electron ion in EI is Pb^+ itself with approximately the same intensity in all three halides which is greater than twenty-five percent. In FAB, it exhibits much higher abundance and the intensity pattern does not change, even after its co-ordination with HMPA. The resemblance in the behaviours of the Lewis acid fragments with their HMPA-co-ordinated counterparts leads us to suspect that the former ions are most probably formed from the corresponding HMPA-containing parent ions by the loss of HMPA. No parent Lewis acid is observed either in EI or in FAB. The intensity patterns of these HMPA adducts of lead are almost the same as those suggested for tin-containing ions in EI [45]. However, fragmentation patterns of the adducts of tin and lead do present some inconsistencies in FAB. The intensity of Ph_3Pb^+ for Ph_3PbX.HMPA decreases from X = Cl to X = Br and then increases for X = I; whereas in FAB the reverse trend is observed.

The positive FAB mass spectra of these compounds are given in Figures 20-22 and the probable fragmentation schemes are described in Figure 23.

Figure 20

Positive ion FAB mass spectrum of $Ph_3PbCl.HMPA$

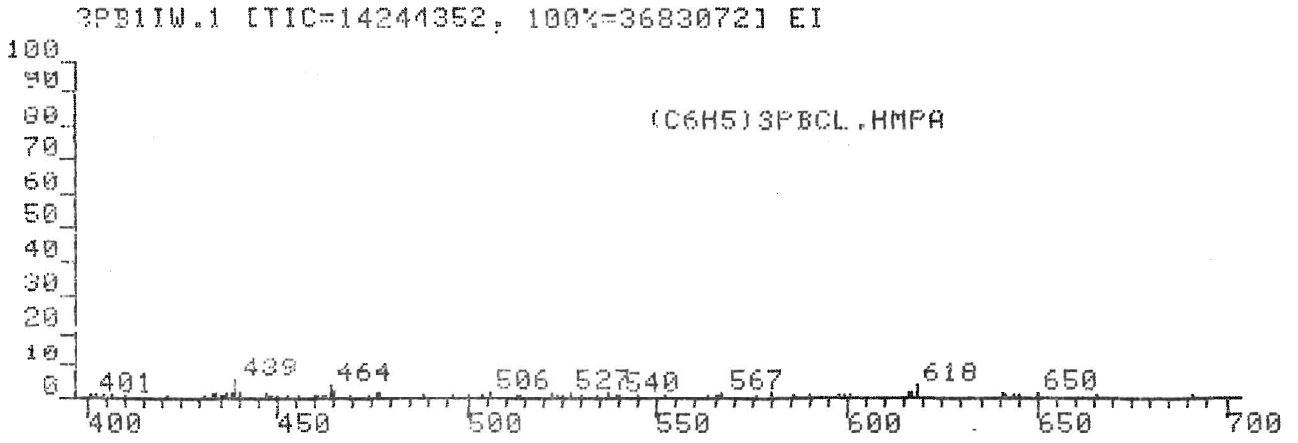
3PB1IW.1 [TIC=14244352, 100%=3683072] EI
(C6H5)3PBCL.HMPA
401
439
464
506
527
540
567
618
650

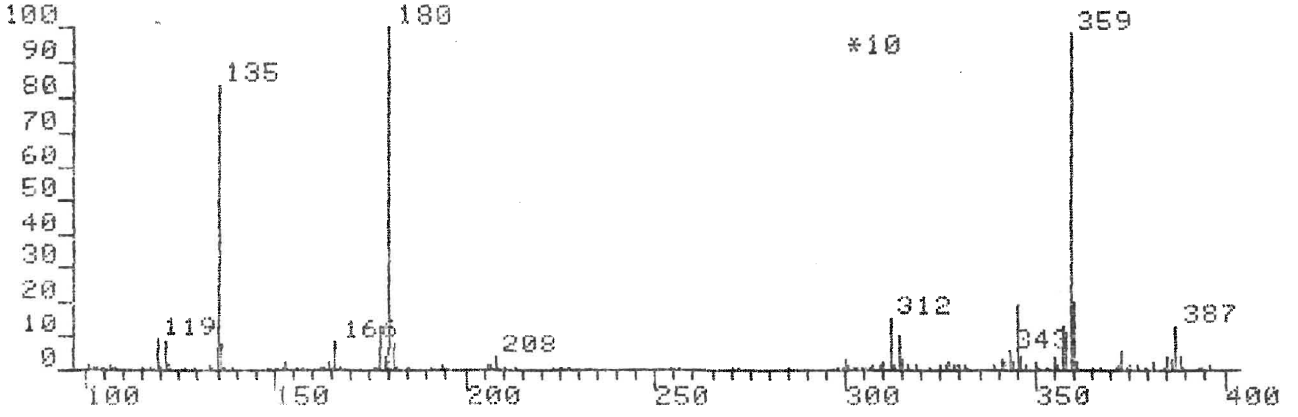
180
135
*10
359
119
208
312
343
387

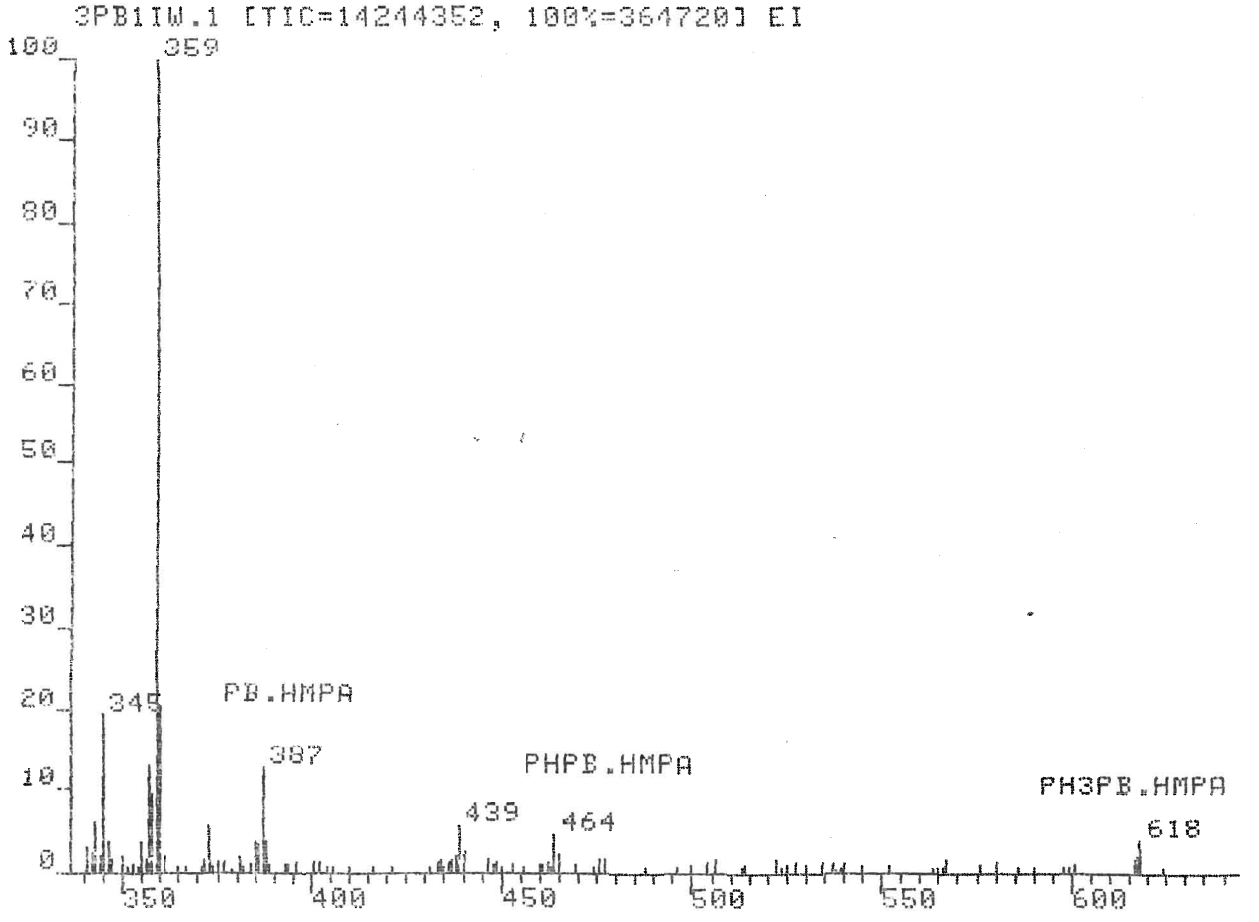
3PB1IW.1 [TIC=14244352, 100%=364720] EI
359
345
PB.HMPA
387
PHPB.HMPA
439
464
PH3PB.HMPA
618

Figure 21

Positive ion FAB mass spectrum of $Ph_3PbBr.HMPA$

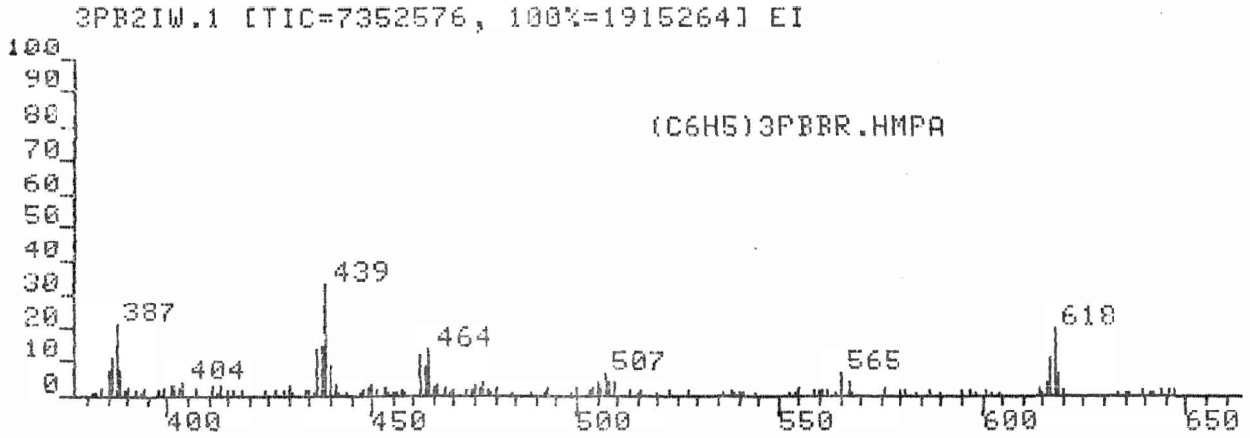
3PB2IW.1 [TIC=7352576, 100%=1915264] EI
(C6H5)3PBBR.HMPA
387
404
439
464
507
565
618

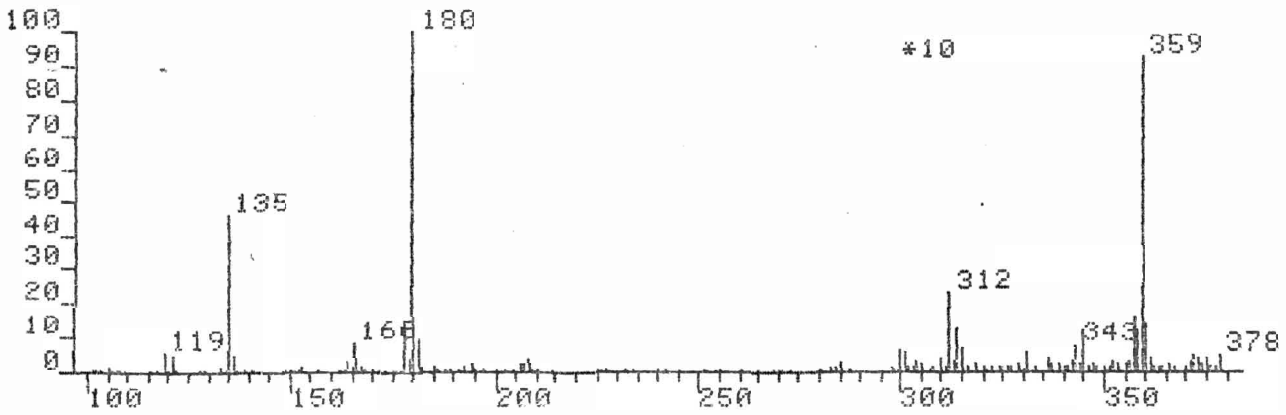
*10
119
135
166
180
312
343
359
378

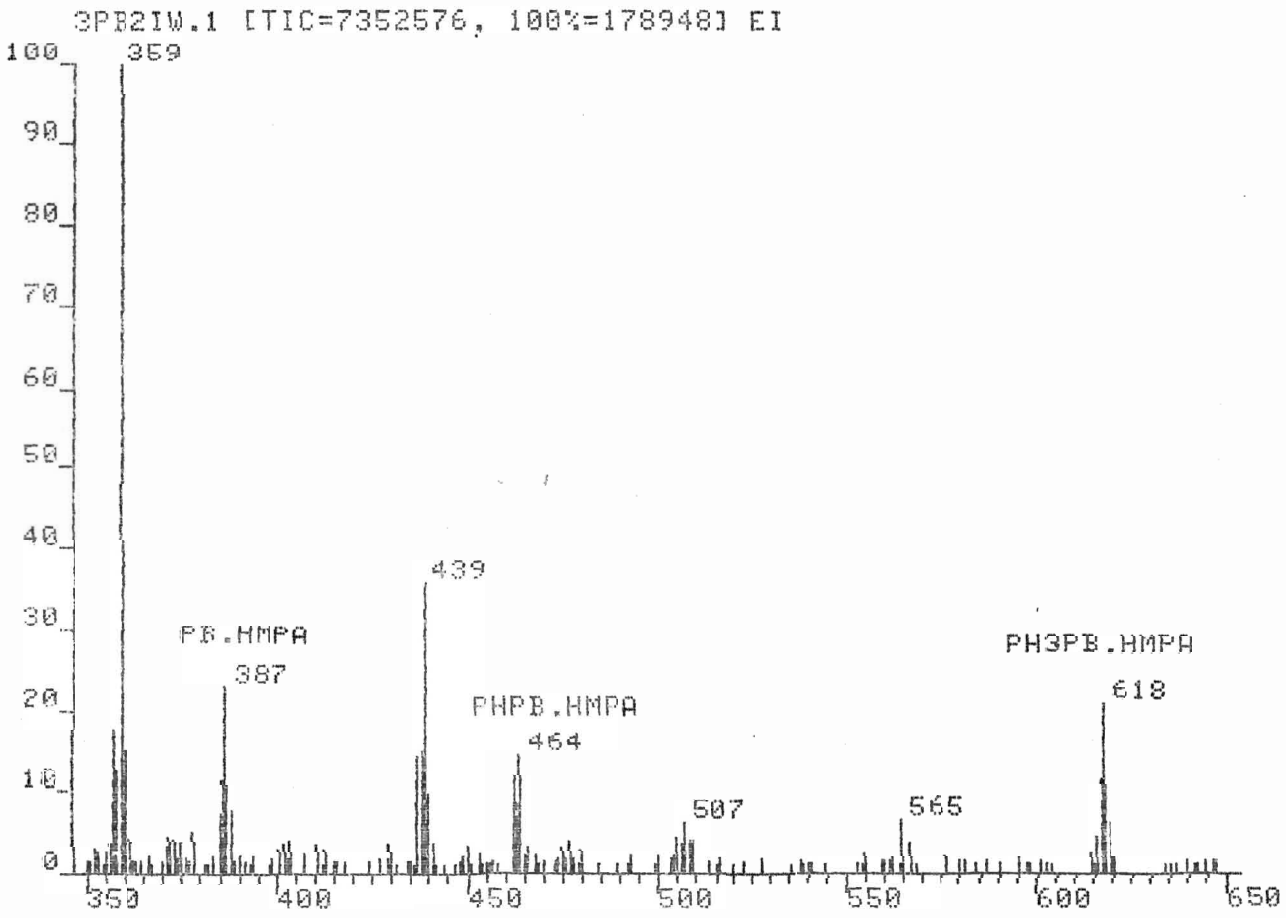
3PB2IW.1 [TIC=7352576, 100%=178948] EI
PB.HMPA
387
PHPB.HMPA
439
464
507
565
PH3PB.HMPA
618
359

Figure 22

Positive ion FAB mass spectrum of $Ph_3PbI.HMPA$

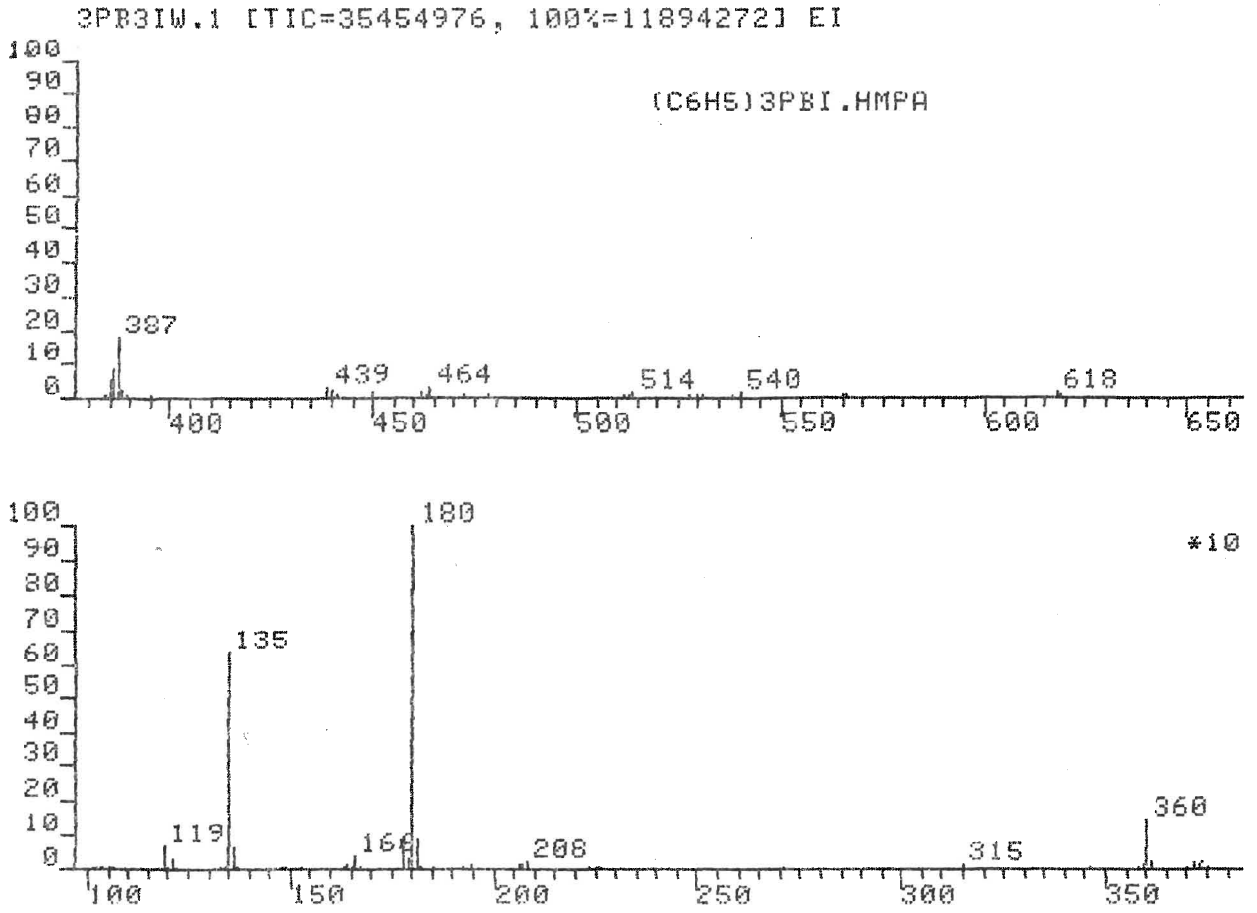
3PB3IW.1 [TIC=35454976, 100%=11894272] EI
(C6H5)3PBI.HMPA
387
439
464
514
540
618
*10
180
135
119
160
208
315
360

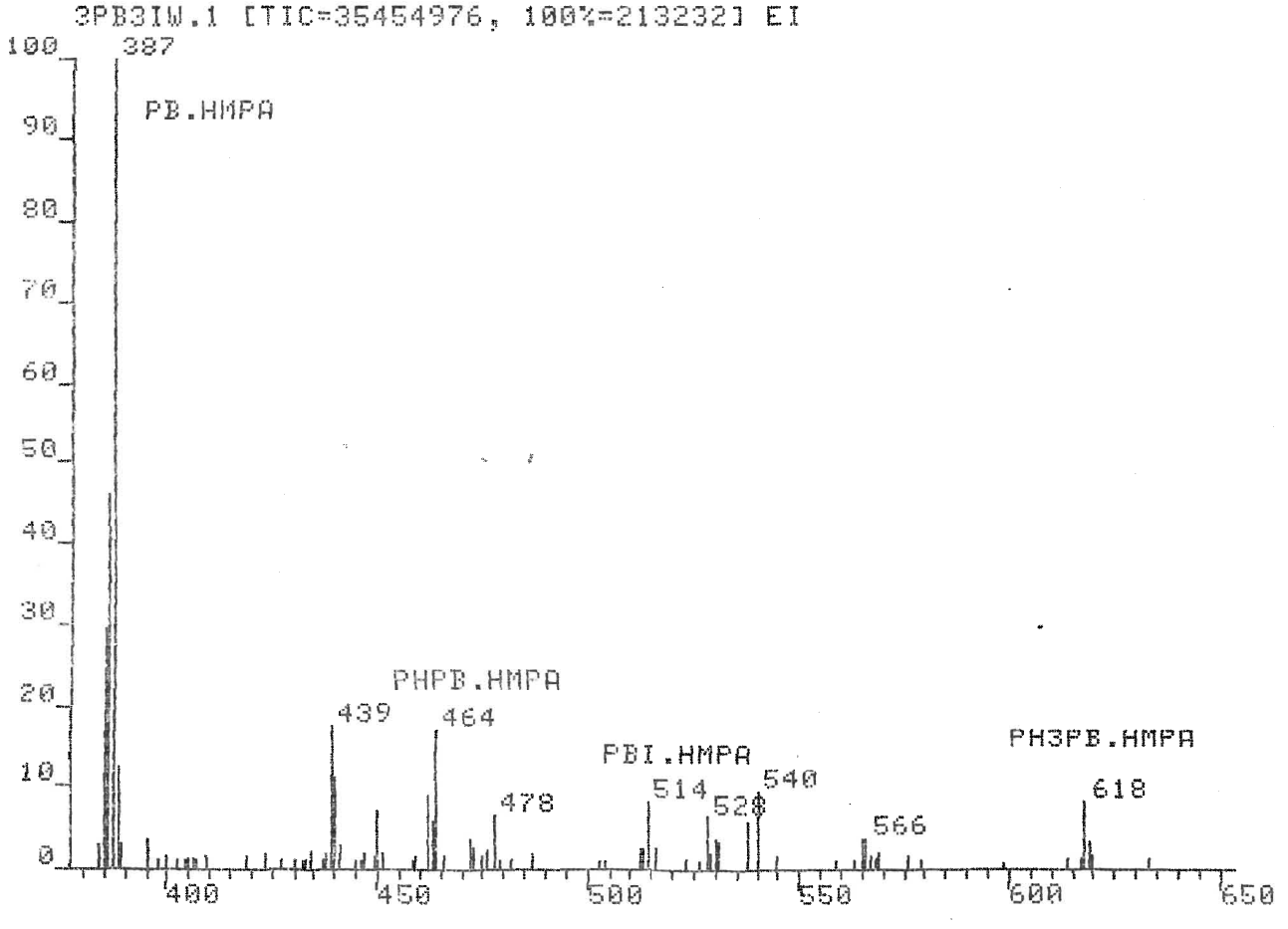
3PB3IW.1 [TIC=35454976, 100%=213232] EI
387
PB.HMPA
PHPB.HMPA
439
464
478
PBI.HMPA
514
528
540
566
PH3PB.HMPA
618

Figure 23

Probable fragmentation schemes for the series $Ph_3PbX.HMPA$ (X = Cl, Br, I)

(A) $Ph_3PbX.HMPA$ (EI)

(B) $Ph_3PbX.HMPA$ (FAB)

(A)

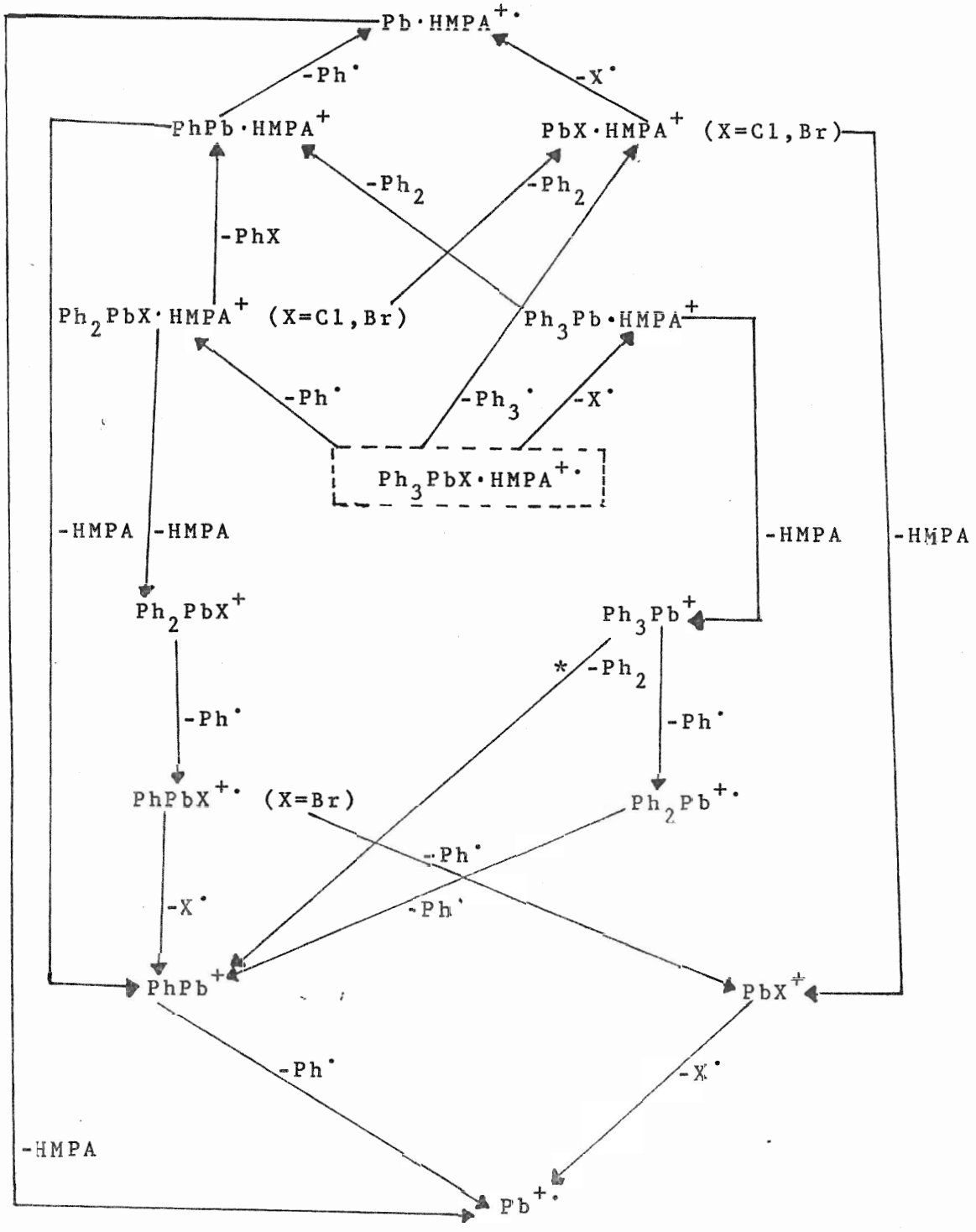

* metastable-confirmed transition [56]

(B)

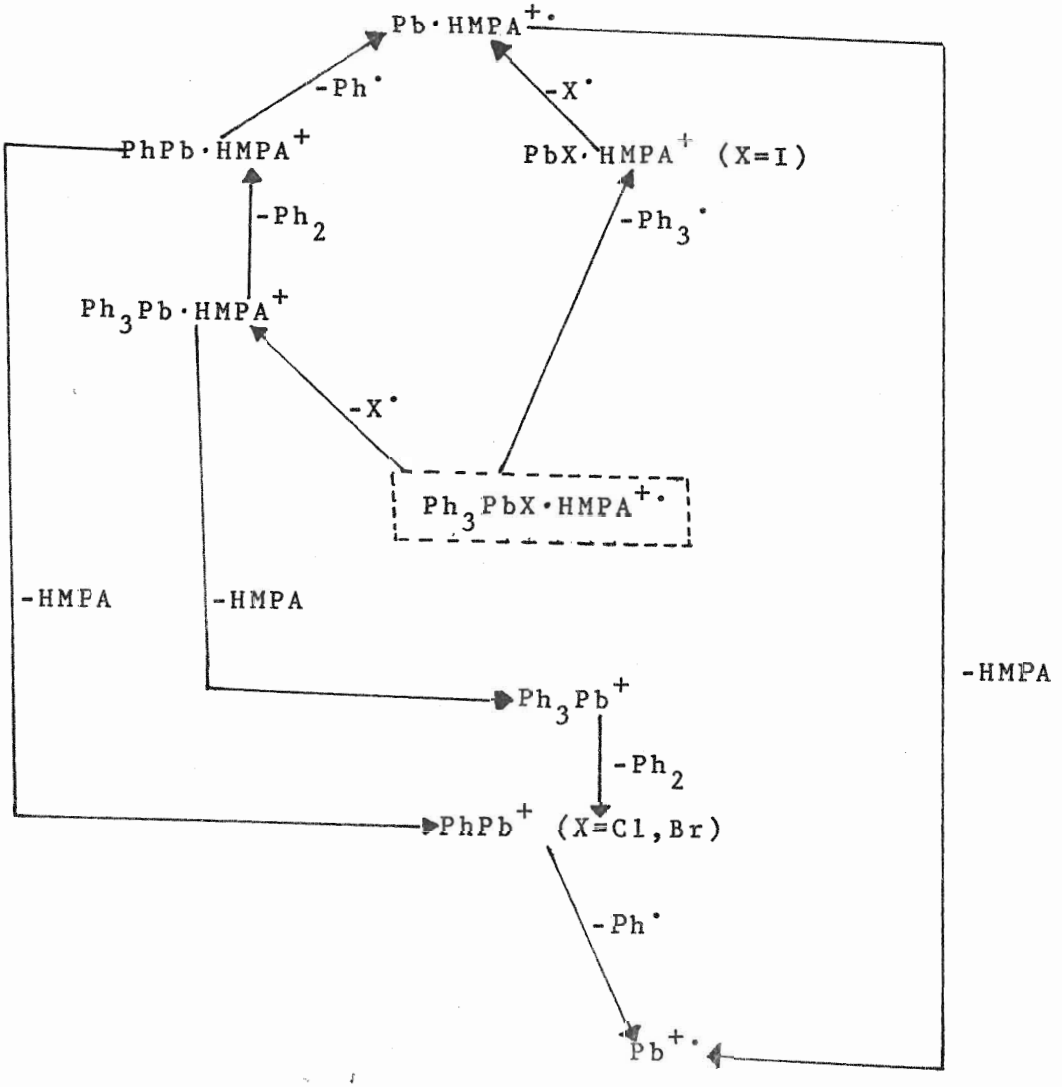
Pb·HMPA+·
-Ph·
-X·
PhPb·HMPA+
PbX·HMPA+ (X=I)
-Ph2
-Ph3·
Ph3Pb·HMPA+
-X·
Ph3PbX·HMPA+·
-HMPA
-HMPA
-HMPA
Ph3Pb+
-Ph2
PhPb+ (X=Cl,Br)
-Ph·
Pb+·

Figure 23a

Comparison of EI and FAB data

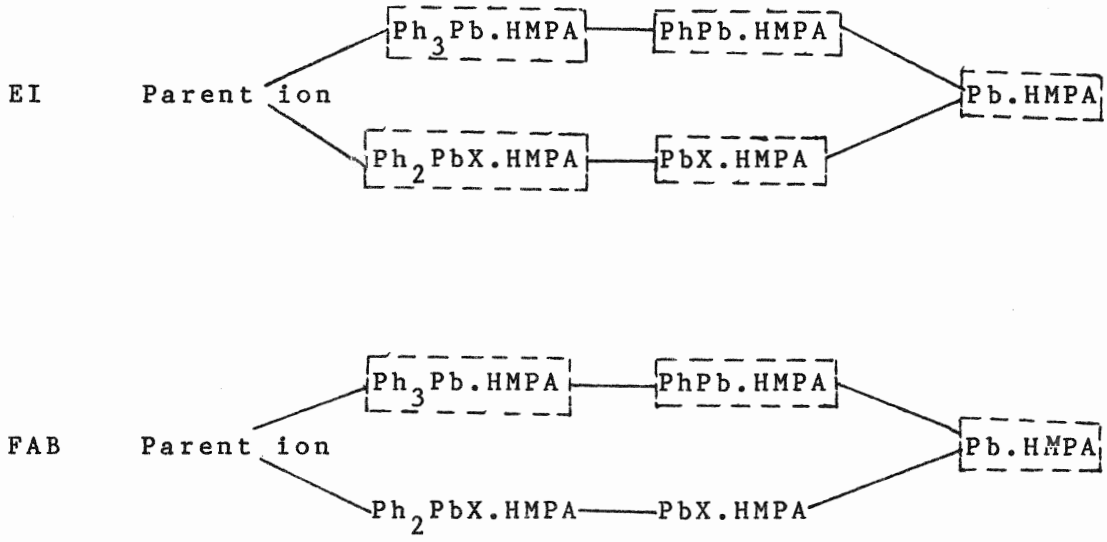

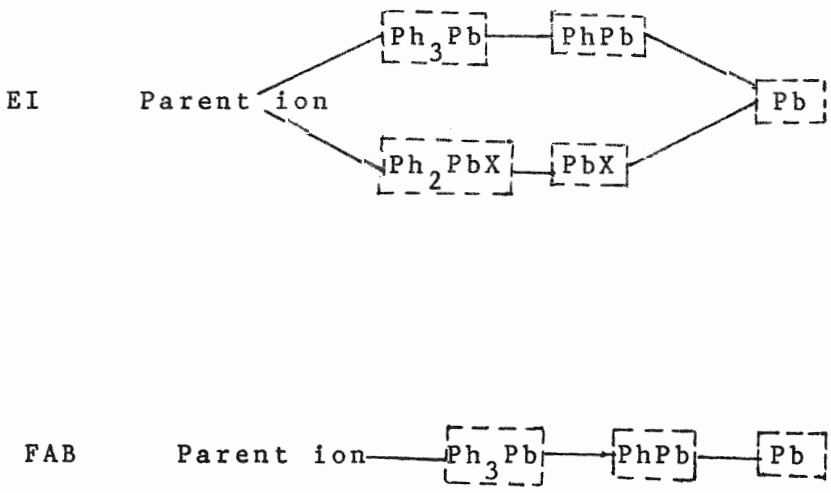

Table VIII.

Comparison of EI and +FAB Data

(lead-containing ions)*

	EI (Ph_2PbX_2.HMPA)		FAB	
Ion^+	X = Br#	X = I	X = Br#	X = I
Ph_2PbX.HMPA	0.4	0.5	4.8	--
PbX.HMPA	0.6	1.1	5.8	6.0
Pb.HMPA	0.4	1.7	8.3	25.3
PbX.2HMPA	--	--	--	1.4
PhPb.HMPA	--	--	9.3	3.0
Ph_3Pb.HMPA	--	--	5.9	--
Ph_2PbX_2	0.2	--	--	--
Ph_2PbX	17.8	11.2	--	--
$PhPbX_2$	4.3	0.3	--	--
PhPbX	0.6	0.6	--	--
PhPb	6.4	14.6	23.6	--
PbX_2	2.5	5.6	--	--
PbX	33.0	25.4	6.7	--
Pb	33.8	39.0	35.5	62.4

* percentage of the total absolute intensity of the metal-containing ions.

the compound is decomposed probably.

(ii) Ph_2PbX_2.HMPA (X = Br, I)

HMPA-containing lead ions are more prominent in FAB. In addition to other ions of higher masses common to both techniques, the ions $PbX.2HMPA^+$, $PhPb.HMPA^+$ and $Ph_3Pb.HMPA^+$ appear in FAB spectra. It is suspected that the presence of $Ph_3Pb.HMPA^+$ (when X = Br) only in FAB is due perhaps to some impurities in the compound (Ph_2PbBr_2.HMPA), but this has not yet been confirmed. A parent Lewis acid ion is observed in the EI spectra for the compound Ph_2PbBr_2.HMPA and the even electron ions such as Ph_2PbX^+, $PhPbX_2^+$, $PhPb^+$, PbX^+ are more pronounced, as usual. On the other hand, in FAB only $PhPb^+$ and PbX^+ appear as stable ions when X = Br. Halogenated lead species for this series of compounds are more dominant than those for the Ph_3PbX.HMPA series. This is probably indicatiave of the lower solvation of these compounds in HMPA-glycerol matrix. FAB as well as EI yields highly intense lead ions and these are more stable when X = I. The same trend is also evident for the $Pb.HMPA^+$ ions. These might have been formed by the preferential loss of iodine from the halogenated lead-containing ions. Figures 24-25 present the positive mass spectra and Figure 26 the possible fragmentation schemes for these two compounds.

Figure 24

Positive ion FAB mass spectrum of Ph_2PbBr_2.HMPA

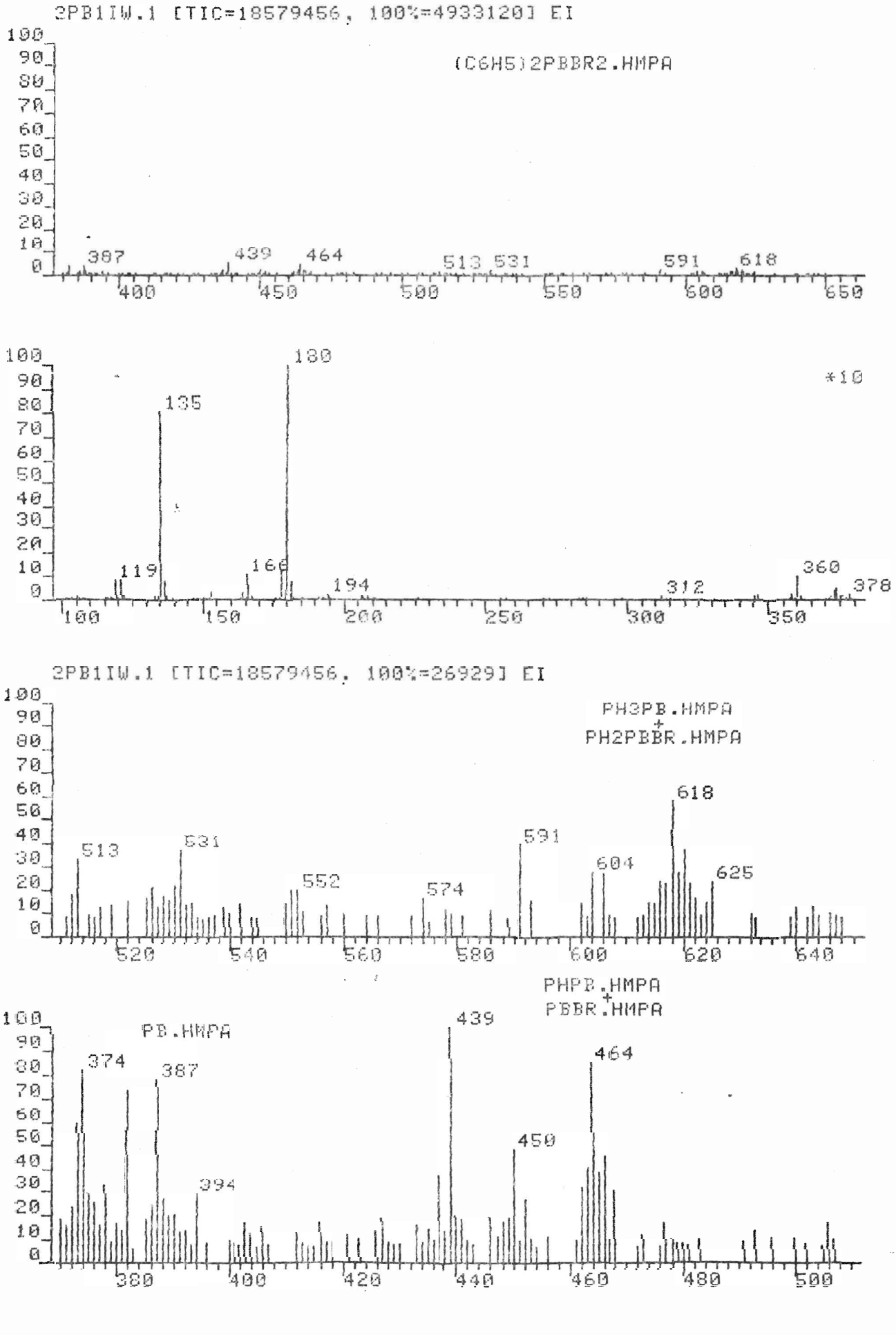
2PB1IW.1 [TIC=18579456, 100%=4933120] EI
(C6H5)2PBBR2.HMPA
387
439
464
513 531
591
618
180
135
119
166
194
312
360
378
*10
2PB1IW.1 [TIC=18579456, 100%=26929] EI
PH3PB.HMPA
+
PH2PBBR.HMPA
513
531
552
574
591
604
618
625
PHPB.HMPA
+
PBBR.HMPA
PB.HMPA
374
387
394
439
450
464

Figure 25

Positive ion FAB mass spectrum of Ph_2PbI_2.HMPA

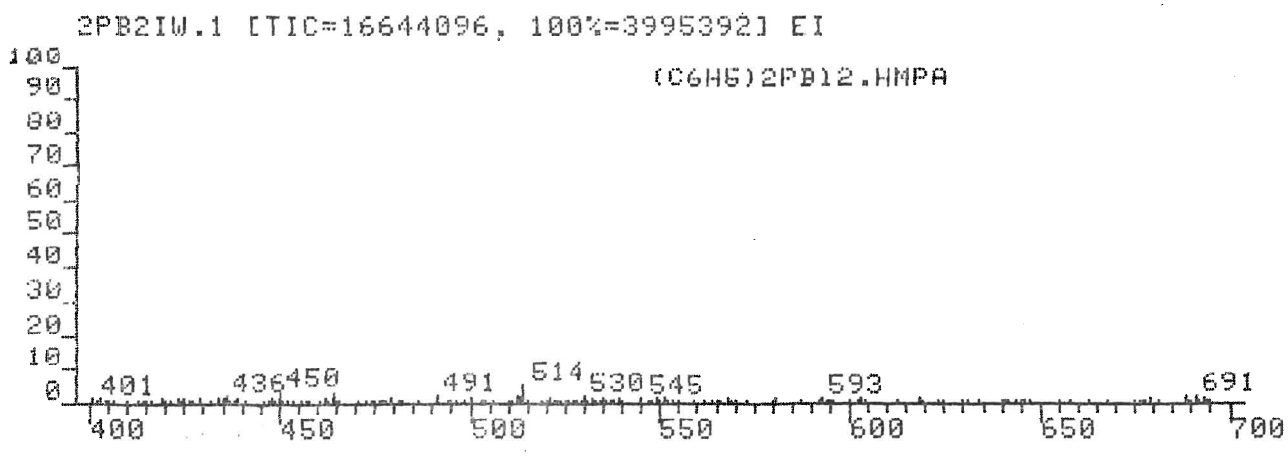
2PB2IW.1 [TIC=16644096, 100%=3995392] EI
(C6H5)2PB12.HMPA
401
436
450
491
514
530
545
593
691

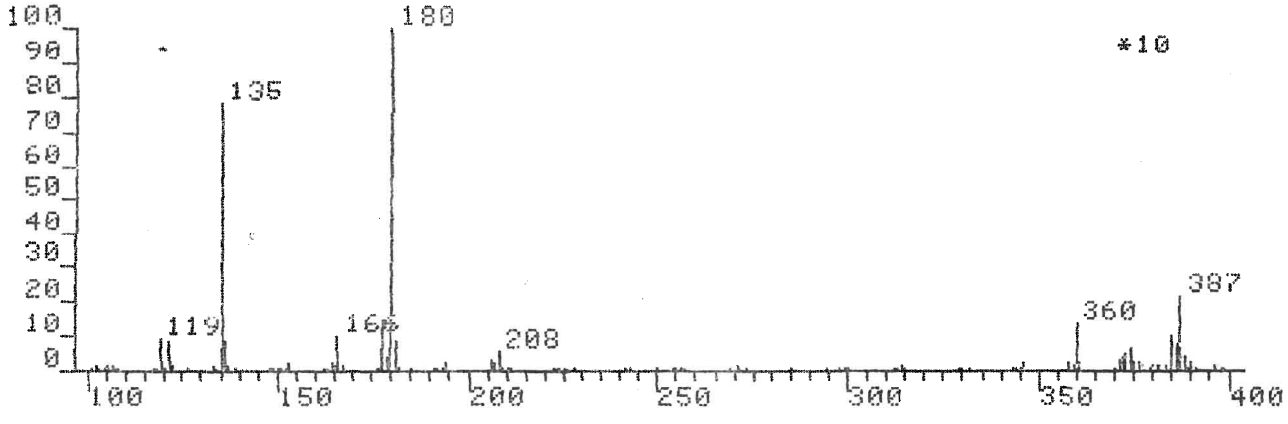
180
135
*10
119
208
360
387

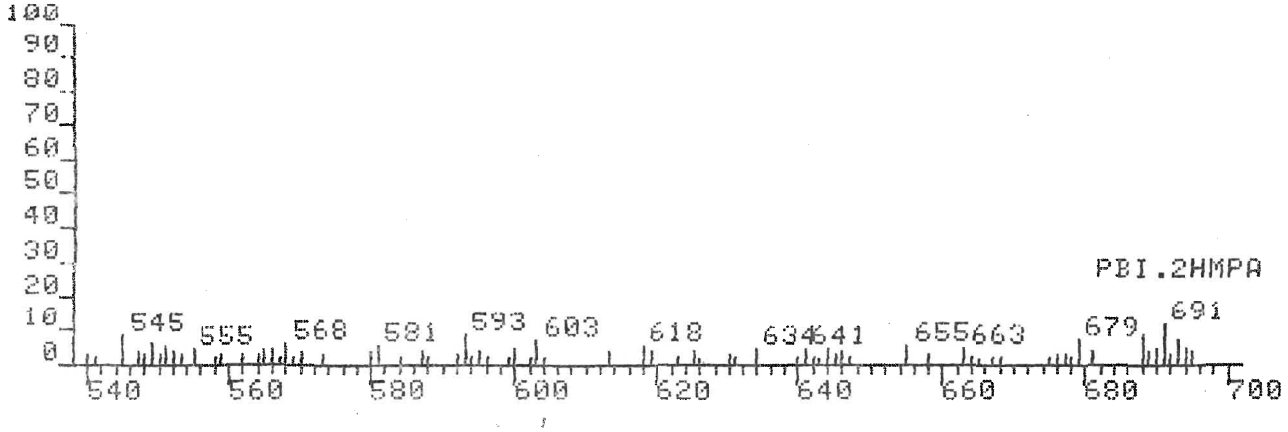
2PB2IW.1 [TIC=16644096, 100%=86772] EI
PBI.2HMPA
545
555
568
581
593
603
618
634
641
655
663
679
691

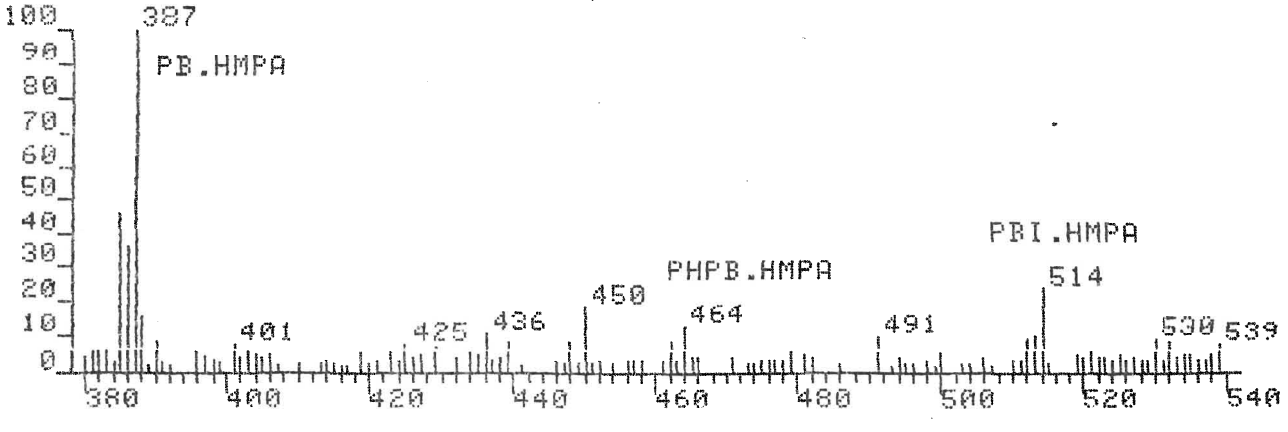
387
PB.HMPA
PBI.HMPA
PHPB.HMPA
514
450
464
401
425
436
491
530
539

Figure 26

Possible fragmentation schemes for the series Ph_2PbX_2.HMPA (X = Br, I).

(A) Ph_2PbX_2.HMPA (EI)

(B) Ph_2PbX_2.HMPA (FAB)

(A)

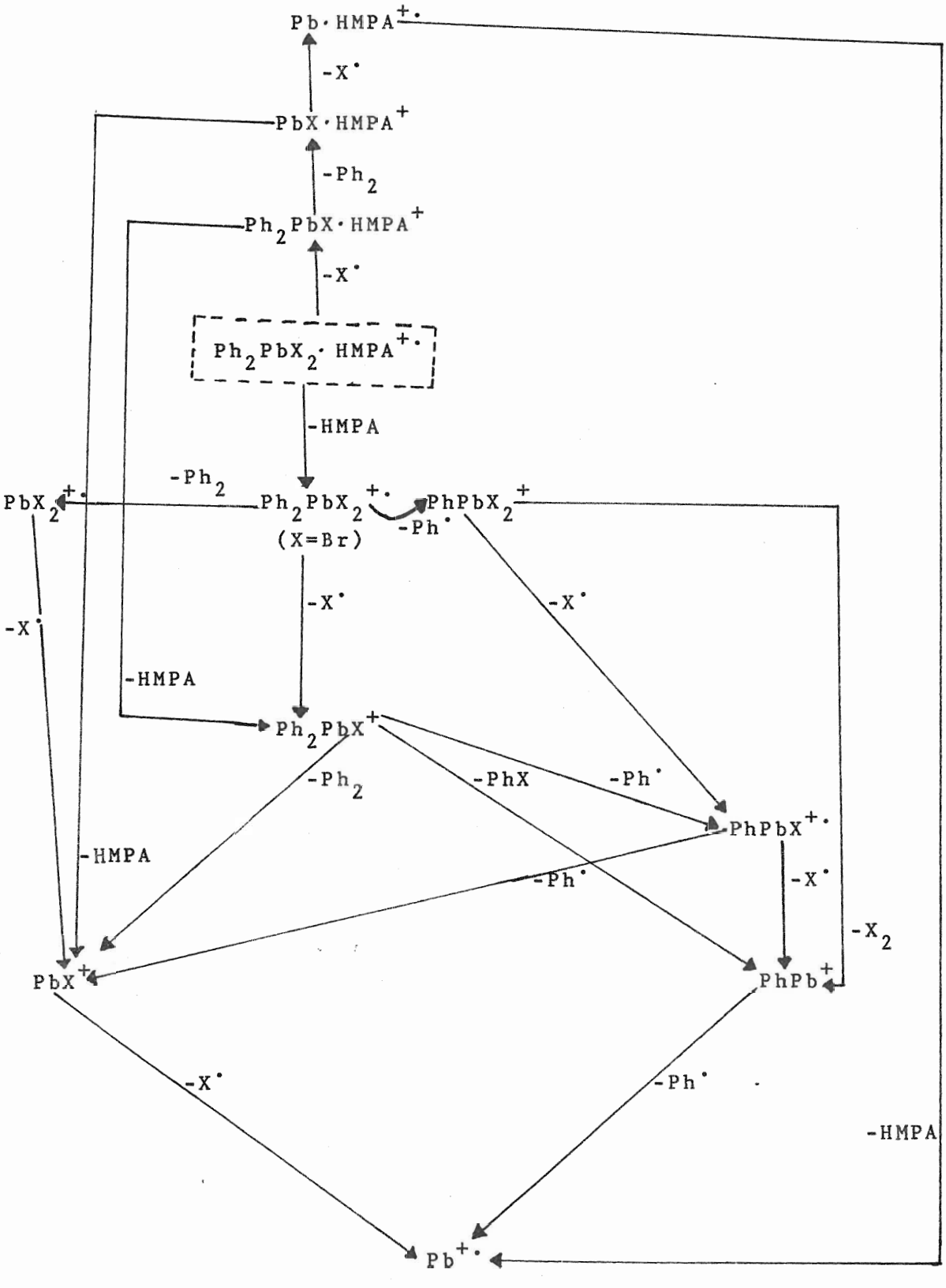
Pb·HMPA+·
-X·
PbX·HMPA+
-Ph2
Ph2PbX·HMPA+
-X·
Ph2PbX2·HMPA+·
-HMPA
-Ph2
PbX2+·
Ph2PbX2+·
(X=Br)
PhPbX2+
-Ph·
-X·
-X·
-HMPA
Ph2PbX+
-Ph2
-PhX
-Ph·
PhPbX+·
-HMPA
-Ph·
-X·
-X2
PbX+
PhPb+
-X·
-Ph·
-HMPA
Pb+·

(B)

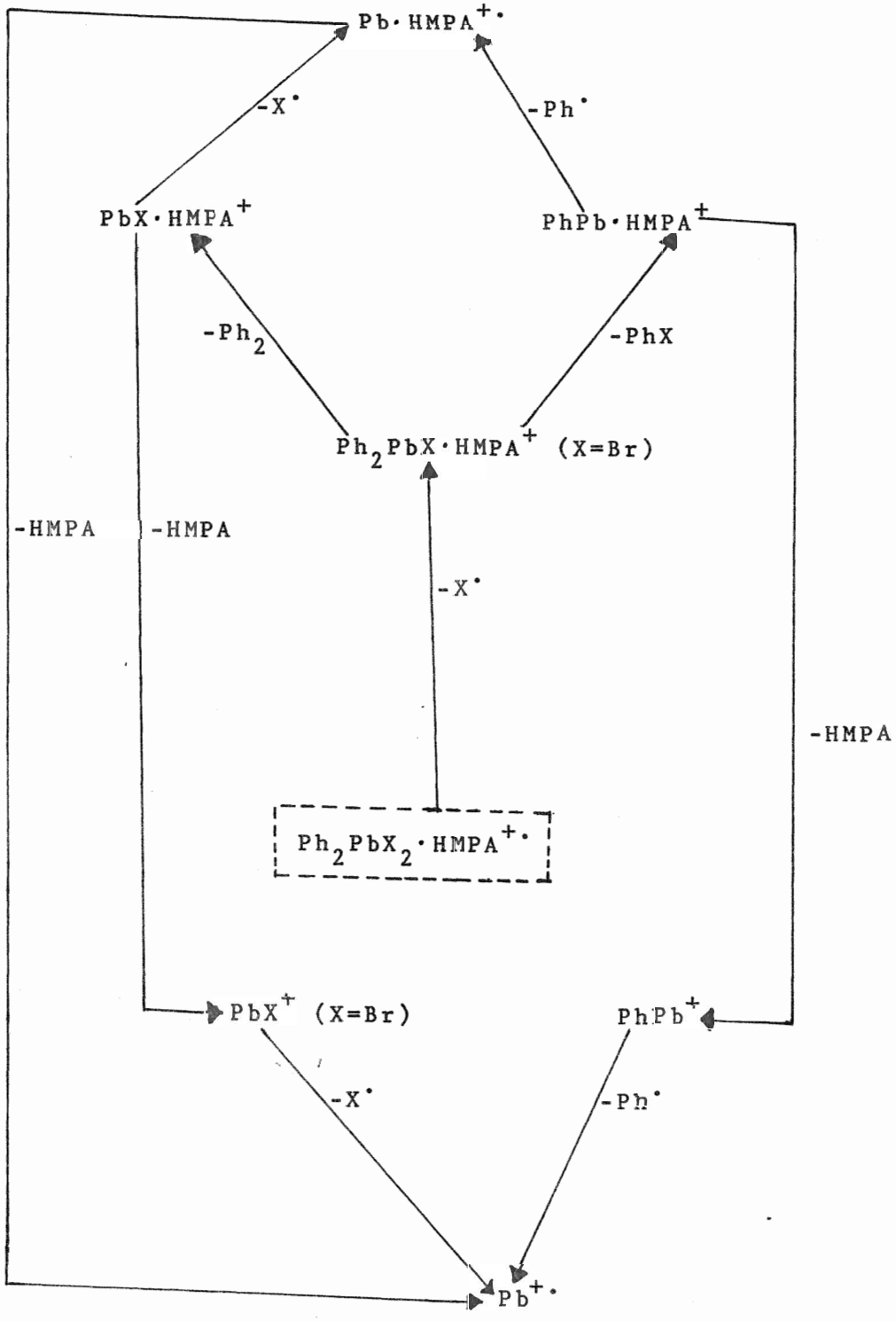
Pb·HMPA+·
-X·
-Ph·
PbX·HMPA+
PhPb·HMPA+
-Ph2
-PhX
Ph2PbX·HMPA+ (X=Br)
-HMPA
-HMPA
-X·
-HMPA
Ph2PbX2·HMPA+·
PbX+ (X=Br)
PhPb+
-X·
-Ph·
Pb+·

Figure 26a

Comparison of EI and FAB data

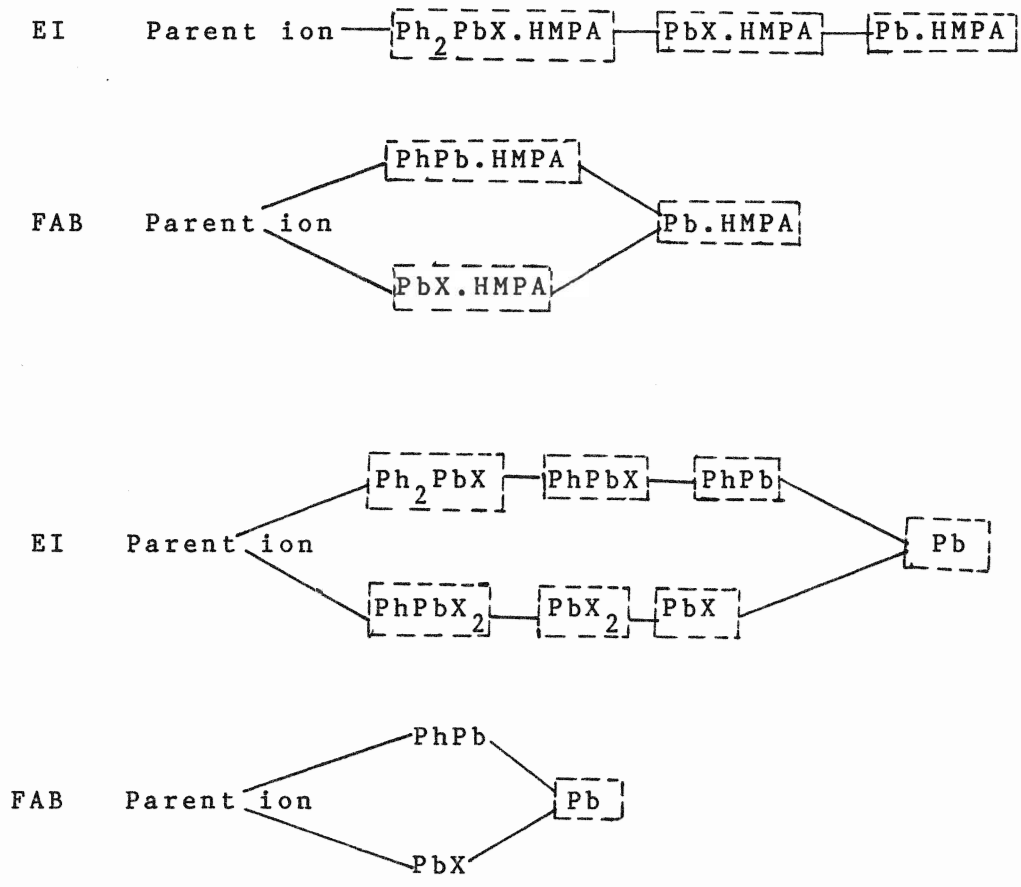

Table IX.

Comparison of EI and +FAB Data

(lead-containing ions)*

	EI (Ph_2PbX_2.2HMPA)			FAB		
ION^+	X = Cl#	X = Br#	X = I	X = Cl#	X = Br#	X = I
Ph_2PbX.HMPA	0.6	0.3	0.4	17.1	--	--
Ph_3Pb.HMPA	--	--	--	9.7	--	--
PbX.HMPA	--	0.3	1.2	11.4	--	11.9
PhPb.HMPA	--	--	--	15.7	13.0	--
PbX.2HMPA	--	--	--	--	--	8.7
Pb.HMPA	1.3	0.3	0.8	6.9	23.7	28.2
Ph_2PbX_2	--	0.3	--	--	--	--
Ph_2PbX	10.2	15.2	24.9	2.0	--	--
$PhPbX_2$	2.6	4.3	0.2	--	--	--
PhPbX	1.9	1.1	1.0	--	--	--
PhPb	9.6	4.5	10.4	20.1	14.9	5.0
PbX_2	--	8.8	7.9	--	--	--
PbX	23.1	41.7	25.0	--	--	--
Pb	50.6	23.3	21.3	16.9	48.3	46.1

* percentage of the total absolute intensity of the metal-containing ions.

these samples seem to be decomposed.

(iii) Ph_2PbX_2.2HMPA (X = Cl, Br, I)

In EI, the addition of another HMPA to the series, Ph_2PbX_2.HMPA, does not make much difference in the relative intensities and intensity patterns of the HMPA-containing lead ions and similarly in FAB most of these ions behave in the same way. The trend in ion intensities of this series is no exception to the dominance of even electron ions over the odd-electron ions in EI. Quite a significant number of lead-containing ions (without HMPA) give almost the same kind of intensities as were observed for Ph_2PbX_2.HMPA. However, in some cases the ion intensities differ. This can be exemplified by Pb^+ ions whose intensities decrease in the present case. This is probably due to the co-ordination of two HMPA molecules instead of one, to the parent Lewis acids. Whether the appearance of Ph_3Pb.HMPA ion is because of the presence of impurities in the lead compounds is not quite clear. When these spectra are compared to those of the corresponding tin compounds, it is seen that most of the EI results agree well but those of FAB vary. This is quite interesting in the sense that the modes of adduct formation by phenyltin and -lead halides are quite different from each other. Tin-ligand bond is formed by an increase in co-ordination number of the central metal atom. On the other hand, the formation of lead-ligand bond does not involve any change in co-ordination number of lead. This is rather formed by the cleavage of halogen bridges [43]. Therefore, it is quite obvious that they should differ in their characteristic properties and FAB strongly

supports this concept, i.e., perhaps reflecting condensed phase species rather than isoated gas phase molecules. Due to the lack of observation of metastable ions (metastables are observed only for the HMPA fragments) for almost all the tin and lead compounds in both EI and FAB, it has not been plausible to propose detailed fragmentation pathways. However, I have attempted to describe the most probable fragmentation schemes. The positive ion FAB mass spectra for these compounds are given in Figures 27-29 and the possible fragmentation schemes in Figure 30.

Figure 27

Positive ion FAB mass spectrum of Ph_2PbCl_2.2HMPA

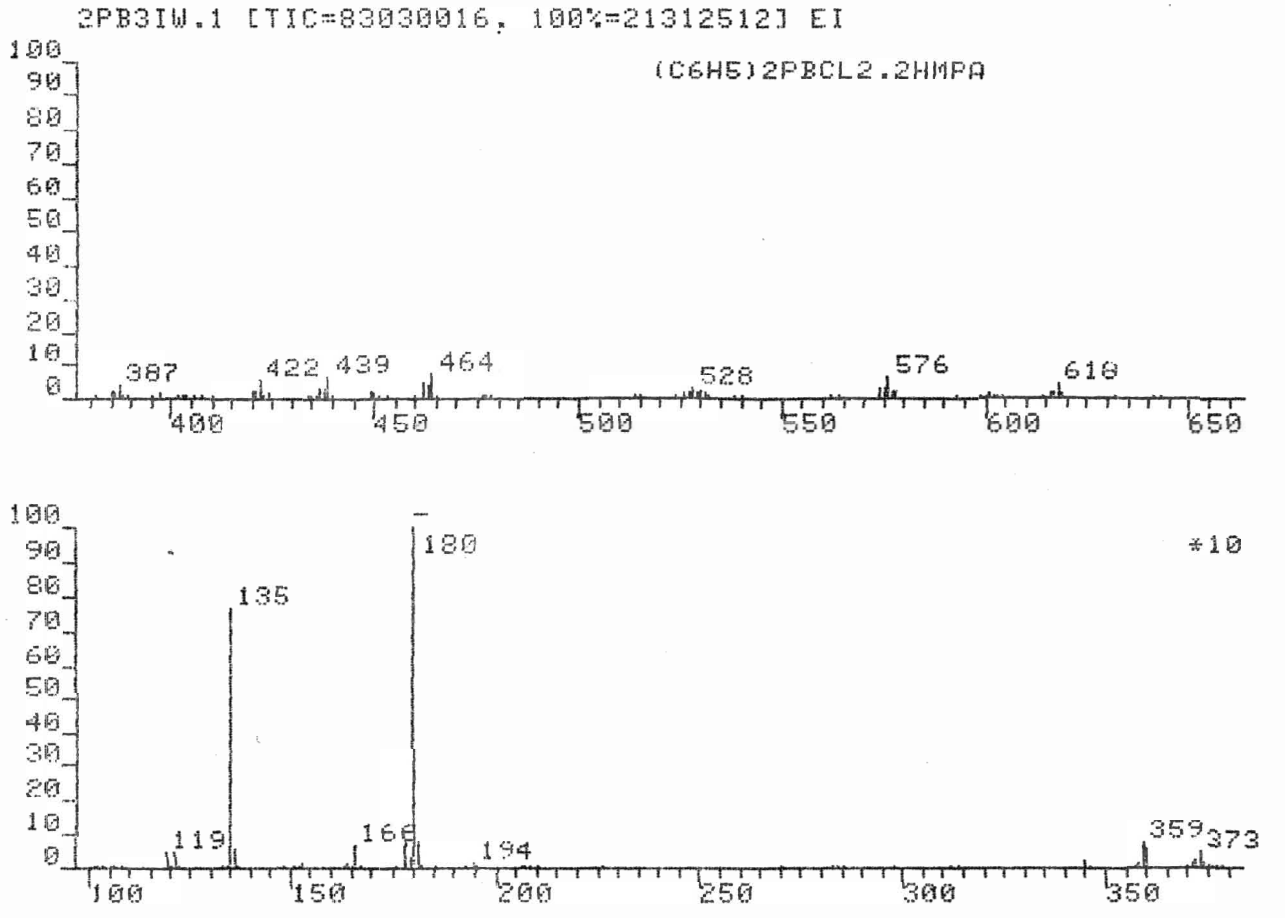
2PB3IW.1 [TIC=83030016, 100%=21312512] EI
(C6H5)2PBCL2.2HMPA
387
422
439
464
528
576
610
180
135
119
166
194
359
373
*10

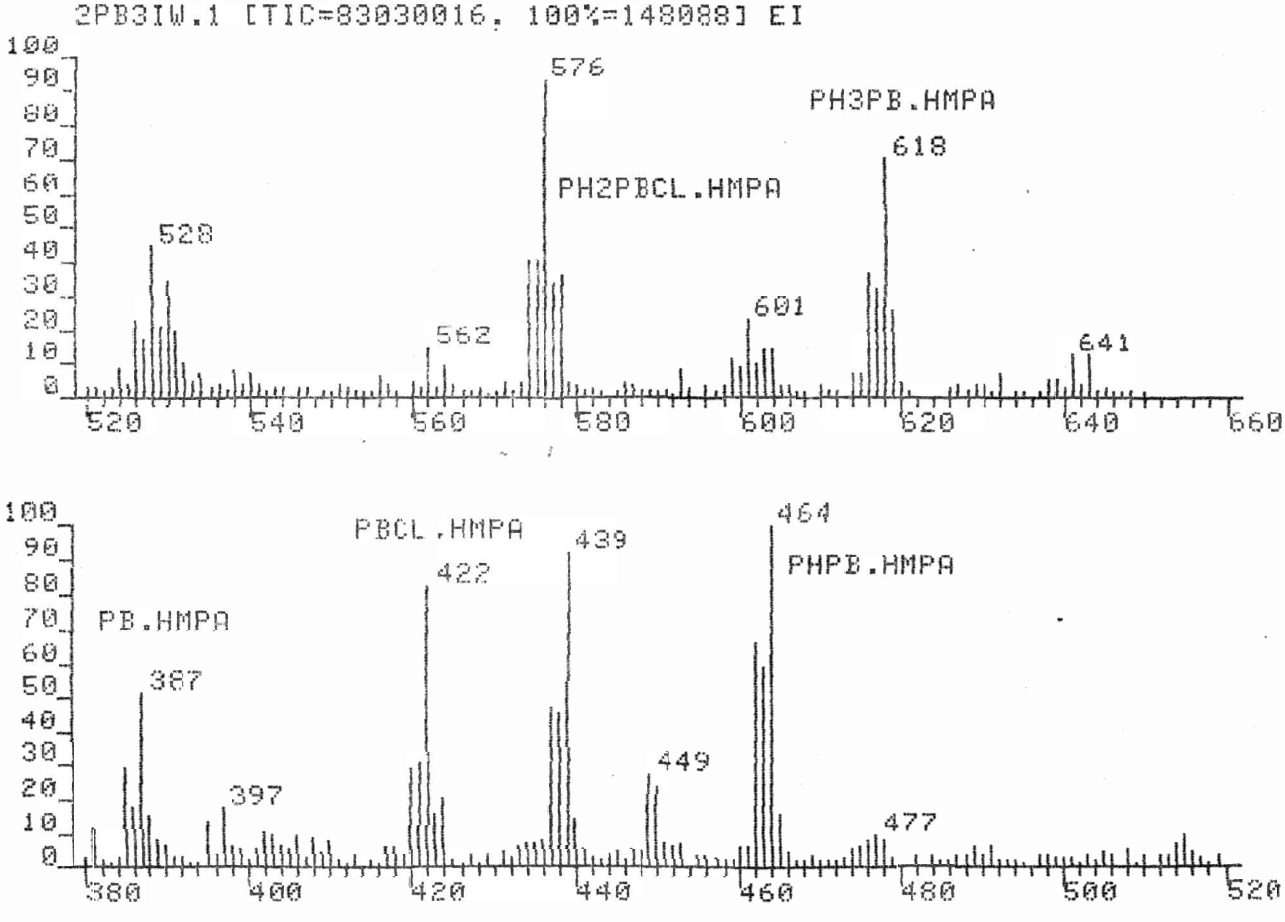
2PB3IW.1 [TIC=83030016, 100%=1480888] EI
576
PH3PB.HMPA
618
PH2PBCL.HMPA
528
562
601
641
PBCL.HMPA
422
439
464
PHPB.HMPA
PB.HMPA
387
397
449
477

Figure 28

Positive ion FAB mass spectrum of $Ph_2PbBr_2.2HMPA$

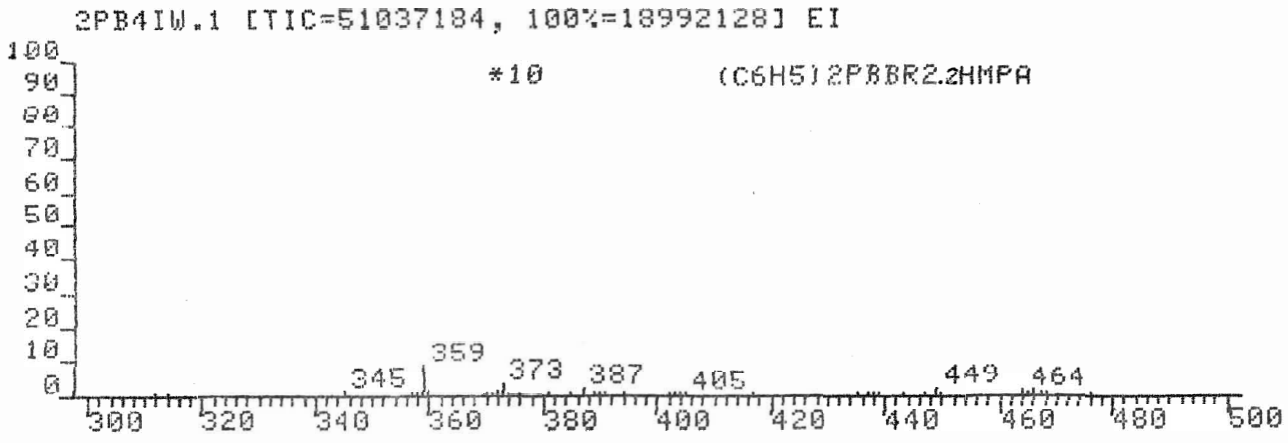
2PB4IW.1 [TIC=51037184, 100%=18992128] EI
*10
(C6H5)2PBBR2.2HMPA
345
359
373
387
405
449
464

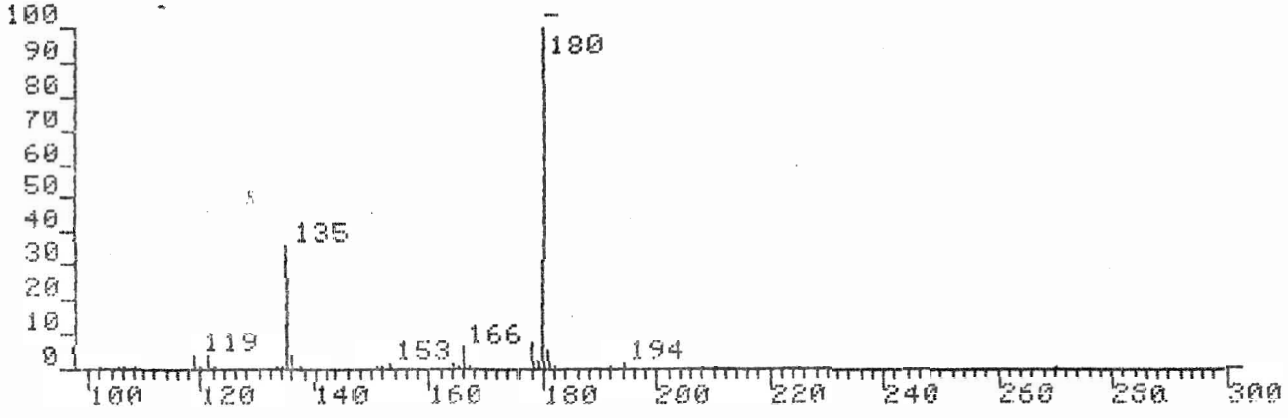
180
135
119
153
166
194

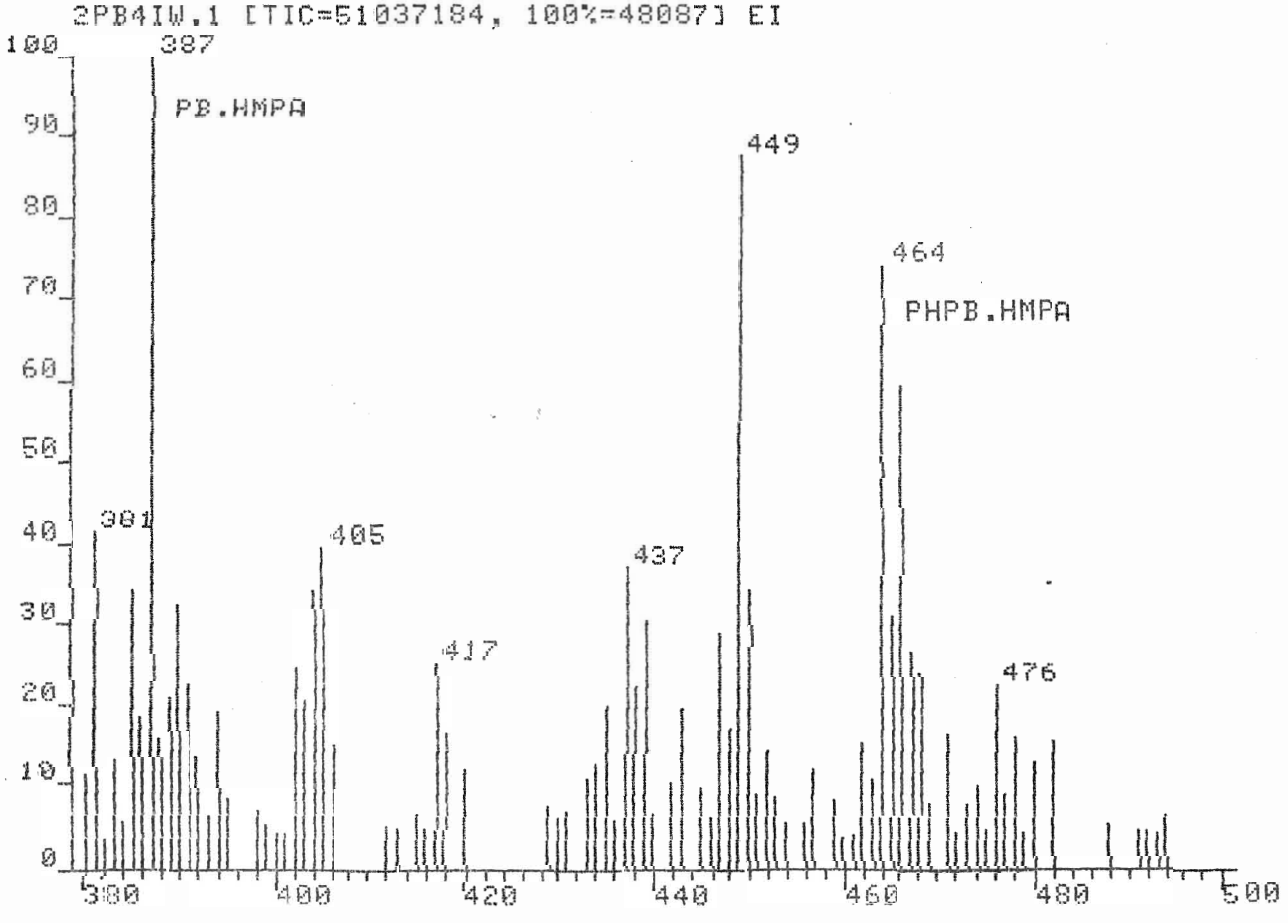
2PB4IW.1 [TIC=51037184, 100%=48087] EI
387
PB.HMPA
449
464
PHPB.HMPA
391
405
437
417
476

Figure 29

Positive ion FAB mass spectrum of Ph_2PbI_2.2HMPA

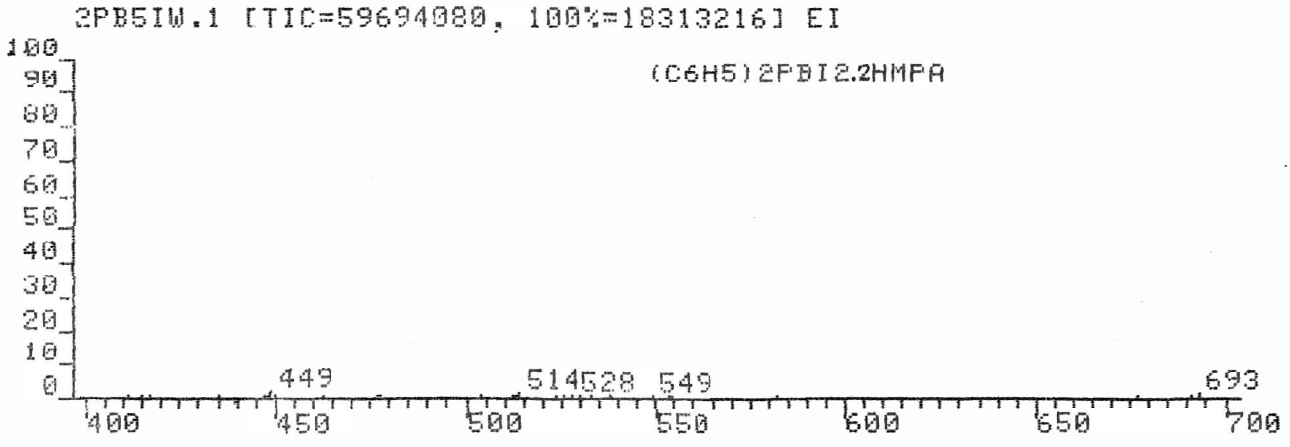
2PB5IW.1 [TIC=59694080, 100%=18313216] EI
(C6H5)2PBI2.2HMPA
449
514
528
549
693

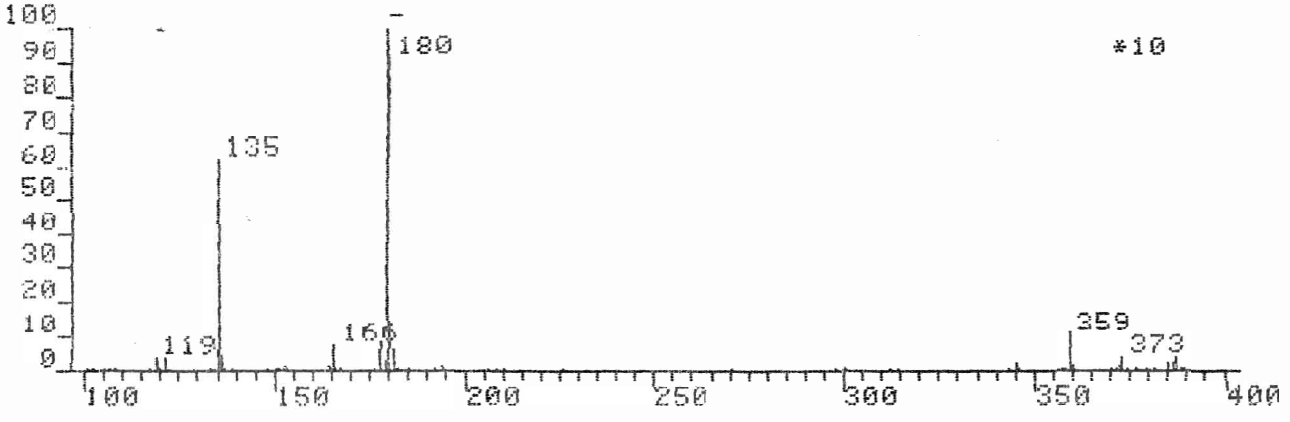
180
*10
135
119
166
359
373

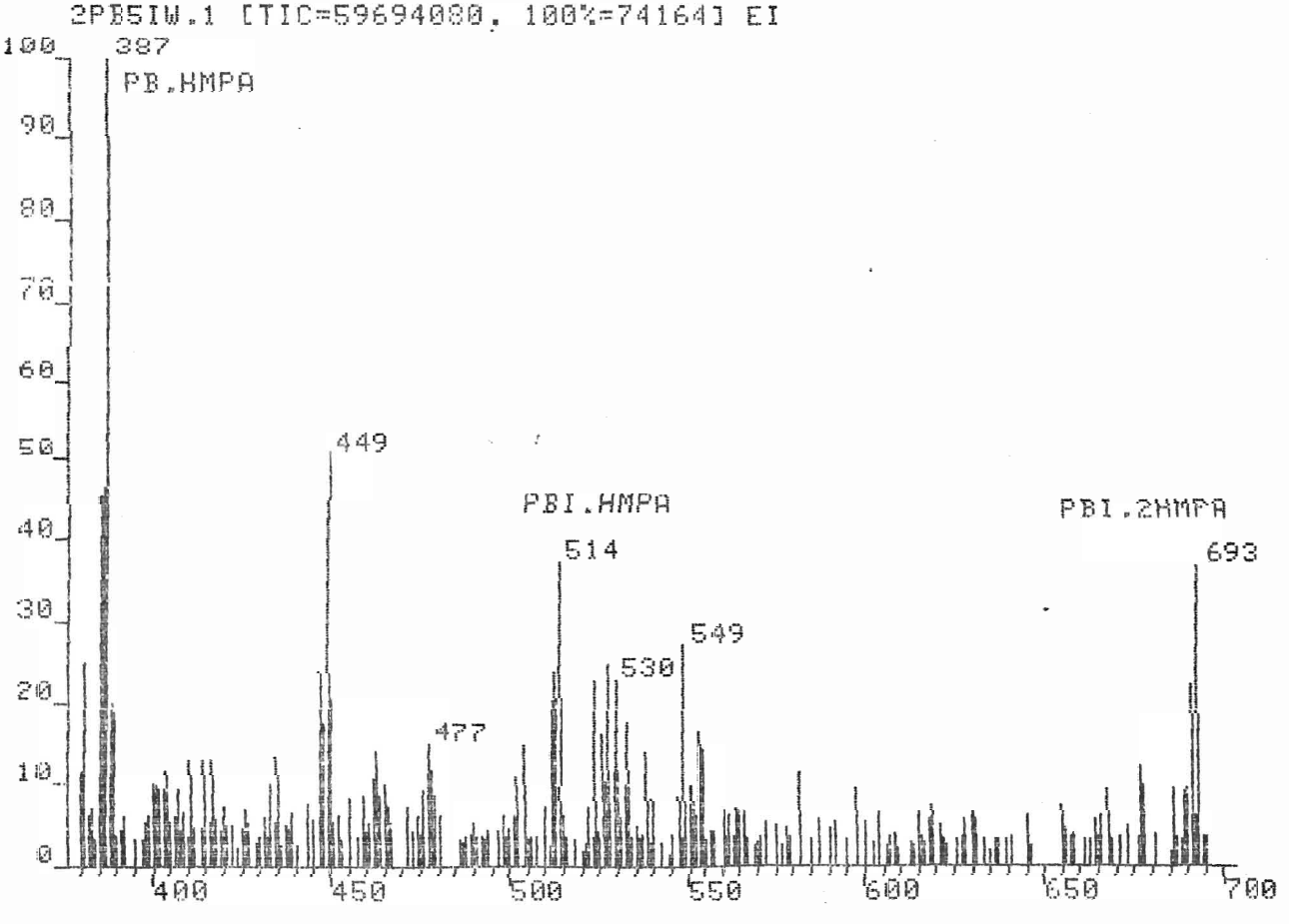
2PB5IW.1 [TIC=59694080, 100%=741641 EI
387
PB.HMPA
449
PBI.HMPA
514
530
549
477
PBI.2HMPA
693

Figure 30

Possible fragmentation schemes for the series $Ph_2PbX_2.2HMPA$ (X = Cl, Br, I)

(A) $Ph_2PbX_2.2HMPA$ (EI)

(B) $Ph_2PbX_2.2HMPA$ (FAB)

(A)

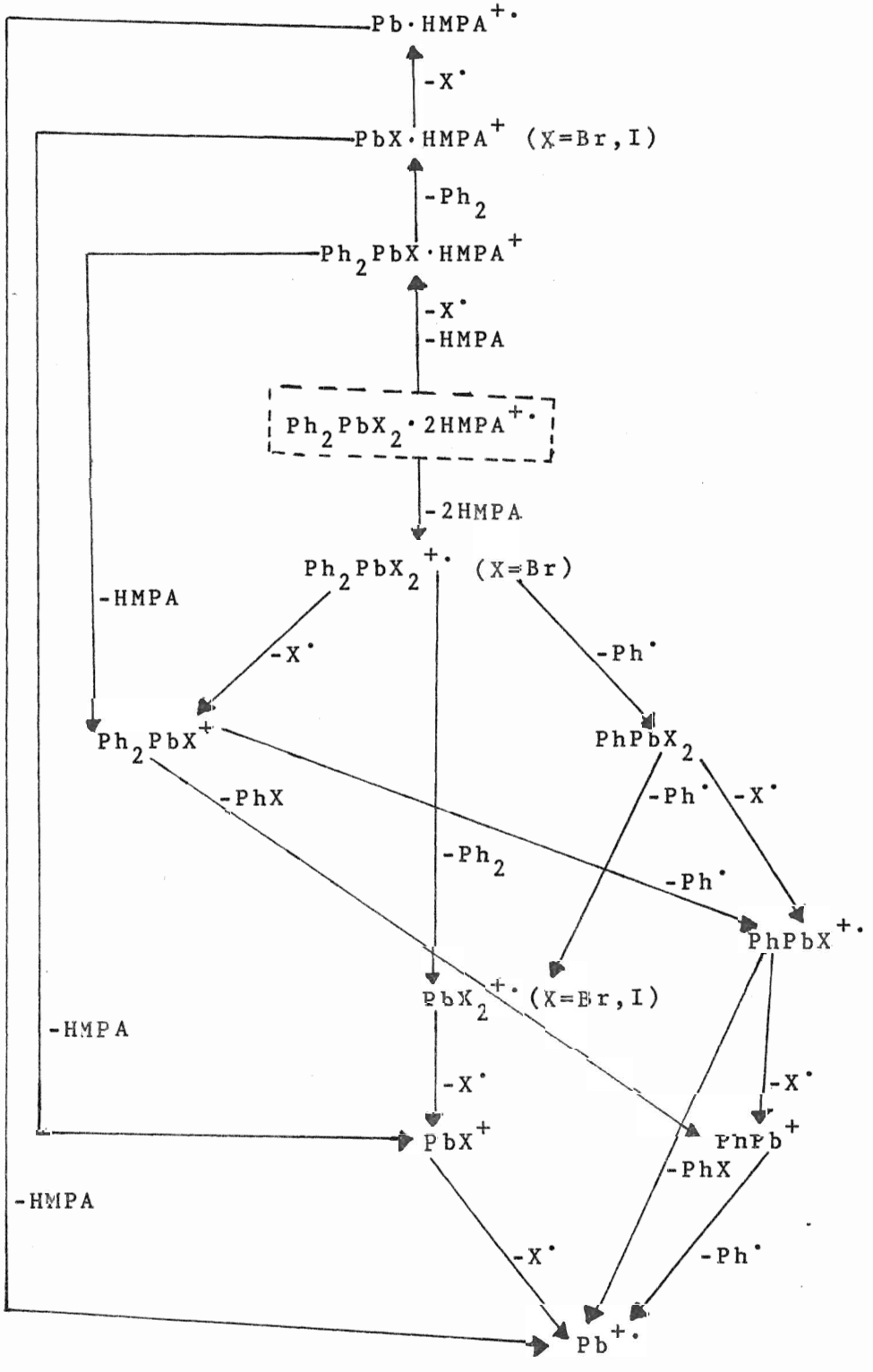
Pb·HMPA+·
-X·
PbX·HMPA+ (X=Br,I)
-Ph2
Ph2PbX·HMPA+
-X·
-HMPA
Ph2PbX2·2HMPA+·
-2HMPA
Ph2PbX2+· (X=Br)
-HMPA
-X·
-Ph·
Ph2PbX+
PhPbX2
-PhX
-Ph·
-X·
-Ph2
-Ph·
PhPbX+·
PbX2+· (X=Br,I)
-HMPA
-X·
-X·
PbX+
PhPb+
-PhX
-HMPA
-X·
-Ph·
Pb+·

(B)

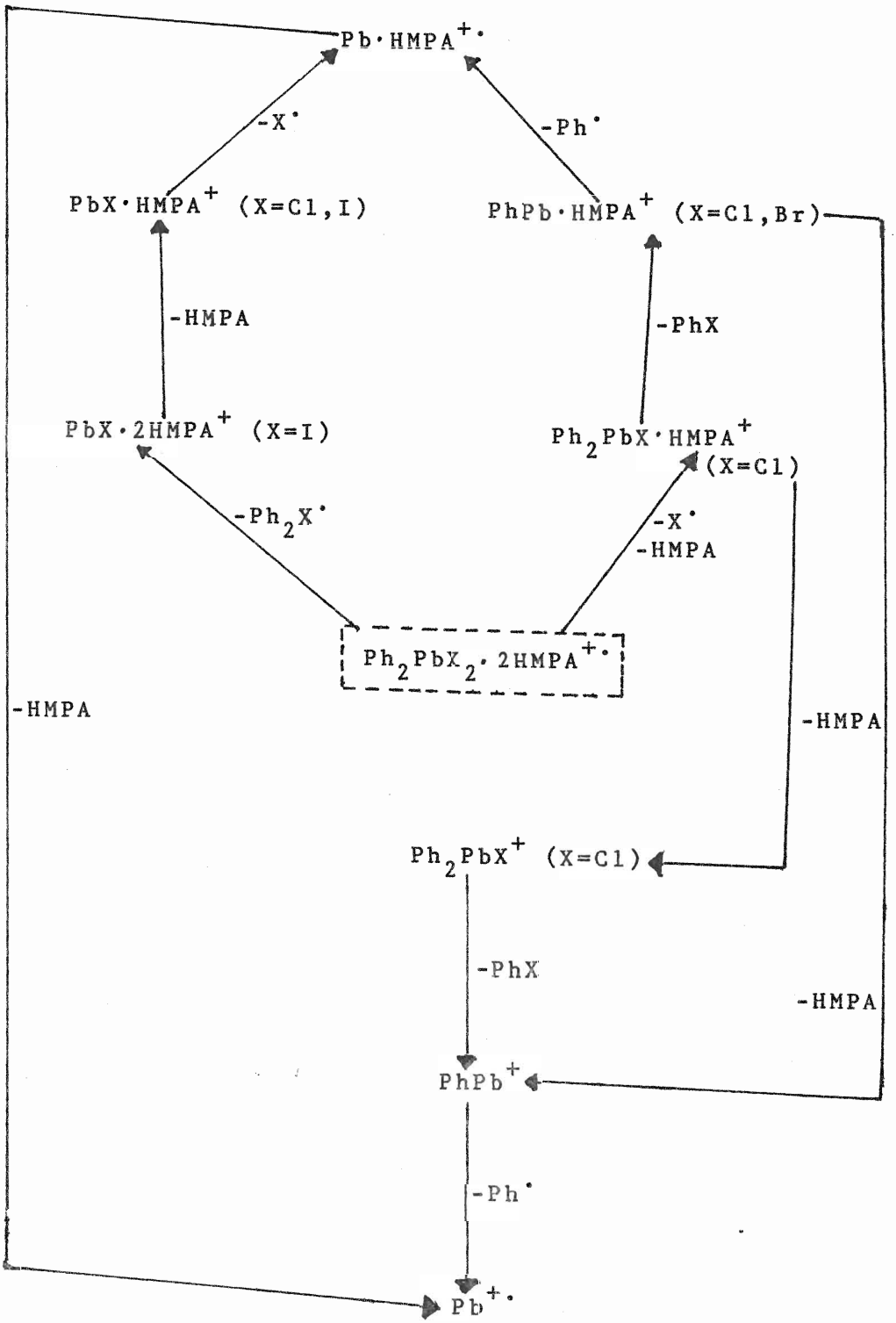
Pb·HMPA+·
-X·
-Ph·
PbX·HMPA+ (X=Cl,I)
PhPb·HMPA+ (X=Cl,Br)
-HMPA
-PhX
PbX·2HMPA+ (X=I)
Ph2PbX·HMPA+ (X=Cl)
-Ph2X·
-X·
-HMPA
Ph2PbX2·2HMPA+·
-HMPA
-HMPA
Ph2PbX+ (X=Cl)
-PhX
-HMPA
PhPb+
-Ph·
Pb+·

Figure 30a

Comparison of EI and FAB data

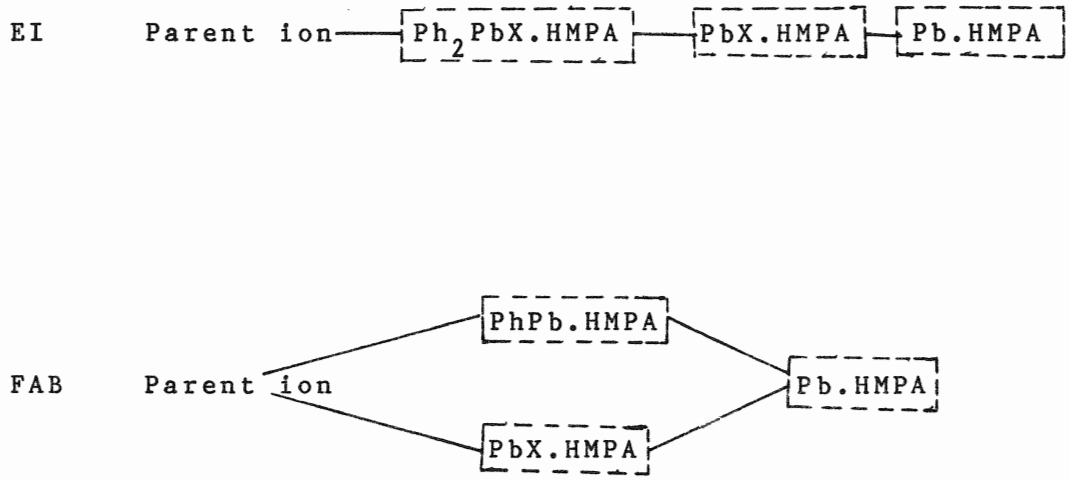

5. Ligand-Exchange Phenomenon:

The positive FAB mass spectrum of Ph_4Sn in HMPA matrix described in section (3) confirmed that the observation of HMPA-containing species in the FAB-MS of HMPA adducts of phenyltin and -lead halides is not an artifact of FAB technique. Matrix liquid co-ordination occurs only if the Lewis acidity of the material is high enough. However, since as has been discussed earlier, ionization of these compounds appears to occur in solution, then solution equilibrium will be reflected in the spectra. The possibility of ligand-exchange is thus illustrated by the observation of the relevant metal-containing ions listed below:

(i) $Ph_3Sn.2HMPA$ for the series $Ph_3SnX.HMPA$ (X = Cl, Br)
(i.e., HMPA exchange)

(ii) $Ph_3Sn.HMPA$ for the series $Ph_2SnX_2.HMPA$ (X = Cl, Br)
(i.e., phenyl exchange)

(iii) Ph_3Sn for the series $Ph_2SnX_2.HMPA$ (X = Cl, Br)
(i.e., phenyl exchange)

(iv) $Ph_3Sn.2HMPA$ for the compound $Ph_2SnCl_2.HMPA$
(i.e., HMPA exchange)

(v) $PbX.2HMPA$ for the compound $Ph_2PbI_2.HMPA$
(i.e., HMPA exchange)

(vi) $Ph_3Pb.HMPA$ for the compound $Ph_2PbBr_2.HMPA$ (impure)
(possibly phenyl exchange)

(vii) $Ph_3Pb.HMPA$ for the compound $Ph_2PbCl_2.2HMPA$ (impure) (possibly phenyl exchange)

Another possibility for the formation of these ions lies in the presence of impurities in the compounds. However, it has been found that all the samples except $Ph_2PbBr_2.HMPA$, $Ph_2PbCl_2.2HMPA$ and $Ph_2PbBr_2.2HMPA$ are pure. Had impurities alone been the cause of these ions, they would not have been observed in the other cases. Therefore, it appears that the presence of an impurity is not the cause of the triphenyl species.

The phenomenon of fast-exchange of free and co-ordinated ligands at room temperature had already been experimentally verified earlier [42,43] by ^{31}P-nmr. The fact that bound X is being fast exchanged by free HMPA ligand from the matrix solution of the parent adduct is strongly supported by the observation of $Ph_3Sn.2HMPA$ ions for compounds $Ph_3SnX.HMPA$ (X = Cl, Br). The exchange process probably takes place as follows:

(i) $Ph_3SnX.HMPA + HMPA^{\prime} \longrightarrow Ph_3Sn.2HMPA^+ + X^-$

(ii) $Ph_2SnX.HMPA^+ + Ph_2SnX_2 \longrightarrow Ph_3Sn.HMPA^+ + PhSnX_3$

(iii) $Ph_2SnX^+ + Ph_2SnX_2.HMPA \longrightarrow Ph_3Sn^+ + PhSnX_3.HMPA$

(iv) $Ph_2SnCl.HMPA^+ + HMPAH^+ \longrightarrow Ph_2Sn.2HMPA^+ + HCl$

or

$Ph_2SnCl.HMPA + HMPA^+ \longrightarrow Ph_2Sn.2HMPA^+ + Cl^-$

(v) $Ph_2PbI.HMPA^+ + HMPA \longrightarrow PbI.2HMPA^+ + Ph_2$

(vi) $Ph_2PbBr.HMPA^+ + Ph_2PbBr_2.HMPA \longrightarrow$

$Ph_3Pb.HMPA^+ + PhPbBr_3.HMPA$

(vii) $Ph_2PbCl.HMPA^+ + Ph_2PbCl_2.HMPA \longrightarrow$

$Ph_3Pb.HMPA^+ + PhPbCl_3.HMPA$

Another interesting aspect in this context is that the phenyl-exchanged species provide much higher stabilities than those formed via exchange of HMPA, as can be seen from the corresponding tables of ion intensities. This also suggests that comparatively small ligands are readily exchangeable.

(6) Moisture sensitive organo-metallics:

Analysis of compounds of this type was attempted by FAB and included

(i) Grignard Reagent (C_6H_5MgBr)

(ii) n-butyllithium (n-BuLi)

The major drawback associated with the analysis of this kind of sample in FAB involves the requirement of placing the sample on the probe tip before insertion into the source. This causes decomposition of the sample due to contact with moisture in the air. The Grignard Reagent was found to be very reactive in matrices like glycerol, sulfolane, triglyme, crown etc. Diphenyl ether was the only matrix which did not react with these two compounds, but that even failed to give any structural identification of these organo-metallics.

(7) Hydrogen bonded systems:

The hydrogen bonded systems of interest are:

(i) tetra-n-butylammonium fluoride-acetophenoxime disolvate

(ii) tetra-n-butylammonium fluoride-dl-camphoroxime disolvate

FAB was applied to these systems to investigate the presence of strong hydrogen bonds that had already been observed by J. H. Clark [44] by other spectroscopic techniques. Glycerol was used as a matrix in both cases as they are quite soluble in it, but unfortunately no confirmation was obtained by FAB.

(8) Trapping of water molecules by tetraalkylammonium fluoride and tetraalkyl- and trialkylarylammonium hydroxide

The quaternary ammonium fluorides, most popular among the aprotic solvent soluble fluoride ion sources were first successfully investigated by FAB to monitor the presence of complex aggregates in solutions that can scavenge and trap large numbers of water molecules. These solutions are thus not always completely anhydrous [58]. NMR-studies had already showed the ability of the ion-aggregates in TBAF-HMPA systems to trap up to 10 mole equivalents of water. For the investigation of this phenomenon in TBAF by FAB, the TBAF was mixed in HMPA in 1:10 ratio and various samples of this compound were prepared by adding different quantities of water to each. An ion at m/z 683 corresponding to $[(Bu_4N^+)_2F^-(H_2O)_{10}]^+$ was observed in the positive mass spectrum of TBAF-HMPA/10H_2O as shown in Figure 31. The peak at m/z 503

Figure 31

Positive ion FAB mass spectrum of TBAF-HMPA/10H_2O

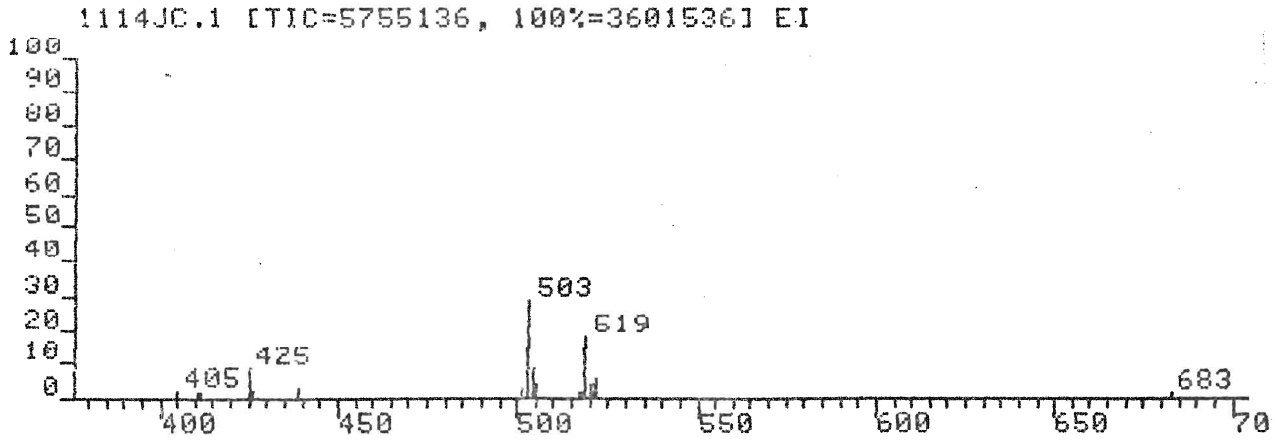
1114JC.1 [TIC=5755136, 100%=3601536] EI
100
90
80
70
60
50
40
30
20
10
0
503
619
425
405
683
400
450
500
550
600
650
70

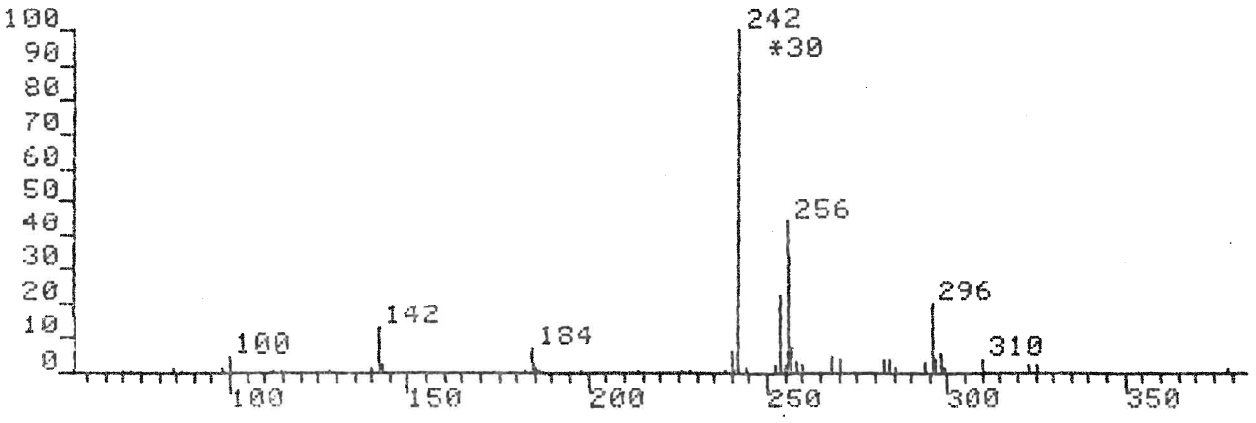
100
90
80
70
60
50
40
30
20
10
0
242
*30
256
296
142
184
100
310
100
150
200
250
300
350

is presumably due to $[(Bu_4N^+)_2F^-]^+$. No other similar species with a small number of water molecules was visible. $[Bu_4N^+)_2F^-]^+$ and its decomposition products were noticed in the solution of TBAF.$3H_2O$ in glycerol or sulfolane matrix. A similar type of experiment was also done by FAB for TBAB-HMPA system, but without any success. This probably tells that fluoride forms stronger hydrogen bonds suggested by Emsley [59]. To explore this ion-aggregation phenomenon in parallel systems, several tetraalkyl- and trialkylarylammonium hydroxides were studied by FAB in glycerol matrix. Samples were mixed in glycerol in 1:1 ratio before the addition of H_2O molecules. Tables X and XI list the individual samples with their respective possible important ions at different masses when $5H_2O$ were added to sample-glycerol (1:1) system.

The interesting part of our research with these samples is the observation of $[(quat.amm^+)_2OH^-.H_2O]^+$ ion in each case except TBAH which is analogous to the result obtained for TBAF-HMPA system by FAB and NMR. The only difference from the fluoride is that instead of $10H_2O$, only a single water molecule is observed along with the anion-cation pair. This may be ascribed to the nature and hydrogen bonding ability of the anion OH^- present in the ion cluster. Five water molecules were observed clustered with the R_4N^+ cation. The probability of complexation of the quaternary ammonium ion with two glycerols was demonstrated only for BTMAH at m/z 336. The feasibility of trapping of five water molecules by the respective cations as observed in each case,

Table X

Sample	m/z	Ion^+
1. BTMAH/GLY/$5H_2O$	151	(BTMA + H)
BTMAH/GLY/$5H_2O$	241	(BTMA.$5H_2O$ + H)
		or (BTMA.C_7H_6 + H)
		or (BTMA.$C_3H_6O_3$ + H)
BTMAH/GLY/$5H_2O$	243	(BTMA.GLY + H)
BTMAH/GLY/$5H_2O$	336	[$(BTMA)_2^+$.OH^-.H_2O + H]
		or $(BTMA)_2^+$.$2H_2O$
		or [BTMA.2GLY + 2H]
2. TMPAH/GLY/$5H_2O$	136	TMPA
TMPAH/GLY/$5H_2O$	226	(TMPA.$5H_2O$)
		or (TMPA.$C_3H_6O_3$)
TMPAH/GLY/$5H_2O$	228	(TMPA.GLY)
TMPAH/GLY/$5H_2O$	307	[$(TMPA)_2^+$.OH^-.H_2O]

BTMAH = benzyltrimethylammonium hydroxide

TMPAH = trimethylphenylammonium hydroxide

GLY = glycerol

Table XI

Sample	m/z	Ion^+
1. TBAH/GLY/$5H_2O$	242	TBA
TBAH/GLY/$5H_2O$	332	(TBA.$5H_2O$)
		or (TBA.$C_3H_6O_3$)
TBAH/GLY/$5H_2O$	296	(TBA.$3H_2O$)
2. TEAH/GLY/$5H_2O$	131	(TEA + H)
TEAH/GLY/$5H_2O$	321	(TEA.$5H_2O$ + H)
		or (TEA.$C_3H_6O_3$ + H)
TEAH/GLY/$5H_2O$	323	(TEA.GLY + H)
TEAH/GLY/$5H_2O$	297	$[(TEA + H)_2^+.OH^-.H_2O]$
3. TMAH/GLY/$5H_2O$	74	TMA
TMAH/GLY/$5H_2O$	165	(TMA.$C_3H_7O_3$)
		or (TMA.$5H_2O$ + H)
		or (TMA.$C_3H_6O_3$ + H)
TMAH/GLY/$5H_2O$	167	(TMA.GLY + H)
TMAH/GLY/$5H_2O$	183	$[(TMA)_2^+.OH^-.H_2O]$

TBAH = tetrabutylammonium hydroxide

TEAH = tetraethylammonium hydroxide

TMAH = tetramethylammonium hydroxide

cannot be confirmed simply by FAB analysis. However, comparing it with other possibilities, assumptions can be made about its existence, but it should also be confirmed by other spectroscopic techniques. Each sample was also run in FAB by adding 10 H_2O to the sample-glycerol system but there was no sign of aggregation of the large numbers of water molecules around the cation.

TBAB = tetrabutylammonium bromide

IV. Conclusion and Suggestions for Future Work

HMPA-containing metal fragments are more prominent in FAB than in EI. Hence it can be said that FAB serves as a better characterization technique for these adducts and in the low mass region too, the ions are indicative of the structures of the corresponding compounds. The only noticeable difference in FAB is that halogenated ion clusters are very weak. McCloskey et al. [61] recently reported that the extensive dehalogenation from the halonucleosides is mainly due to easy exchange of halogens by H^+ from glycerol matrix. Albeit the same reasoning cannot be directly implied to the M-X bond instabilities of these organo-metallics, but at the same time this possibility cannot also be ignored. Thus it can be concluded that the presence of a polar matrix makes the metal-halogen bond unstable, or susceptible to exchange, certainly with energy deposition into the matrix by the bombarding atom. Most of the compounds in the present study show greater intensities of the bare metal ions in FAB. The Sn-HMPA bond was found to be less stable than that of the Pb-HMPA based on relative abundances. In EI, parent ions are not obtainable, while in FAB, they may exist but are still too weak to be easily detected with our instrumentation. Their presence was hinted at but could not be confirmed. Argon was used as bombarding atom. Hopefully, by the use of more sensitive colliding atoms like xenon and mercury (with greater momenta) and better matrices, the intensities of the parent ions can be enhanced in FAB.

Research regarding the ligand-exchange phenomena by FAB is still in its infancy and absolute conclusions are premature unless bolstered by other complementary techniques. However, the parallelism of solution chemistry with the FAB technique that has been reported earlier [26,29], leads us to forecast that ligand-exchange phenomena together with the similar kind of mechanisms involved in solution chemistry will be explored by FAB in the near future. As far as the analysis of the moisture sensitive compounds are concerned, probably by using NPOE as a matrix or with the advent of other suitable matrices and design of a convenient dry bag in front of the FAB source, their analysis may succeed. The formation of strong hydrogen bonds of aromatic carboxylic acids, alcohols, amines, amides etc. has already been shown earlier by Clark and Miller [60] with the help of two major spectroscopic techniques, namely NMR and IR. It would be very interesting if they could be investigated by FAB and sufficient structural information obtained before their X-ray studies.

It is suspected that the crystalline forms of TBAF-β-diketones and similar complexes are H^+-transferred species. It would be of great interest if we can monitor when this transfer occurs, by FAB. The investigation of the scavenging and trapping of water molecules by the complex aggregates in solutions of quaternary ammonium fluorides and hydroxides by FAB is also at an experimental stage. Various other matrices whose decomposition fragments (having mass equivalent to that of $5H_2O$ or $10H_2O$) have the least possibility of attaching

themselves to the corresponding aggregates, should be attempted to clarify this concept.

REFERENCES

1. M. S. B. Munson and F. H. Field: J. Am. Chem. Soc., 88 , 2621 (1966).

2. H. D. Beckey: Field Ionization Mass Spectrometry. Pergamon Press (1971).

3. H. D. Beckey: Int. J. Mass Spectrom. and Ion Physics, 2 , 500 (1969).

4. R. D. Macfarlane and D. F. Torgenson: Science, 191 , 920 (1976).

5. R. D. Macfarlane: Analytical Chemistry, 55 , 12, 1260A (1983).

6. D. J. Surman and J. C. Vickerman: J. Chem. Soc. Chem. Comm. 324 (1981).

7. M. A. Rudat, G. H. Morrison: Anal. Chem. Acta, 112 , 1 (1979).

8. A. Benninghoven, W. Sichtermann: Org. Mass Spectrom., 12 , 595 (1977).

9. H. Grade, N. Winograd, R. G. Cooks: J. Am. Chem. Soc., 99 , 7725 (1977).

10. H. Kambara, S. Hishida: Org. Mass Spectrom., 16 , 167 (1981).

11. D. J. Surman and J. C. Vickerman: J. Chem. Soc. Chem. Comm., 324 (1981).

12. M. Barber, R. S. Bordoli, R. D. Sedgwick and A. N. Tyler: J. Chem. Soc. Chem. Comm. 325 (1981).

13. H. R. Schulten, H. M. Schiebel: Naturwissenschaften, 65 , 223 (1978).

14. M. Barber, R. S. Bordoli and R. D. Sedgwick, in "Soft Ionization Biological Mass Spectrometry", H. R. Morris ed., Heyden, London, 137-152 (1981).

15. M. Barber, R. S. Bordoli, R. D. Sedgwick and A. N. Tyler: Biomed. Mass Spec., 8 , 492 (1981).

16. M. Barber, R. S. Bordoli, R. D. Sedgwick and A. N. Tyler: Nature, 293 , 270 (1981).

17. M. Barber, R. S. Bordoli, R. D. Sedgwick and A. N. Tyler: Biochem. and Biophys. Res. Commun., 101 , 632 (1981).

18. H. Schwarz, K. Eckart, F. Lester and C. E. Tyler: Org. Mass Spectrom., 17 (9) 458 (1982).

19. A. Dell, R. C. Hider, M. Barber, R. S. Bordoli, R. D. Sedgwick, A. N. Tyler and J. B. Neilands: Biomed. Mass Spec., 9 , 158-161 (1982).

20. G. Puzo, J. C. Prome, J. P. Macquet and I. A. S. Lewis: Biomed. Mass Spec., 9 , 552-556 (1982).

21. R. D. Minard and G. L. Geoffroy: Abstracts, 30th Annual Conference on Mass Spectrometry and Allied Topics, Honolulu, June (1982), 321.

22. H. M. Schiebel and H. R. Schulten: Biomed. Mass Spec. 9 , 354 (1982)

23. J. van der Greef and M. C. ten Noever de Brauw: Int. J. of Mass Spec. and Ion Phys., 46 , 379-382 (1983).

24. I. Tkatchenko, D. Neibecker, D. Fraisse, F. Gomez and D. F. Barofsky: Int. J. of Mass Spec. and Ion Phys., 46 , 499-502 (1983).

25. R. A. W. Johnstone and I. A. S. Lewis: Int. J. of Mass Spec. and Ion Phys. 46 , 451-454 (1983).

26. R. A. W. Johnstone, I. A. S. Lewis and M. E. Rose: Tetrahedron, 39 , 1597 (1983).

27. Reg Davis, Ian F. Groves, J. L. A. Durrant, P. Brooks and I. Lewis: J. of Organometallic Chemistry, 241 , C27-C30 (1983).

28. B. R. James and L. D. Markham: Inorg. Chem., 13 , 97 (1974); P. R. Hoffman and K. G. Caulton: J. Am. Chem. Soc., 97 , 4221 (1975).

29. R. L. Cerny, B. Patrick Sullivan, M. M. Bursey and T. J. Meyer: Analytical Chemistry, 55 . 1954-1958 (1983).

30. R. L. Cerny, M. M. Bursey and J. R. Hass: Abstr. 31st Conference ASMS, Boston, 369, May (1983).

31. C. E. Costello, J. W. Brodack, A. G. Jones, A. Davison, D. L. Johnson, S. Kasina and A. R. Fritzberg: J. Nucl. Med., 24 , 353-355 (1983).

32. C. E. Costello, H. Pang, A. Davison and A. G. Jones: Abstr. 31st Conf. ASMS, Boston, 377, May (1983).

33. A. I. Cohen, K. A. Glavan and J. F. Kronauge: Biomed. Mass Spec., 10 . 287-291, (1983).

34. G. Hansen, D. Heller, J. Yergey, R. J. Cotter and C. Fenselau: Chem., Biomed., and Environ. Instru., 12 , 275-288 (1982-1983).

35. J. Meili and J. Seibl: 31st Annual Conference on Mass Spec. (ASMS) Boston, May (1983).

36. J. M. Miller: paper presented at Annual Conference, Chemical Inst. of Canada, Calgary, June (1983).

37. J. M. Miller: paper presented at International Conference on the Organometallic and Coordination Chemistry of Ge, Sn and Pb, Montreal, August (1983).

38. M. Farquharson and J. S. Hartman: J. Chem. Soc. Chem. Comm. 256-257 (1984).

39. T. R. Sharp, M. R. White, J. F. Davis and P. J. Stang: Org. Mass Spec. 19 , 107-112 (1984).

40. B. Gregory, C. R. Jablonski and Y-P. Wang: private communication to Dr. J. M. Miller (1984).

41. S. E. Unger: Anal. Chem. 56 , 363-368 (1984).

42. I. Wharf, M. Onyszchuk, D. M. Tallett and J. M. Miller: Can. J. Spectroscopy, 24 , 123-131 (1979).

43. I. Wharf, M. Onyszchuk, J. M. Miller and T. R. B. Jones: J. Orgmet. Chem., 190 , 417-433 (1980).

44. J. H. Clark: Can. J. Chem. 57 , 1481-1487 (1979).

45. J. M. Miller, T. R. B. Jones, J. H. Clark, D. M. Goodall and M. S. White: Can. J. Chem. (submitted 1984).

46. AEI MS-30 Instruction Manual.

47. K. L. Rinehart, Jr.: Science, 218 , 254-260 (1982).

48. J. Franks: Int. J. of Mass Spec. and Ion Phys., 46 , 343-346 (1983).

49. J. Mahoney, J. Perel and S. Taylor: Am. Laboratory, March 1984.

50. S. A. Martin, C. E. Costello and K. Blemann: Anal. Chem., 84 , 2362-2368 (1982).

51. M. E. Hemling, J. C. Cook, Jr., K. L. Rinehart, Jr. and K. L. Olson: Abstr. 30th Annual Conf. Mass Spectrom. and Allied Topics, Honolulu, June 1982 . p. 564.

52. A. I. Vogel: A Text Book of Practical Organic Chemistry, including Qualitative Organic Analysis, (Scottiswoode, Ballantyne and Co. Ltd., 1962). p. 813.

53. J. M. Miller: "Fast Atom Bombardment Mass Spectrometry and Related Techniques", in Adv. Inorg. Chem. and Radiochem., H. J. Emeleus and A. G. Sharpe, eds., Academic Press, New York, 28 in press (1984).

54. F. Glockling: "Mass Spectrometry of Metal Complexes", J. Charalambous, ed., Butterworth, London (1975), Ch. 5.

55. D. B. Chambers, F. Glockling and M. Weston: J. Chem. Soc. (A), 1759 (1967).

56. M. R. Litzow and T. R. Spalding: "Mass Spectrometry of Inorganic and Organometallic Compounds", Elsevier, Amsterdam (1973).

57. F. A. Cotton and G. Wilkinson: "Advanced Inorganic Chemistry, a Comprehensive Text", Wiley-Interscience, U. S. A. (1980). Ch. 12.

58. J. H. Clark: Chem. Rev., 80 , 429 (1980).

59. J. Emsley, J. Chem. Soc. (A), 2702 (1971).

60. J. H. Clark and J. M. Miller: J. Am. Chem. Soc., 99 , 498 (1977).

61. S. K. Sethi, C. C. Nelson and J. A. McCloskey: Anal. Chem., 56 , 1975-1977 (1984).

APPENDIX

SCAN: 1. 1/ 3/84 14:47

$(C_6H_5)_3SnCl.HMPA$

IONISATION: EI
NO. PEAKS: 481
BASE/NREF INT: 1858240./ 1858240.
TIC: 11746048.
MASS RANGE: 68 - 798
RETN TIME/MISC: 0: 0/ 0/ 0/ 0

PEAK NO.	MEASURED MASS	NO. POINTS	ABSOLUTE INTENSITY	% INT. BASE	% INT. NREF	% TOT. ION
88	534	103	19725.	1.1	1.1	0.2*
90	532	103	22753.	1.2	1.2	0.2
91	531	119	32949.	1.8	1.8	0.3
92	530	119	115828.	6.2	6.2	1.0
93	529	103	57685.	3.1	3.1	0.5
94	528	143	99808.	5.4	5.4	0.8*
95	527	143	45537.	2.5	2.5	0.4*
96	526	119	55520.	3.0	3.0	0.5*
106	516	119	48111.	2.6	2.6	0.4
108	514	119	38335.	2.1	2.1	0.3*
110	512	87	19776.	1.1	1.1	0.2
149	452	87	19482.	1.0	1.0	0.2
201	376	103	36799.	2.0	2.0	0.3
203	374	103	32492.	1.7	1.7	0.3
204	373	143	20544.	1.1	1.1	0.2*
217	360	143	25170.	1.4	1.4	0.2
218	359	143	136944.	7.4	7.4	1.2*
219	358	119	28452.	1.5	1.5	0.2*
220	357	143	84284.	4.5	4.5	0.7*
222	355	143	23428.	1.3	1.3	0.2
224	353	103	20921.	1.1	1.1	0.2
225	352	103	24365.	1.3	1.3	0.2
226	351	143	121184.	6.5	6.5	1.0
227	350	119	41572.	2.2	2.2	0.4
228	349	143	87144.	4.7	4.7	0.7
229	348	119	40980.	2.2	2.2	0.3*
230	347	143	62533.	3.4	3.4	0.5*
232	345	119	39142.	2.1	2.1	0.3
234	343	119	22129.	1.2	1.2	0.2*
256	314	119	19585.	1.1	1.1	0.2*
257	313	119	19337.	1.0	1.0	0.2*
258	312	143	99652.	5.4	5.4	0.8*
267	300	87	10240.	0.6	0.6	0.1*
268	299	103	13931.	0.7	0.7	0.1
269	298	143	39881.	2.1	2.1	0.3
270	297	119	13253.	0.7	0.7	0.1*
271	296	87	11004.	0.6	0.6	0.1*
272	295	71	8118.	0.4	0.4	0.1*
273	294	71	6998.	0.4	0.4	0.1*
275	291	71	11076.	0.6	0.6	0.1
355	201	103	18547.	1.0	1.0	0.2
357	199	103	16493.	0.9	0.9	0.1
359	197	143	108244.	5.8	5.8	0.9*
360	196	143	43744.	2.4	2.4	0.4*
361	195	175	90976.	4.9	4.9	0.8
362	194	207	107840.	5.8	5.8	0.9*
363	193	175	66964.	3.6	3.6	0.6*
364	192	143	29529.	1.6	1.6	0.3*
365	191	103	21191.	1.1	1.1	0.2*
397	155	59	7443.	0.4	0.4	0.1*
399	153	119	92012.	5.0	5.0	0.9
400	152	143	49658.	2.7	2.7	0.4*
401	151	119	26633.	1.4	1.4	0.2*
402	150	103	21153.	1.1	1.1	0.2
403	149	119	19912.	1.1	1.1	0.2*
404	148	103	21204.	1.1	1.1	0.2*
405	147	87	11677.	0.6	0.6	0.1*
406	146	71	8460.	0.5	0.5	0.1*
413	139	103	27469.	1.5	1.5	0.2
415	137	175	43197.	2.3	2.3	0.4*
416	136	207	146580.	7.9	7.9	1.2*
417	135	415	1858240.	100.0	100.0	15.8*
418	134	175	47593.	2.6	2.6	0.4*
419	133	175	75552.	4.1	4.1	0.6*
420	132	59	7462.	0.4	0.4	0.1*
425	126	87	14800.	0.8	0.8	0.1
429	122	175	60105.	3.2	3.2	0.5*
430	121	207	334912.	18.0	18.0	2.9*
431	120	239	65540.	3.5	3.5	0.6*
432	119	239	170900.	9.2	9.2	1.5*
433	118	207	49639.	2.7	2.7	0.4*
434	117	207	53588.	2.9	2.9	0.5*

DP4:3SN2IW.MS
SCAN: 1, 1/ 3/84 15:13 $(C_6H_5)_3SnBr.HMPA$

IONISATION: EI
NO. PEAKS: 496
BASE/NREF INT: 1811008./ 1811008.
TIC: 10352384.
MASS RANGE: 69 - 796
RETN TIME/MISC: 0: 0/ 0/ 0/ 0

PEAK NO.	MEASURED MASS	NO. POINTS	ABSOLUTE INTENSITY	% INT. BASE	% INT. NREF	% TOT. ION
72	534	119	39884.	2.2	2.2	0.4*
74	532	119	42896.	2.4	2.4	0.4*
75	531	119	53132.	2.9	2.9	0.5
76	530	175	213744.	11.8	11.8	2.1
77	529	143	98776.	5.5	5.5	1.0*
78	528	143	155184.	8.6	8.6	1.5
79	527	143	65271.	3.6	3.6	0.6*
80	526	143	81420.	4.5	4.5	0.8*
90	516	87	13415.	0.7	0.7	0.1
92	514	87	12426.	0.7	0.7	0.1
142	453	87	15290.	0.8	0.8	0.1
143	452	87	18494.	1.0	1.0	0.2*
144	451	103	17489.	1.0	1.0	0.2*
145	450	87	15391.	0.8	0.8	0.1*
196	380	87	10970.	0.6	0.6	0.1*
198	378	87	11203.	0.6	0.6	0.1*
199	377	71	12541.	0.7	0.7	0.1*
200	376	143	61485.	3.4	3.4	0.6*
201	375	103	23985.	1.3	1.3	0.2*
202	374	119	52292.	2.9	2.9	0.5
203	373	103	24905.	1.4	1.4	0.2*
204	372	103	30723.	1.7	1.7	0.3*
215	360	119	46220.	2.6	2.6	0.4*
216	359	175	261172.	14.4	14.4	2.5*
217	358	103	29066.	1.6	1.6	0.3*
218	357	103	19119.	1.1	1.1	0.2*
220	355	103	20715.	1.1	1.1	0.2*
222	353	103	20611.	1.1	1.1	0.2
223	352	87	18801.	1.0	1.0	0.2*
224	351	143	99500.	5.5	5.5	1.0*
225	350	143	41883.	2.3	2.3	0.4*
226	349	143	81012.	4.5	4.5	0.8*
227	348	119	33242.	1.8	1.8	0.3*
228	347	119	41779.	2.3	2.3	0.4*
230	345	119	27640.	1.5	1.5	0.3*
258	314	119	34005.	1.9	1.9	0.3
260	312	119	24044.	1.3	1.3	0.2*
271	300	103	13507.	0.7	0.7	0.1*
272	299	119	21390.	1.2	1.2	0.2*
273	298	119	30104.	1.7	1.7	0.3*
274	297	87	12154.	0.7	0.7	0.1*
275	296	119	20065.	1.1	1.1	0.2*
287	284	143	27333.	1.5	1.5	0.3*
289	282	103	13626.	0.8	0.8	0.1*
291	280	71	9511.	0.5	0.5	0.1*
296	275	87	10795.	0.6	0.6	0.1*
297	274	35	3750.	0.2	0.2	0.0*
298	273	71	8726.	0.5	0.5	0.1*
299	272	59	6009.	0.3	0.3	0.1*
300	271	71	10815.	0.6	0.6	0.1*
301	270	103	13783.	0.8	0.8	0.1*
302	269	59	6098.	0.3	0.3	0.1*
303	268	35	4013.	0.2	0.2	0.0*
368	201	103	13813.	0.8	0.8	0.1*
370	199	87	11953.	0.7	0.7	0.1*
372	197	143	70160.	3.9	3.9	0.7*
373	196	119	40190.	2.2	2.2	0.4*
374	195	175	59689.	3.3	3.3	0.6*
375	194	207	52159.	2.9	2.9	0.5*
376	193	143	47279.	2.6	2.6	0.5*
446	122	143	21386.	1.2	1.2	0.2*
447	121	175	117900.	6.5	6.5	1.1*
448	120	239	74692.	4.1	4.1	0.7*
449	119	287	226432.	12.5	12.5	2.2*
450	118	143	28838.	1.6	1.6	0.3*
451	117	143	22755.	1.3	1.3	0.2*
452	116	119	19431.	1.1	1.1	0.2*
453	115	87	13699.	0.8	0.8	0.1*

$(C_6H_5)_3SnI.HMPA$

DP0:3SN3IW.MS
SCAN: 1, 1/ 3/84 15:37

IONISATION: EI
NO. PEAKS: 221
BASE/NREF INT: 319456./ 319456.
TIC: 1807872.
MASS RANGE: 70 - 743
RETN TIME/MISC: 0: 0/ 0/ 0/ 0
PAGE 1

PEAK NO.	MEASURED MASS	NO. POINTS	ABSOLUTE INTENSITY	% INT. BASE	% INT. NREF	% TOT. ION
9	547	21	2390.	0.75	0.75	0.13
10	544	43	4422.	1.38	1.38	0.24*
11	534	71	8764.	2.74	2.74	0.48*
12	533	35	3589.	1.12	1.12	0.20
13	532	59	6629.	2.08	2.08	0.37*
14	531	119	20086.	6.29	6.29	1.11*
15	530	119	61682.	19.31	19.31	3.41
16	529	103	29086.	9.10	9.10	1.61*
17	528	119	40500.	12.68	12.68	2.24
18	527	103	21269.	6.66	6.66	1.18*
19	526	119	26329.	8.24	8.24	1.46
20	524	43	4495.	1.41	1.41	0.25*
21	516	59	4628.	1.45	1.45	0.26*
22	515	59	5876.	1.84	1.84	0.33*
23	514	43	5342.	1.67	1.67	0.30*
24	513	25	2082.	0.65	0.65	0.12
25	510	25	1526.	0.48	0.48	0.08
26	497	21	1109.	0.35	0.35	0.06
27	481	25	1486.	0.47	0.47	0.08
28	477	21	1314.	0.41	0.41	0.07
29	473	25	1028.	0.32	0.32	0.06
30	468	21	1237.	0.39	0.39	0.07
31	464	25	1482.	0.46	0.46	0.08
32	455	21	1752.	0.55	0.55	0.10
33	454	25	1356.	0.42	0.42	0.08
34	453	35	3060.	0.96	0.96	0.17*
35	452	35	2918.	0.91	0.91	0.16
36	451	35	3707.	1.16	1.16	0.21
37	450	51	2815.	0.88	0.88	0.16*

PAGE 2

PEAK NO.	MEASURED MASS	NO. POINTS	ABSOLUTE INTENSITY	% INT. BASE	% INT. NREF	% TOT. ION
38	449	29	1871.	0.59	0.59	0.10
39	426	25	2956.	0.93	0.93	0.16
40	422	29	2392.	0.75	0.75	0.13
41	404	29	1929.	0.60	0.60	0.11
42	402	25	2203.	0.69	0.69	0.12
43	401	29	2041.	0.64	0.64	0.11
44	399	29	3233.	1.01	1.01	0.18
45	397	25	1069.	0.33	0.33	0.06
46	394	35	3179.	1.00	1.00	0.18
47	393	21	1482.	0.46	0.46	0.08
48	386	21	2110.	0.66	0.66	0.12
49	380	35	4816.	1.51	1.51	0.27
50	379	25	2258.	0.71	0.71	0.12
51	378	87	9315.	2.92	2.92	0.52
52	377	35	2003.	0.63	0.63	0.11
53	376	119	23771.	7.44	7.44	1.31
54	375	59	5547.	1.74	1.74	0.31*
55	374	87	18620.	5.83	5.83	1.03*
56	373	51	4492.	1.41	1.41	0.25*
57	372	71	12771.	4.00	4.00	0.71*
58	370	21	1328.	0.42	0.42	0.07
59	366	21	1639.	0.51	0.51	0.09
60	365	29	1304.	0.41	0.41	0.07
61	363	25	1906.	0.60	0.60	0.11
62	362	25	1365.	0.43	0.43	0.08
63	361	25	2075.	0.65	0.65	0.11
64	360	29	2775.	0.87	0.87	0.15
65	359	35	3216.	1.01	1.01	0.18
66	358	29	2466.	0.77	0.77	0.14

PAGE 3

PEAK NO.	MEASURED MASS	NO. POINTS	ABSOLUTE INTENSITY	% INT. BASE	% INT. NREF	% TOT ION
67	357	25	1975.	0.62	0.62	0.11
68	356	25	2306.	0.72	0.72	0.13
69	355	59	6597.	2.07	2.07	0.36*
70	354	35	3089.	0.97	0.97	0.17
71	353	71	7255.	2.27	2.27	0.40*
72	352	71	7048.	2.21	2.21	0.39*
73	351	119	48638.	15.23	15.23	2.69
74	350	103	20336.	6.37	6.37	1.12*
75	349	143	36313.	11.37	11.37	2.01
76	348	87	14336.	4.49	4.49	0.79
77	347	103	19596.	6.13	6.13	1.08
78	346	35	3297.	1.03	1.03	0.18
79	345	29	2185.	0.68	0.68	0.12
80	344	21	1461.	0.46	0.46	0.08
81	343	29	1827.	0.57	0.57	0.10
82	335	29	1803.	0.56	0.56	0.10
83	333	29	1268.	0.40	0.40	0.07
154	197	143	44130.	13.81	13.81	2.44*
156	195	103	27769.	8.69	8.69	1.54*
158	193	103	19506.	6.11	6.11	1.08
166	180	143	89128.	27.90	27.90	4.93
168	178	103	19740.	6.18	6.18	1.09
188	136	119	20162.	6.31	6.31	1.12*
189	135	175	319456.	100.00	100.00	17.67*
193	124	51	3548.	1.11	1.11	0.20*
194	122	21	1658.	0.52	0.52	0.09
195	121	119	25375.	7.94	7.94	1.40*
196	120	119	22898.	7.17	7.17	1.27*
197	119	175	45818.	14.34	14.34	2.53*

PAGE 4

PEAK NO.	MEASURED MASS	NO. POINTS	ABSOLUTE INTENSITY	% INT. BASE	% INT. NREF	% TOT. ION
198	118	103	19787.	6.19	6.19	1.09
199	117	87	11543.	3.61	3.61	0.64*
200	116	87	10829.	3.39	3.39	0.60*
201	107	21	1767.	0.55	0.55	0.10
202	106	29	2213.	0.69	0.69	0.12
203	105	43	4378.	1.37	1.37	0.24*
204	103	21	3510.	1.10	1.10	0.19
205	102	25	2222.	0.70	0.70	0.12

$(C_6H_5)_2SnCl_2$.HMPA

DP4:2SN1IW.MS
SCAN: 1, 1/ 3/84 15:58

IONISATION: EI
NO. PEAKS: 545
BASE/NREF INT: 2846912./ 2846912.
TIC: 11490816.
MASS RANGE: 68 - 791
RETN TIME/MISC: 0: 0/ 0/ 0/ 0

PEAK NO.	MEASURED MASS	NO. POINTS	ABSOLUTE INTENSITY	% INT. BASE	% INT. NREF	% TOT. ION
106	534	87	21383.	0.7	0.7	0.2*
108	532	103	20677.	1.0	1.0	0.2*
109	531	103	39833.	1.4	1.4	0.3
110	530	143	131340.	4.6	4.6	1.1
111	529	143	63685.	2.2	2.2	0.6
112	528	143	103660.	3.6	3.6	0.9*
113	527	119	51359.	1.8	1.8	0.4*
114	526	103	56028.	2.0	2.0	0.5
148	490	87	12786.	0.4	0.4	0.1*
150	488	103	32850.	1.2	1.2	0.3
151	487	87	13942.	0.5	0.5	0.1*
152	486	119	27281.	1.0	1.0	0.2*
154	484	87	13010.	0.5	0.5	0.1
183	453	87	12368.	0.4	0.4	0.1*
184	452	87	19263.	0.7	0.7	0.2*
185	451	71	13551.	0.5	0.5	0.1*
186	450	87	16914.	0.6	0.6	0.1*
187	449	71	11824.	0.4	0.4	0.1*
245	380	71	11511.	0.4	0.4	0.1*
249	376	119	55308.	1.9	1.9	0.5
250	375	103	22226.	0.8	0.8	0.2*
251	374	119	45155.	1.6	1.6	0.4*
252	373	119	24653.	0.9	0.9	0.2
253	372	103	23523.	0.8	0.8	0.2
265	360	143	65321.	2.3	2.3	0.6*
266	359	175	391072.	13.7	13.7	3.4*
267	358	143	38903.	1.4	1.4	0.3*
268	357	103	11444.	0.4	0.4	0.1*
270	355	71	10181.	0.4	0.4	0.1*
272	353	71	10418.	0.4	0.4	0.1*
273	352	71	14966.	0.5	0.5	0.1*
274	351	119	56224.	2.0	2.0	0.5*
275	350	103	25277.	0.9	0.9	0.2
276	349	103	43670.	1.5	1.5	0.4*
277	348	103	19755.	0.7	0.7	0.2
278	347	103	22941.	0.8	0.8	0.2*
279	346	59	5169.	0.2	0.2	0.1*
280	345	103	23763.	0.8	0.8	0.2*
294	341	59	5485.	0.2	0.2	0.1
311	313	87	9612.	0.3	0.3	0.1*
312	312	119	23455.	0.8	0.8	0.2*
315	309	87	15172.	0.5	0.5	0.1*
317	307	71	7033.	0.2	0.2	0.1*
323	301	51	5709.	0.2	0.2	0.0*
324	300	87	13108.	0.5	0.5	0.1*
325	299	87	14367.	0.5	0.5	0.1
326	298	119	23358.	0.8	0.8	0.2
327	297	103	13749.	0.5	0.5	0.1*
328	296	87	15632.	0.5	0.5	0.1*
329	295	71	10638.	0.4	0.4	0.1*
330	294	71	8651.	0.3	0.3	0.1*
333	291	71	9961.	0.3	0.3	0.1*
418	201	71	11190.	0.4	0.4	0.1*
420	199	71	9714.	0.3	0.3	0.1*
422	197	143	75000.	2.6	2.6	0.7*
423	196	103	26881.	0.9	0.9	0.2*
424	195	143	59467.	2.1	2.1	0.5*
425	194	175	41310.	1.5	1.5	0.4*
426	193	143	39370.	1.4	1.4	0.3*
427	192	103	12954.	0.5	0.5	0.1*
436	182	119	22683.	0.8	0.8	0.2*
437	181	207	238192.	8.4	8.4	2.1*
438	180	415	2846912.	100.0	100.0	24.8*
439	179	207	88028	3.1	3.1	0.8*
463	155	103	8947.	0.3	0.3	0.1*
465	153	143	32934.	1.2	1.2	0.3*
466	152	87	13708.	0.5	0.5	0.1*
467	151	87	11002.	0.4	0.4	0.1*
468	150	59	9877.	0.3	0.3	0.1*
469	149	87	12311.	0.4	0.4	0.1*
470	148	103	13669.	0.5	0.5	0.1*
480	137	175	35585.	1.2	1.2	0.3*
481	136	175	205780.	7.2	7.2	1.8*
482	135	415	2267328.	79.6	79.6	19.7*
483	134	119	18173.	0.6	0.6	0.2*
484	133	143	34508.	1.2	1.2	0.3*
495	122	143	23098.	0.8	0.8	0.2*
496	121	175	136276.	4.8	4.8	1.2*
497	120	207	51652.	1.8	1.8	0.4*
498	119	239	216668.	7.6	7.6	1.9*
499	118	143	26301.	0.9	0.9	0.2*
500	117	143	19874.	0.7	0.7	0.2*
501	116	103	14877.	0.5	0.5	0.1*

DP4:2SN2IW.MS
SCAN: 1, 1/ 3/84 16:19

$(C_6H_5)_2SnBr_2$.HMPA

IONISATION: EI
NO. PEAKS: 290
BASE/NREF INT: 875376./ 875376.
TIC: 4188864.
MASS RANGE: 68 - 799
RETN TIME/MISC: 0: 0/ 0/ 0/ 0

PEAK NO.	MEASURED MASS	NO. POINTS	ABSOLUTE INTENSITY	% INT. BASE	% INT. NREF	% TOT. ION
30	535	143	20127.	2.3	2.3	0.5%
31	534	59	9247.	1.1	1.1	0.2
32	533	175	50335.	5.8	5.8	1.2%
33	532	103	23049.	2.6	2.6	0.6
34	531	143	60420.	6.9	6.9	1.4%
35	530	103	30495.	3.5	3.5	0.7
36	529	143	45502.	5.2	5.2	1.1%
37	528	87	14810.	1.7	1.7	0.4%
38	527	87	14490.	1.7	1.7	0.3%
69	452	87	8926.	1.0	1.0	0.2%
71	450	71	10375.	1.2	1.2	0.2
87	388	87	17670.	2.0	2.0	0.4
89	378	143	31474.	3.6	3.6	0.8%
90	377	87	11817.	1.3	1.3	0.3
91	376	143	40193.	4.6	4.6	1.0%
92	375	87	13926.	1.6	1.6	0.3
93	374	119	29378.	3.4	3.4	0.7
95	372	71	10618.	1.2	1.2	0.3%
103	360	87	10877.	1.2	1.2	0.3%
104	359	143	83656.	9.6	9.6	2.0%
109	354	87	11886.	1.4	1.4	0.3%
110	353	51	9064.	1.0	1.0	0.2
111	352	51	8872.	1.0	1.0	0.2%
112	351	71	9337.	1.1	1.1	0.2
113	350	71	9117.	1.0	1.0	0.2%
134	314	71	8790.	1.0	1.0	0.2%
140	300	43	4188.	0.5	0.5	0.1%
141	299	71	7553.	0.9	0.9	0.2%
142	298	87	12472.	1.4	1.4	0.3%
143	297	59	6373.	0.7	0.7	0.2%
144	296	87	9288.	1.1	1.1	0.2%
145	295	51	4022.	0.5	0.5	0.1%
146	294	51	5291.	0.6	0.6	0.1%
147	293	25	1400.	0.2	0.2	0.0
148	290	25	2409.	0.3	0.3	0.1
149	289	43	3801.	0.4	0.4	0.1
150	288	25	2578.	0.3	0.3	0.1
151	287	71	5720.	0.7	0.7	0.1%
152	286	29	2048.	0.2	0.2	0.0
153	285	21	1061.	0.1	0.1	0.0
154	284	71	10050.	1.1	1.1	0.2%
155	283	71	5842.	0.7	0.7	0.1%
156	282	43	4190.	0.5	0.5	0.1
157	281	25	2549.	0.3	0.3	0.1
158	280	43	5312.	0.6	0.6	0.1
159	278	25	2330.	0.3	0.3	0.1
160	277	25	2261.	0.3	0.3	0.1
161	276	21	2670.	0.3	0.3	0.1
162	275	25	3046.	0.3	0.3	0.1
163	274	43	3746.	0.4	0.4	0.1
164	273	29	1740.	0.2	0.2	0.0
165	272	43	4668.	0.5	0.5	0.1%
166	271	43	4659.	0.5	0.5	0.1%
167	269	25	2455.	0.3	0.3	0.1
168	268	21	2003.	0.2	0.2	0.0
199	201	103	12582.	1.4	1.4	0.3%
201	199	87	8683.	1.0	1.0	0.2%
202	198	43	4465.	0.5	0.5	0.1%
203	197	143	34775.	4.0	4.0	0.8
204	196	87	14737.	1.7	1.7	0.4%
205	195	119	21449.	2.5	2.5	0.5%
206	194	175	21508.	2.5	2.5	0.5%
207	193	119	19071.	2.2	2.2	0.5%
208	192	35	3972.	0.5	0.5	0.1%
209	191	51	3955.	0.5	0.5	0.1
212	185	59	7537.	0.9	0.9	0.2%
213	182	43	4808.	0.5	0.5	0.1%
214	181	143	72196.	8.2	8.2	1.7%
215	180	287	875376.	100.0	100.0	20.9%
216	179	119	25852.	3.0	3.0	0.6%
217	178	143	101620.	11.6	11.6	2.4
222	167	43	5407.	0.6	0.6	0.1
223	166	143	35186.	4.0	4.0	0.8
224	165	35	5650.	0.6	0.6	0.1
225	164	119	18494.	2.1	2.1	0.4%
226	163	43	4818.	0.6	0.6	0.1%
227	162	71	5065.	0.6	0.6	0.1%
228	160	71	5663.	0.6	0.6	0.1%
229	159	35	4111.	0.5	0.5	0.1
230	156	29	4158.	0.5	0.5	0.1
232	153	59	10040.	1.1	1.1	0.2
233	152	43	4185.	0.5	0.5	0.1%
234	151	51	7434.	0.8	0.8	0.2
236	149	71	8483.	1.0	1.0	0.2%
237	148	51	5149.	0.6	0.6	0.1%
241	139	59	6225.	0.7	0.7	0.1
242	137	143	17098.	2.0	2.0	0.4%
244	135	287	868928.	99.3	99.3	20.7%
245	134	87	9806.	1.1	1.1	0.2%
246	133	87	12874.	1.5	1.5	0.3
247	131	35	3513.	0.4	0.4	0.1%
248	130	35	3974.	0.5	0.5	0.1
249	128	35	3959.	0.5	0.5	0.1
250	126	51	4734.	0.5	0.5	0.1
252	122	87	18006.	0.9	0.9	0.2%
253	121	143	58551.	6.7	6.7	1.4%
254	120	143	19386.	2.2	2.2	0.5%
255	119	175	97920.	11.2	11.2	2.3%
256	118	103	11737.	1.3	1.3	0.3%
257	117	71	8146.	0.9	0.9	0.2%
258	116	87	10495.	1.2	1.2	0.3%

DP0:2SN4IW.MS
SCAN: 1, 1/ 4/84 9:28

$(C_6H_5)_2SnBr_2.2HMPA$

IONISATION: EI
NO. PEAKS: 326
BASE/NREF INT: 686336./ 686336.
TIC: 3099392.
MASS RANGE: 69 - 779
RETN TIME/MISC: 0: 0/ 0/ 0/ 0
PAGE 1

PEAK NO.	MEASURED MASS	NO. POINTS	ABSOLUTE INTENSITY	% INT. BASE	% INT. NREF	% TOT. ION
33	600	29	3523.	0.51	0.51	0.11
42	544	43	3943.	0.57	0.57	0.13*
51	534	87	11095.	1.62	1.62	0.36*
52	533	35	4777.	0.70	0.70	0.15*
53	532	103	14222.	2.07	2.07	0.46
54	531	71	7418.	1.08	1.08	0.24*
55	530	87	15279.	2.23	2.23	0.49*
56	529	71	6522.	0.95	0.95	0.21*
57	528	71	7203.	1.05	1.05	0.23*
58	527	43	3696.	0.54	0.54	0.12*
62	519	43	4996.	0.73	0.73	0.16*
68	512	35	3999.	0.58	0.58	0.13
85	457	35	3966.	0.58	0.58	0.13
87	452	43	5872.	0.86	0.86	0.19*
91	450	59	6286.	0.92	0.92	0.20*
92	449	35	3498.	0.51	0.51	0.11*
104	395	51	4302.	0.63	0.63	0.14
109	391	43	4366.	0.64	0.64	0.14*
109	380	51	5349.	0.78	0.78	0.17*
111	378	71	7129.	1.04	1.04	0.23*
113	376	103	18518.	2.70	2.70	0.60*
114	375	51	5182.	0.76	0.76	0.17*
115	374	103	13004.	1.89	1.89	0.42*
116	373	43	5097.	0.74	0.74	0.16*
117	372	43	4680.	0.68	0.68	0.15*
126	360	103	16759.	2.44	2.44	0.54*
127	359	175	92924.	13.54	13.54	3.00*
128	358	71	8940.	1.30	1.30	0.29*
129	357	43	4185.	0.61	0.61	0.14*

PAGE 2

PEAK NO.	MEASURED MASS	NO. POINTS	ABSOLUTE INTENSITY	% INT. BASE	% INT NREF	% TOT. ION
132	353	43	4036.	0.59	0.59	0.13*
134	351	71	7025.	1.02	1.02	0.23*
135	350	43	4433.	0.65	0.65	0.14*
136	349	59	5960.	0.87	0.87	0.19*
140	345	87	12969.	1.89	1.89	0.42*
142	343	35	3961.	0.58	0.58	0.13*
159	314	87	12123.	1.77	1.77	0.39*
161	312	71	8852.	1.29	1.29	0.29*
170	299	43	4002.	0.58	0.58	0.13*
171	298	71	8824.	1.29	1.29	0.28*
172	297	59	5270.	0.77	0.77	0.17*
173	296	59	5611.	0.82	0.82	0.18*
174	295	51	3882.	0.57	0.57	0.13*
175	294	43	4235.	0.62	0.62	0.14
176	293	59	5037.	0.73	0.73	0.16
184	284	71	6455.	0.94	0.94	0.21*
186	282	35	4659.	0.68	0.68	0.15
187	281	43	4070.	0.59	0.59	0.13*
195	270	43	3685.	0.54	0.54	0.12*
214	226	51	5884.	0.86	0.86	0.19*
215	225	35	3610.	0.53	0.53	0.12*
218	211	43	4175.	0.61	0.61	0.13
225	202	59	5403.	0.79	0.79	0.17
226	201	59	5931.	0.86	0.86	0.19*
227	199	51	3900.	0.57	0.57	0.13*
228	198	43	3044.	0.44	0.44	0.10*
229	197	103	22335.	3.25	3.25	0.72*
230	196	71	7190.	1.05	1.05	0.23*
231	195	103	15793.	2.30	2.30	0.51*

PAGE 3

PEAK NO.	MEASURED MASS	NO. POINTS	ABSOLUTE INTENSITY	% INT. BASE	% INT. NREF	% TOT. ION
232	194	103	11082.	1.61	1.61	0.36*
233	193	87	9991.	1.46	1.46	0.32*
234	192	35	3658.	0.53	0.53	0.12*
241	180	239	686336.	100.00	100.00	22.14*
243	178	143	87424.	12.74	12.74	2.82*
274	135	287	618896.	90.17	90.17	19.97*
281	124	35	2983.	0.43	0.43	0.10*
282	122	59	5191.	0.76	0.76	0.17*
283	121	175	59789.	8.71	8.71	1.93*
284	120	143	20912.	3.05	3.05	0.67*
285	119	207	69740.	10.16	10.16	2.25*
286	118	87	11782.	1.72	1.72	0.38*
287	117	87	9150.	1.33	1.33	0.30*
288	116	59	6991.	1.02	1.02	0.23*
289	115	29	2064.	0.30	0.30	0.07
290	112	43	3029.	0.44	0.44	0.10*
291	108	51	5801.	0.85	0.85	0.19*
292	107	71	6445.	0.94	0.94	0.21*
293	106	51	5942.	0.87	0.87	0.19*
294	105	71	8131.	1.18	1.18	0.26*
295	104	21	1818.	0.26	0.26	0.06
296	103	25	2672.	0.39	0.39	0.09
297	102	35	3079.	0.45	0.45	0.10*
298	101	29	2974.	0.43	0.43	0.10*
299	100	21	1237.	0.18	0.18	0.04

DP4:2SNSIW.MS
SCAN: 1, 1/ 4/84 9:51

$(C_6H_5)_2SnI_2 \cdot 2HMPA$

IONISATION: EI
NO. PEAKS: 154
BASE/NREF INT: 1465024./ 1465024.
TIC: 4170560.
MASS RANGE: 69 - 850
RETN TIME/MISC: 0: 0/ 0/ 0/ 0

PEAK NO.	MEASURED MASS	NO. POINTS	ABSOLUTE INTENSITY	% INT. BASE	% INT. NREF	% TOT. ION
8	585	25	1520.	0.1	0.1	0.0
9	584	43	2911.	0.2	0.2	0.1
10	583	21	1124.	0.1	0.1	0.0
11	582	51	4256.	0.3	0.3	0.1
12	581	71	5371.	0.4	0.4	0.1*
13	580	87	24868.	1.7	1.7	0.6
14	579	87	11576.	0.8	0.8	0.3
15	578	87	16915.	1.2	1.2	0.4
16	577	51	7541.	0.5	0.5	0.2
17	576	87	14312.	1.0	1.0	0.3*
18	572	29	2008.	0.1	0.1	0.0
19	553	21	2057.	0.1	0.1	0.0
20	548	21	1403.	0.1	0.1	0.0
21	544	29	2795.	0.2	0.2	0.1
22	542	35	3260.	0.2	0.2	0.1
23	541	21	1065.	0.1	0.1	0.0
24	532	21	1248.	0.1	0.1	0.0
25	531	21	899.	0.1	0.1	0.0
26	530	51	5563.	0.4	0.4	0.1*
27	529	25	1871.	0.1	0.1	0.0
28	528	59	8331.	0.6	0.6	0.2*
29	527	35	3093.	0.2	0.2	0.1
30	526	43	4537.	0.3	0.3	0.1
31	502	21	1713.	0.1	0.1	0.0
32	488	43	4090.	0.3	0.3	0.1
33	479	25	2028.	0.1	0.1	0.0
34	470	25	2038.	0.1	0.1	0.0
35	464	35	2545.	0.2	0.2	0.1
36	452	35	1712.	0.1	0.1	0.0
37	451	21	1794.	0.1	0.1	0.0
38	450	21	1958.	0.1	0.1	0.0
39	430	21	1563.	0.1	0.1	0.0
40	426	71	6777.	0.5	0.5	0.2*
41	425	29	2350.	0.2	0.2	0.1
42	424	21	2604.	0.2	0.2	0.1
43	422	21	2457.	0.2	0.2	0.1
44	421	21	1194.	0.1	0.1	0.0
45	400	25	2294.	0.2	0.2	0.1
46	399	35	2450.	0.2	0.2	0.1
47	398	35	2035.	0.1	0.1	0.0
48	381	35	2561.	0.2	0.2	0.1
49	377	35	2004.	0.1	0.1	0.0
50	376	71	11319.	0.8	0.8	0.3
51	375	71	4996.	0.3	0.3	0.1
52	374	87	13671.	0.9	0.9	0.3*
53	373	43	5250.	0.4	0.4	0.1
54	372	21	2007.	0.1	0.1	0.0
55	361	35	3894.	0.3	0.3	0.1
56	360	119	37266.	2.5	2.5	0.9*
57	359	175	211072.	14.4	14.4	5.1
58	358	103	18807.	1.3	1.3	0.5
59	357	21	2163.	0.1	0.1	0.1
62	347	25	2116.	0.1	0.1	0.1
63	345	59	7322.	0.5	0.5	0.2
64	344	21	2405.	0.2	0.2	0.1
65	332	29	2154.	0.1	0.1	0.1
67	329	21	2013.	0.1	0.1	0.0
68	315	35	3292.	0.2	0.2	0.1
69	314	87	17352.	1.2	1.2	0.4
70	300	29	2531.	0.2	0.2	0.1
71	298	71	8360.	0.6	0.6	0.2*
72	297	21	3020.	0.2	0.2	0.1
73	296	29	2730.	0.2	0.2	0.1
74	295	25	2547.	0.2	0.2	0.1
95	197	71	9644.	0.7	0.7	0.2
96	196	43	3971.	0.3	0.3	0.1
97	195	71	7175.	0.5	0.5	0.2*
98	194	51	7220.	0.5	0.5	0.2*
99	193	35	2824.	0.2	0.2	0.1*
100	188	21	2448.	0.2	0.2	0.1
101	185	21	1912.	0.1	0.1	0.0
102	182	59	7661.	0.5	0.5	0.2*
103	181	175	130816.	8.9	8.9	3.1*
104	180	239	1465024.	100.0	100.0	35.1*
105	179	143	59367.	4.1	4.1	1.4
106	178	143	117692.	8.0	8.0	2.8
107	176	21	1484.	0.1	0.1	0.0
108	167	43	3452.	0.2	0.2	0.1
109	166	87	29616.	2.0	2.0	0.7
110	165	29	2196.	0.1	0.1	0.1
111	164	71	7488.	0.5	0.5	0.2*
112	163	43	4004.	0.3	0.3	0.1*
113	162	25	1691.	0.1	0.1	0.0
114	159	25	2401.	0.2	0.2	0.1
115	153	59	7256.	0.5	0.5	0.2*
116	149	71	7783.	0.5	0.5	0.2
117	145	25	2234.	0.2	0.2	0.1
118	137	103	12831.	0.9	0.9	0.3*
119	136	175	85380.	5.8	5.8	2.0*
120	135	287	958464.	65.4	65.4	23.0*
121	134	59	6521.	0.4	0.4	0.2*
122	133	71	9810.	0.7	0.7	0.2
123	131	21	1470.	0.1	0.1	0.0
124	124	35	2127.	0.1	0.1	0.1
125	122	59	6430.	0.4	0.4	0.2*
126	121	103	27808.	1.9	1.9	0.7
127	120	119	15836.	1.1	1.1	0.4*
128	119	175	95820.	6.5	6.5	2.3*
129	118	51	5251.	0.4	0.4	0.1*
130	117	43	4108.	0.3	0.3	0.1*
131	116	25	1684.	0.1	0.1	0.0

DP0:3PB1IW.MS $(C_6H_5)_3PbCl.HMPA$ 107
SCAN: 1. 1/ 5/84 9:47

IONISATION: EI
NO. PEAKS: 346
BASE/NREF INT: 3683072./ 3683072.
TIC: 14244352.
MASS RANGE: 68 - 809
RETN TIME/MISC: 0: 0/ 0/ 0/ 0
PAGE 1

PEAK NO.	MEASURED MASS	NO. POINTS	ABSOLUTE INTENSITY	% INT. BASE	% INT. NREF	% TOT. ION
15	650	103	6044.	0.16	0.16	0.04
17	644	103	3826.	0.10	0.10	0.03*
19	641	119	5219.	0.14	0.14	0.04*
21	618	207	14165.	0.38	0.38	0.10*
22	617	143	6537.	0.18	0.18	0.05*
23	616	119	6382.	0.17	0.17	0.04*
29	580	103	4860.	0.13	0.13	0.03*
31	567	103	6011.	0.16	0.16	0.04
37	540	71	4410.	0.12	0.12	0.03
40	537	119	4605.	0.13	0.13	0.03*
41	534	103	4048.	0.11	0.11	0.03
43	527	119	4750.	0.13	0.13	0.03*
46	522	143	5407.	0.15	0.15	0.04*
49	506	87	6122.	0.17	0.17	0.04
50	504	87	4242.	0.12	0.12	0.03
54	477	87	4916.	0.13	0.13	0.03
55	476	87	6197.	0.17	0.17	0.04
57	469	71	3740.	0.10	0.10	0.03
58	465	207	8283.	0.22	0.22	0.06*
59	464	287	16392.	0.45	0.45	0.12*
61	462	103	4074.	0.11	0.11	0.03*
67	449	87	3926.	0.11	0.11	0.03
69	447	71	4874.	0.13	0.13	0.03
70	440	143	8896.	0.24	0.24	0.06
71	439	287	19997.	0.54	0.54	0.14*
72	438	143	6680.	0.18	0.18	0.05*
73	437	143	6401.	0.17	0.17	0.04*
74	436	71	4017.	0.11	0.11	0.03
76	434	143	5566.	0.15	0.15	0.04*

PAGE 2

PEAK NO.	MEASURED MASS	NO. POINTS	ABSOLUTE INTENSITY	% INT. BASE	% INT. NREF	% TOT. ION
77	433	71	4869.	0.13	0.13	0.03
84	402	71	4296.	0.12	0.12	0.03
85	401	87	4379.	0.12	0.12	0.03
86	396	71	4055.	0.11	0.11	0.03
90	388	175	12385.	0.34	0.34	0.09*
91	387	415	46656.	1.27	1.27	0.33*
92	386	239	11079.	0.30	0.30	0.08*
93	385	207	12912.	0.35	0.35	0.09*
96	381	119	7461.	0.20	0.20	0.05
98	377	71	4041.	0.11	0.11	0.03
99	375	87	4032.	0.11	0.11	0.03
101	373	287	20823.	0.57	0.57	0.15*
102	372	119	4993.	0.14	0.14	0.04*
221	208	575	125368.	3.40	3.40	0.88*
222	207	415	48210.	1.31	1.31	0.34*
223	206	479	51580.	1.40	1.40	0.36*
242	180	959	3683072.	100.00	100.00	25.86*
244	178	831	481936.	13.09	13.09	3.38*
282	135	959	3080640.	83.64	83.64	21.63*

DR0:3PB2IW.MS $(C_6H_5)_3PbBr.HMPA$
SCAN: 1. 1/ 5/84 10:48

IONISATION: EI
NO. PEAKS: 460
BASE/NREF INT: 1915264./ 1915264.
TIC: 7352576.
MASS RANGE: 68 - 841
RETN TIME/MISC: 0: 0/ 0/ 0/ 0
PAGE 1

PEAK NO.	MEASURED MASS	NO. POINTS	ABSOLUTE INTENSITY	% INT. BASE	% INT. NREF	% TOT. ION
54	619	175	11870.	0.62	0.62	0.16*
55	618	351	37277.	1.95	1.95	0.51*
56	617	287	21170.	1.11	1.11	0.29*
57	616	175	7874.	0.41	0.41	0.11*
59	614	87	4670.	0.24	0.24	0.06
71	576	71	4000.	0.21	0.21	0.05
73	567	103	7235.	0.38	0.38	0.10
74	565	175	12249.	0.64	0.64	0.17*
80	555	119	4496.	0.23	0.23	0.06*
95	509	143	7800.	0.41	0.41	0.11*
96	508	175	7392.	0.39	0.39	0.10*
97	507	239	11468.	0.60	0.60	0.16*
98	506	143	6029.	0.31	0.31	0.08*
99	505	175	8281.	0.43	0.43	0.11*
100	504	103	4252.	0.22	0.22	0.06
108	480	143	5023.	0.26	0.26	0.07*
111	477	87	7293.	0.38	0.38	0.10
113	475	119	5377.	0.28	0.28	0.07*
118	468	87	4076.	0.21	0.21	0.06
119	466	119	5914.	0.31	0.31	0.08
121	464	287	26151.	1.37	1.37	0.36*
122	463	287	15817.	0.83	0.83	0.22*
123	462	287	21811.	1.14	1.14	0.30*
129	453	71	4576.	0.24	0.24	0.06
131	450	119	5393.	0.28	0.28	0.07*
137	441	143	6209.	0.32	0.32	0.08*
138	440	287	17372.	0.91	0.91	0.24*
139	439	415	63757.	3.33	3.33	0.87*
140	438	287	27079.	1.41	1.41	0.37
141	437	351	25819.	1.35	1.35	0.35*
146	430	119	6117.	0.32	0.32	0.08
153	413	119	5318.	0.28	0.28	0.07
155	411	87	6080.	0.32	0.32	0.08
156	407	87	4753.	0.25	0.25	0.06
157	404	175	7450.	0.39	0.39	0.10*
159	402	143	6044.	0.32	0.32	0.08*
160	401	71	5078.	0.27	0.27	0.07
166	390	87	3941.	0.21	0.21	0.05
168	388	207	13799.	0.72	0.72	0.19*
169	387	351	40807.	2.13	2.13	0.56
170	386	239	20766.	1.08	1.08	0.28*
171	385	287	13780.	0.72	0.72	0.19*
172	383	87	4238.	0.22	0.22	0.06*
175	378	103	9395.	0.49	0.49	0.13
178	375	143	6828.	0.36	0.36	0.09
180	373	175	7600.	0.40	0.40	0.10*
181	372	175	8332.	0.44	0.44	0.11*
182	371	103	5690.	0.30	0.30	0.08*
190	360	287	26855.	1.40	1.40	0.37*
191	359	575	178948.	9.34	9.34	2.43*
192	358	287	22548.	1.18	1.18	0.31*
193	357	351	31674.	1.65	1.65	0.43*
204	345	287	21714.	1.13	1.13	0.30*
227	314	287	25959.	1.36	1.36	0.35*
229	312	415	44917.	2.35	2.35	0.61*
241	298	287	22529.	1.18	1.18	0.31*
253	285	415	52823.	2.76	2.76	0.72
254	284	351	27577.	1.44	1.44	0.38*
255	283	287	26528.	1.39	1.39	0.36*
327	208	575	73848.	3.86	3.86	1.00*
328	207	415	34949.	1.82	1.82	0.48*
329	206	351	36310.	1.90	1.90	0.49*
355	180	959	1915264.	100.00	100.00	26.05*
357	178	703	276864.	14.46	14.46	3.77*
395	135	831	882624.	46.08	46.08	12.00*

DP0:3PB3IW.MS $(C_6H_5)_3PbI.HMPA$
SCAN: 1. 1/ 5/84 11:34

IONISATION: EI
NO. PEAKS: 337
BASE/NREF INT: 11894272./ 11894272.
TIC: 35454976.
MASS RANGE: 68 - 874
RETN TIME/MISC: 0: 0/ 0/ 0/ 0
PAGE 1

PEAK NO.	MEASURED MASS	NO. POINTS	ABSOLUTE INTENSITY	% INT. BASE	% INT. NREF	% TOT. ION
17	619	175	6511.	0.05	0.05	0.02*
18	618	415	17241.	0.14	0.14	0.05*
24	569	71	4042.	0.03	0.03	0.01
27	566	143	7905.	0.07	0.07	0.02
28	565	207	7289.	0.06	0.06	0.02*
32	540	287	20520.	0.17	0.17	0.06*
33	538	239	11319.	0.10	0.10	0.03*
34	531	143	6548.	0.06	0.06	0.02
35	530	143	7837.	0.07	0.07	0.02
36	529	103	3830.	0.03	0.03	0.01*
37	528	175	12967.	0.11	0.11	0.04
40	516	87	5274.	0.04	0.04	0.01
41	514	287	17391.	0.15	0.15	0.05*
42	513	143	5754.	0.05	0.05	0.02*
43	512	143	5741.	0.05	0.05	0.02*
46	487	143	3839.	0.03	0.03	0.01*
49	478	175	14116.	0.12	0.12	0.04
50	476	87	4621.	0.04	0.04	0.01
52	473	143	5254.	0.04	0.04	0.01*
53	472	143	7302.	0.06	0.06	0.02*
55	464	415	36539.	0.31	0.31	0.10*
56	463	207	11676.	0.10	0.10	0.03*
57	462	207	18924.	0.16	0.16	0.05
60	451	71	3908.	0.03	0.03	0.01
61	450	239	14832.	0.12	0.12	0.04*
63	447	71	4152.	0.03	0.03	0.01
66	441	143	6381.	0.05	0.05	0.02*
67	440	351	23445.	0.20	0.20	0.07*
68	439	479	37857.	0.32	0.32	0.11*

PAGE 2

PEAK NO.	MEASURED MASS	NO. POINTS	ABSOLUTE INTENSITY	% INT. BASE	% INT. NREF	% TOT. ION
69	438	87	3981.	0.03	0.03	0.01
71	434	103	4830.	0.04	0.04	0.01
76	423	87	4309.	0.04	0.04	0.01
77	419	87	3801.	0.03	0.03	0.01
84	400	103	3693.	0.03	0.03	0.01*
86	395	143	7411.	0.06	0.06	0.02*
87	389	103	5987.	0.05	0.05	0.02
88	388	351	26329.	0.22	0.22	0.07*
89	387	703	213232.	1.79	1.79	0.60*
90	386	415	98512.	0.83	0.83	0.28
91	385	415	63049.	0.53	0.53	0.18
92	384	87	6253.	0.05	0.05	0.02
95	375	103	4091.	0.03	0.03	0.01*
96	374	415	22718.	0.19	0.19	0.06*
97	373	415	18022.	0.15	0.15	0.05*
98	372	351	26741.	0.22	0.22	0.08*
107	360	959	1755904.	14.76	14.76	4.95*
208	208	703	282032.	2.37	2.37	0.80*
209	207	575	129224.	1.09	1.09	0.36
210	206	959	180988.	1.52	1.52	0.51*
233	180	959	11894272.	100.00	100.00	33.55*
272	135	959	7520000.	63.22	63.22	21.21*

DP0:2PB1IW.MS $(C_6H_5)_2PbBr_2$.HMPA
SCAN: 1, 1/ 5/84 11:52

IONISATION: EI
NO. PEAKS: 479
BASE/NREF INT: 4933120./ 4933120.
TIC: 18579456.
MASS RANGE: 68 - 844
RETN TIME/MISC: 0: 0/ 0/ 0/ 0
PAGE 1

PEAK NO.	MEASURED MASS	NO. POINTS	ABSOLUTE INTENSITY	% INT. BASE	% INT. NREF	% TOT. ION
33	695	103	5963.	0.12	0.12	0.03*
53	625	119	6426.	0.13	0.13	0.03
57	621	143	6231.	0.13	0.13	0.03*
58	620	143	9966.	0.20	0.20	0.05*
59	619	143	7330.	0.15	0.15	0.04*
60	618	239	15538.	0.31	0.31	0.08*
61	617	143	6119.	0.12	0.12	0.03*
62	616	103	6437.	0.13	0.13	0.03
69	606	143	7241.	0.15	0.15	0.04*
70	604	143	7447.	0.15	0.15	0.04*
74	591	239	10656.	0.22	0.22	0.06*
89	552	119	5375.	0.11	0.11	0.03*
90	551	143	5355.	0.11	0.11	0.03*
103	531	143	9986.	0.20	0.20	0.05*
104	530	143	5834.	0.12	0.12	0.03
108	526	103	5607.	0.11	0.11	0.03*
115	513	143	8900.	0.18	0.18	0.05*
135	468	175	8406.	0.17	0.17	0.05
137	466	175	12242.	0.25	0.25	0.07*
138	465	207	10350.	0.21	0.21	0.06*
139	464	287	22916.	0.46	0.46	0.12*
140	463	175	10932.	0.22	0.22	0.06*
141	462	175	8668.	0.18	0.18	0.05*
146	452	175	7397.	0.15	0.15	0.04*
148	450	175	13016.	0.26	0.26	0.07*
149	449	103	5180.	0.11	0.11	0.03
150	448	103	4947.	0.10	0.10	0.03*
152	446	143	5371.	0.11	0.11	0.03*
155	441	119	5020.	0.10	0.10	0.03*

PAGE 2

PEAK NO.	MEASURED MASS	NO. POINTS	ABSOLUTE INTENSITY	% INT. BASE	% INT. NREF	% TOT. ION
156	440	143	5598.	0.11	0.11	0.03*
157	439	287	26929.	0.55	0.55	0.14*
159	437	207	10127.	0.21	0.21	0.05*
167	427	87	5237.	0.11	0.11	0.03
187	394	143	7975.	0.16	0.16	0.04*
191	390	119	5673.	0.11	0.11	0.03*
192	389	119	5436.	0.11	0.11	0.03*
193	388	143	7430.	0.15	0.15	0.04*
194	387	239	21136.	0.43	0.43	0.11*
195	386	143	6630.	0.13	0.13	0.04*
196	385	119	4983.	0.10	0.10	0.03*
198	382	287	19836.	0.40	0.40	0.11*
202	378	103	9116.	0.18	0.18	0.05
204	376	119	6841.	0.14	0.14	0.04*
205	375	175	8076.	0.16	0.16	0.04*
206	374	351	22083.	0.45	0.45	0.12*
207	373	287	16054.	0.33	0.33	0.09*
208	372	143	6450.	0.13	0.13	0.03*
216	360	703	496048.	10.06	10.06	2.67*
346	208	479	84748.	1.72	1.72	0.46*
348	206	415	55311.	1.12	1.12	0.30*
373	180	959	4933120.	100.00	100.00	26.55*
375	178	575	620960.	12.59	12.59	3.34
386	166	703	537808.	10.90	10.90	2.89*
413	135	959	3984960.	80.78	80.78	21.45*

$(C_6H_5)_2PbI_2$.HMPA

DP0:2PB2IW.MS
SCAN: 1, 1/ 5/84 13:14

IONISATION: EI
NO. PEAKS: 496
BASE/NREF INT: 3995392./ 3995392.
TIC: 16644096.
MASS RANGE: 68 - 896
RETN TIME/MISC: 0: 0/ 0/ 0/ 0
PAGE 1

PEAK NO.	MEASURED MASS	NO. POINTS	ABSOLUTE INTENSITY	% INT. BASE	% INT. NREF	% TOT. ION
28	693	143	6132.	0.15	0.15	0.04*
30	691	175	9995.	0.25	0.25	0.06
33	688	143	7948.	0.20	0.20	0.05*
35	679	119	6002.	0.15	0.15	0.04*
44	663	87	4459.	0.11	0.11	0.03
46	655	87	4716.	0.12	0.12	0.03
62	618	103	4891.	0.12	0.12	0.03*
65	603	143	5966.	0.15	0.15	0.04*
72	593	143	7129.	0.18	0.18	0.04*
77	581	71	4841.	0.12	0.12	0.03
82	568	87	5334.	0.13	0.13	0.03
93	551	87	5104.	0.13	0.13	0.03
95	549	103	5592.	0.14	0.14	0.03*
98	545	143	7174.	0.18	0.18	0.04*
101	539	119	6493.	0.16	0.16	0.04
102	538	87	4621.	0.12	0.12	0.03
105	535	87	4822.	0.12	0.12	0.03
108	532	175	7075.	0.18	0.18	0.04
110	530	175	8088.	0.20	0.20	0.05*
115	525	103	4631.	0.12	0.12	0.03*
119	521	71	5294.	0.13	0.13	0.03
121	519	71	4401.	0.11	0.11	0.03
123	514	287	21249.	0.53	0.53	0.13*
124	513	207	8627.	0.22	0.22	0.05*
125	512	143	7828.	0.20	0.20	0.05*
132	500	119	5146.	0.13	0.13	0.03*
139	491	143	8875.	0.22	0.22	0.05*
142	481	119	4617.	0.12	0.12	0.03*
143	479	143	5193.	0.13	0.13	0.03*
153	464	287	11530.	0.29	0.29	0.07*
155	462	103	7407.	0.19	0.19	0.04
163	450	175	16008.	0.40	0.40	0.10*
165	448	119	6875.	0.17	0.17	0.04*
169	439	175	7119.	0.18	0.18	0.04*
172	436	175	9203.	0.23	0.23	0.06*
173	435	87	4869.	0.12	0.12	0.03*
174	434	103	5409.	0.14	0.14	0.03*
176	429	143	6203.	0.16	0.16	0.04*
179	425	143	6342.	0.16	0.16	0.04*
181	423	119	5240.	0.13	0.13	0.03*
184	419	119	5571.	0.14	0.14	0.03*
192	406	87	4582.	0.11	0.11	0.03
194	404	119	4730.	0.12	0.12	0.03*
195	403	103	5169.	0.13	0.13	0.03*
197	401	119	6643.	0.17	0.17	0.04*
201	396	87	5240.	0.13	0.13	0.03*
204	390	143	7507.	0.19	0.19	0.05*
206	388	207	13323.	0.33	0.33	0.08*
207	387	479	86772.	2.17	2.17	0.52*
208	386	415	31452.	0.79	0.79	0.19*
209	385	351	40138.	1.00	1.00	0.24*
211	383	119	5012.	0.13	0.13	0.03*
212	382	103	5288.	0.13	0.13	0.03
213	381	119	5359.	0.13	0.13	0.03
217	377	103	5775.	0.14	0.14	0.03*
218	376	143	8516.	0.21	0.21	0.05*
219	375	143	7123.	0.18	0.18	0.04*
220	374	351	25456.	0.64	0.64	0.15*
221	373	287	17993.	0.45	0.45	0.11*
222	372	207	16276.	0.41	0.41	0.10*
223	371	143	12409.	0.31	0.31	0.07
362	208	575	203164.	5.08	5.08	1.22*
363	207	479	86568.	2.17	2.17	0.52*
364	206	575	101440.	2.54	2.54	0.61*
390	180	959	3995392.	100.00	100.00	24.00*
392	178	831	581040.	14.54	14.54	3.49*
403	166	575	412912.	10.33	10.33	2.48*
431	135	959	313766[illegible]	78.57	[illegible]	[illegible]*

DP4:2PB3IW.MS $(C_6H_5)_2PbCl_2.2HMPA$
SCAN: 1. 1/ 5/84 13:37

IONISATION: EI
NO. PEAKS: 695
BASE/NREF INT: 21312512./ 21312512.
TIC: 83030016.
MASS RANGE: 68 - 895
RETN TIME/MISC: 0: 0/ 0/ 0/ 0

PEAK NO.	MEASURED MASS	NO. POINTS	ABSOLUTE INTENSITY	% INT. BASE	% INT. NREF	% TOT. ION
161	619	351	37915.	0.2	0.2	0.0*
162	618	415	104904.	0.5	0.5	0.1
163	617	351	47586.	0.2	0.2	0.1*
164	616	351	55264.	0.3	0.3	0.1*
174	604	239	22423.	0.1	0.1	0.0
175	603	287	22496.	0.1	0.1	0.0
177	601	287	35540.	0.2	0.2	0.0*
198	578	415	54102.	0.3	0.3	0.1*
199	577	351	49540.	0.2	0.2	0.1*
200	576	479	138676.	0.7	0.7	0.2*
201	575	415	60733.	0.3	0.3	0.1*
202	574	351	60714.	0.3	0.3	0.1*
214	562	287	22687.	0.1	0.1	0.0*
242	531	351	28761.	0.1	0.1	0.0
243	530	351	51205.	0.2	0.2	0.1*
244	529	351	30826.	0.1	0.1	0.0*
245	528	575	65632.	0.3	0.3	0.1*
246	527	351	25627.	0.1	0.1	0.0*
247	526	351	33858.	0.2	0.2	0.0*
302	465	287	23798.	0.1	0.1	0.0
303	464	479	148088.	0.7	0.7	0.2*
304	463	415	88524.	0.4	0.4	0.1
305	462	479	98092.	0.5	0.5	0.1
316	450	415	35734.	0.2	0.2	0.0*
317	449	287	41870.	0.2	0.2	0.1*
326	440	351	21924.	0.1	0.1	0.0*
327	439	479	137124.	0.6	0.6	0.2
328	438	415	69036.	0.3	0.3	0.1
329	437	415	70772.	0.3	0.3	0.1
341	424	351	31108.	0.1	0.1	0.0*
342	423	287	24492.	0.1	0.1	0.0
343	422	479	122844.	0.6	0.6	0.1*
344	421	415	45641	0.2	0.2	0.1*
345	420	479	44346.	0.2	0.2	0.1*
367	397	287	25676	0.1	0.1	0.0*
376	388	287	22712.	0.1	0.1	0.0*
377	387	575	76248.	0.4	0.4	0.1*
378	386	351	27177.	0.1	0.1	0.0*
379	385	415	44160.	0.2	0.2	0.1*
390	374	351	27408.	0.1	0.1	0.0*
391	373	703	100656.	0.5	0.5	0.1*
392	372	415	51125.	0.2	0.2	0.1*
393	371	351	34506.	0.2	0.2	0.0*
403	360	831	1214144.	5.7	5.7	1.5*
404	359	575	1574464.	7.4	7.4	1.9*
462	298	575	66896.	0.3	0.3	0.1*
475	285	575	212480.	1.0	1.0	0.3*
476	284	575	120516.	0.6	0.6	0.1*
477	283	575	94416.	0.4	0.4	0.1*
490	270	575	98464.	0.5	0.5	0.1*
534	226	479	74172.	0.3	0.3	0.1*
550	210	415	65784.	0.3	0.3	0.1*
552	208	703	184428.	0.9	0.9	0.2*
553	207	703	83016.	0.4	0.4	0.1*
554	206	575	91732.	0.4	0.4	0.1*
580	180	959	6451200.	30.3	30.3	7.8*
581	180	703	9417728.	44.2	44.2	11.3* ^
582	180	959	21312512.	100.0	100.0	25.7* ^
627	135	959	12090112.	56.7	56.7	14.6*
628	135	959	4237312.	19.9	19.9	5.1*

DP4:2PB4IW.MS $(C_6H_5)_2PbBr_2.2HMPA$
SCAN: 1, 1/ 5/84 14:23

IONISATION: EI
NO. PEAKS: 512
BASE/NREF INT: 18992128./ 18992128.
TIC: 51037184.
MASS RANGE: 68 - 896
RETN TIME/MISC: 0: 0/ 0/ 0/ 0
PAGE 1

PEAK NO.	MEASURED MASS	NO. POINTS	ABSOLUTE INTENSITY	% INT. BASE	% INT. NREF	% TOT. ION
155	466	351	28514.	0.2	0.2	0.1*
157	464	479	35524.	0.2	0.2	0.1*
170	449	415	42055.	0.2	0.2	0.1*
196	405	287	19070.	0.1	0.1	0.0*
208	391	207	10843.	0.1	0.1	0.0*
209	390	207	15643.	0.1	0.1	0.0*
210	389	175	10017.	0.1	0.1	0.0*
212	387	479	48087.	0.3	0.3	0.1
214	385	175	16499.	0.1	0.1	0.0*
218	381	287	20025.	0.1	0.1	0.0*
226	373	415	75340.	0.4	0.4	0.1
227	372	351	27940.	0.1	0.1	0.1*
238	361	415	25403.	0.1	0.1	0.0*
239	360	703	285888.	1.5	1.5	0.6*
240	359	831	1652544.	8.7	8.7	3.2*
241	358	575	163412.	0.9	0.9	0.3*
242	357	575	154456.	0.8	0.8	0.3*
244	355	287	23696.	0.1	0.1	0.0*
252	346	287	41672.	0.2	0.2	0.1*
253	345	575	266560.	1.4	1.4	0.5*
254	344	351	46804.	0.2	0.2	0.1
255	343	351	53977.	0.3	0.3	0.1*
264	331	239	25087.	0.1	0.1	0.0*
277	315	287	32788.	0.2	0.2	0.1*
278	314	479	105196.	0.6	0.6	0.2*
279	313	287	24094.	0.1	0.1	0.0*
280	312	479	120096.	0.6	0.6	0.2*
291	300	479	56370.	0.3	0.3	0.1*
292	299	479	30897.	0.2	0.2	0.1*

PAGE 2

PEAK NO.	MEASURED MASS	NO. POINTS	ABSOLUTE INTENSITY	% INT. BASE	% INT. NREF	% TOT. ION
293	298	479	51990.	0.3	0.3	0.1*
304	286	287	24985.	0.1	0.1	0.0*
305	285	351	21518.	0.1	0.1	0.0*
306	284	351	35194.	0.2	0.2	0.1*
307	283	351	19501.	0.1	0.1	0.0*
318	271	287	19878.	0.1	0.1	0.0*
319	270	351	55880.	0.3	0.3	0.1*
330	258	415	28287.	0.1	0.1	0.1*
332	256	415	52412.	0.3	0.3	0.1*
334	254	351	34292.	0.2	0.2	0.1
345	240	287	34296.	0.2	0.2	0.1*
346	239	351	25550.	0.1	0.1	0.1*
357	227	287	28764.	0.2	0.2	0.1*
358	226	287	41384.	0.2	0.2	0.1
359	225	575	69060.	0.4	0.4	0.1*
372	211	351	48377.	0.3	0.3	0.1
373	210	415	61791.	0.3	0.3	0.1*
375	208	479	85328.	0.4	0.4	0.2*
376	207	415	27126.	0.1	0.1	0.1*
377	206	351	19126.	0.1	0.1	0.0*
381	202	287	28862.	0.2	0.2	0.1*

DP4:2PB5IW.MS $(C_6H_5)_2PbI_2 \cdot 2HMPA$
SCAN: 1, 1/ 5/84 14: 9

IONISATION: EI
NO. PEAKS: 564
BASE/NREF INT: 18313216./ 18313216.
TIC: 59694080.
MASS RANGE: 68 - 870
RETN TIME/MISC: 0: 0/ 0/ 0/ 0

NO.	MASS	POINTS	INTENSITY	BASE	NREF	ION
43	693	287	27506.	0.2	0.2	0.0*
45	691	239	16782.	0.1	0.1	0.0*
54	677	207	9241.	0.1	0.1	0.0*
125	554	143	10682.	0.1	0.1	0.0*
126	553	175	12382.	0.1	0.1	0.0
130:	549	239	20188.	0.1	0.1	0.0
138	538	207	10464.	0.1	0.1	0.0*
143	533	239	13411.	0.1	0.1	0.0*
146	530	287	17173.	0.1	0.1	0.0*
148	528	239	18563.	0.1	0.1	0.0*
150	526	239	12108.	0.1	0.1	0.0*
152	524	287	17104.	0.1	0.1	0.0*
160	514	287	27697.	0.2	0.2	0.0
161	513	239	17787.	0.1	0.1	0.0
162	512	207	14937.	0.1	0.1	0.0*
168	504	175	11261.	0.1	0.1	0.0*
187	477	143	11153.	0.1	0.1	0.0*
197	463	239	10407.	0.1	0.1	0.0*
207	450	239	15250.	0.1	0.1	0.0*
208	449	351	37751.	0.2	0.2	0.1*
209	448	207	13203.	0.1	0.1	0.0*
210	447	287	17633.	0.1	0.1	0.0
218	435	207	10002.	0.1	0.1	0.0*
234	417	143	9602.	0.1	0.1	0.0*
236	415	175	9858.	0.1	0.1	0.0*
239	411	143	9814.	0.1	0.1	0.0*
260	387	479	74164.	0.4	0.4	0.1
261	386	351	34909.	0.2	0.2	0.1*
262	385	351	34103.	0.2	0.2	0.1*
266	381	287	18381.	0.1	0.1	0.0*
273	374	287	18557.	0.1	0.1	0.0*
274	373	479	75856.	0.4	0.4	0.1*
275	372	239	21107.	0.1	0.1	0.0*
285	361	207	31125.	0.2	0.2	0.1*
286	360	703	308352.	1.7	1.7	0.5*
287	359	959	1974144.	10.8	10.8	3.3*
288	358	351	98216.	0.5	0.5	0.2*
289	357	479	183328.	1.0	1.0	0.3*
299	346	351	69144.	0.4	0.4	0.1*
300	345	575	334144.	1.8	1.8	0.6*
301	344	351	32672.	0.2	0.2	0.1*
302	343	415	69276.	0.4	0.4	0.1*
314	331	351	36733.	0.2	0.2	0.1*
316	329	287	27810.	0.2	0.2	0.0*
327	315	351	40621.	0.2	0.2	0.1*
328	314	479	120024.	0.7	0.7	0.2*
329	313	287	23969.	0.1	0.1	0.0*
330	312	479	127404.	0.7	0.7	0.2
339	300	479	54455.	0.3	0.3	0.1*
340	299	415	31969.	0.2	0.2	0.1*
341	298	479	60216.	0.3	0.3	0.1*
351	286	239	23829.	0.1	0.1	0.0*
353	284	287	25305.	0.1	0.1	0.0*
364	272	415	45150.	0.2	0.2	0.1*
365	271	351	34997.	0.2	0.2	0.1*
366	270	479	113676.	0.6	0.6	0.2*
367	269	287	19540.	0.1	0.1	0.0*
368	268	287	28234.	0.2	0.2	0.0*
379	256	287	19789.	0.1	0.1	0.0*
381	254	351	40076.	0.2	0.2	0.1*
383	252	287	22923.	0.1	0.1	0.0*
392	240	287	42949.	0.2	0.2	0.1
404	227	351	30314.	0.2	0.2	0.1*
405	226	479	67800.	0.4	0.4	0.1*
406	225	415	35343.	0.2	0.2	0.1*
407	224	479	28763.	0.2	0.2	0.0*
421	210	479	93364.	0.5	0.5	0.2
423	208	703	134092.	0.7	0.7	0.2*
424	207	479	41486.	0.2	0.2	0.1*
425	206	479	58619.	0.3	0.3	0.1*
429	202	351	23903.	0.1	0.1	0.0*

DP1:712AF2.MS $(C_6H_5)_4Sn$/Sulfolane
SCAN: 1, 7/12/84 10:46

IONISATION: EI
NO. PEAKS: 206
BASE/NREF INT: 149296./ 149296.
TIC: 1740160.
MASS RANGE: 76 - 663
RETN TIME/MISC: 0: 0/ 0/ 0/ 0
PAGE 1

PEAK NO.	MEASURED MASS	NO. POINTS	ABSOLUTE INTENSITY	% INT. BASE	% INT. NREF	% TOT. ION
1	663	35	2300.	1.5	1.5	0.1
2	623	29	1689.	1.1	1.1	0.1
3	621	35	2218.	1.5	1.5	0.1
4	591	35	3169.	2.1	2.1	0.2
5	589	29	2373.	1.6	1.6	0.1
6	545	43	2727.	1.8	1.8	0.2
9	487	35	2471.	1.7	1.7	0.1
10	477	29	1766.	1.2	1.2	0.1
11	475	43	5355.	3.6	3.6	0.3
12	473	43	6915.	4.6	4.6	0.4
13	472	43	7184.	4.8	4.8	0.4
14	471	51	26689.	17.9	17.9	1.5
15	470	59	14515.	9.7	9.7	0.8
16	469	51	22773.	15.3	15.3	1.3
17	468	43	11421.	7.6	7.6	0.7
18	467	59	17958.	12.0	12.0	1.0
19	466	43	5155.	3.5	3.5	0.3
20	465	51	4201.	2.8	2.8	0.2
21	464	43	3560.	2.4	2.4	0.2
22	463	43	3212.	2.2	2.2	0.2
23	455	35	3755.	2.5	2.5	0.2
24	453	35	3741.	2.5	2.5	0.2
25	451	29	2718.	1.8	1.8	0.2
26	437	29	2412.	1.6	1.6	0.1
27	435	29	2766.	1.9	1.9	0.2
29	429	29	2404.	1.6	1.6	0.1
30	428	29	2085.	1.4	1.4	0.1
31	427	43	6092.	4.1	4.1	0.4
32	426	35	3679.	2.5	2.5	0.2
33	425	43	5599.	3.8	3.8	0.3
34	424	29	1542.	1.0	1.0	0.1
35	423	43	5002.	3.4	3.4	0.3
56	355	59	18046.	12.1	12.1	1.0
58	353	51	16137.	10.8	10.8	0.9
59	352	51	19106.	12.8	12.8	1.1
60	351	71	102832.	68.9	68.9	5.9
61	350	71	42575.	28.5	28.5	2.4
62	349	71	82160.	55.0	55.0	4.7
63	348	71	43254.	29.0	29.0	2.5
64	347	87	93272.	62.5	62.5	5.4
65	346	59	23434.	15.7	15.7	1.3
66	345	71	37897.	25.4	25.4	2.2
67	344	59	14652.	9.8	9.8	0.8
68	343	59	20779.	13.9	13.9	1.2
77	317	51	12451.	8.3	8.3	0.7
79	315	51	9495.	6.4	6.4	0.5
81	313	51	7634.	5.1	5.1	0.4
91	291	43	8585.	5.8	5.8	0.5
102	275	59	9059.	6.1	6.1	0.5
103	274	51	7557.	5.1	5.1	0.4
104	273	71	17751.	11.9	11.9	1.0
106	271	51	10329.	6.9	6.9	0.6
108	269	71	11976.	8.0	8.0	0.7
146	201	59	17416.	11.7	11.7	1.0
147	199	59	12469.	8.4	8.4	0.7
149	197	87	91528.	61.3	61.3	5.3
150	196	71	30521.	20.4	20.4	1.8
151	195	71	68864.	46.1	46.1	4.0
152	194	59	26310.	17.6	17.6	1.5
153	193	87	41178.	27.6	27.6	2.4
181	135	103	16505.	11.1	11.1	0.9
190	122	103	15473.	10.4	10.4	0.9
192	120	119	149296.	100.0	100.0	8.6
193	119	103	13196.	8.8	8.8	0.8
194	118	103	25443.	17.0	17.0	1.5
196	116	71	14802.	9.9	9.9	0.9

703MD2.1 [TIC=7755008, 100%=1694784] EI

BTMAH/GLY/5H2O

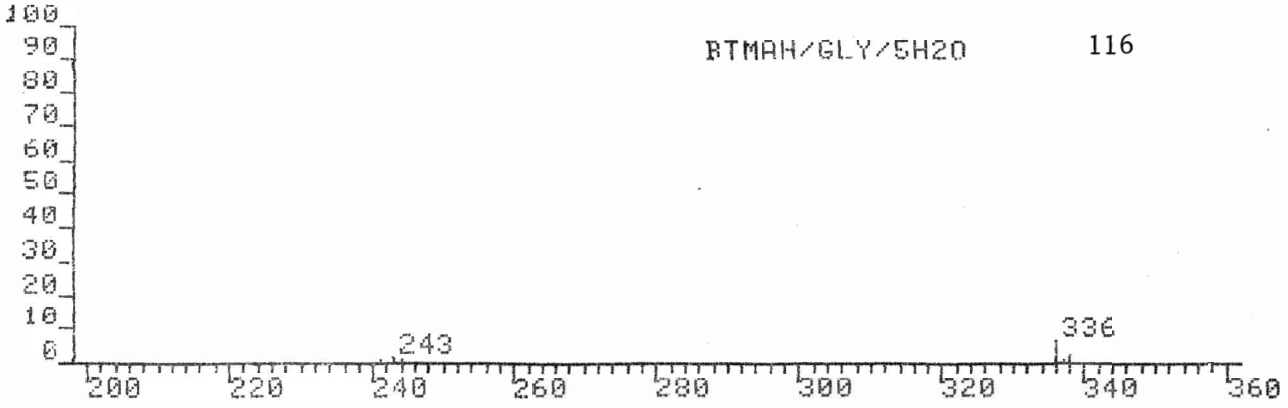

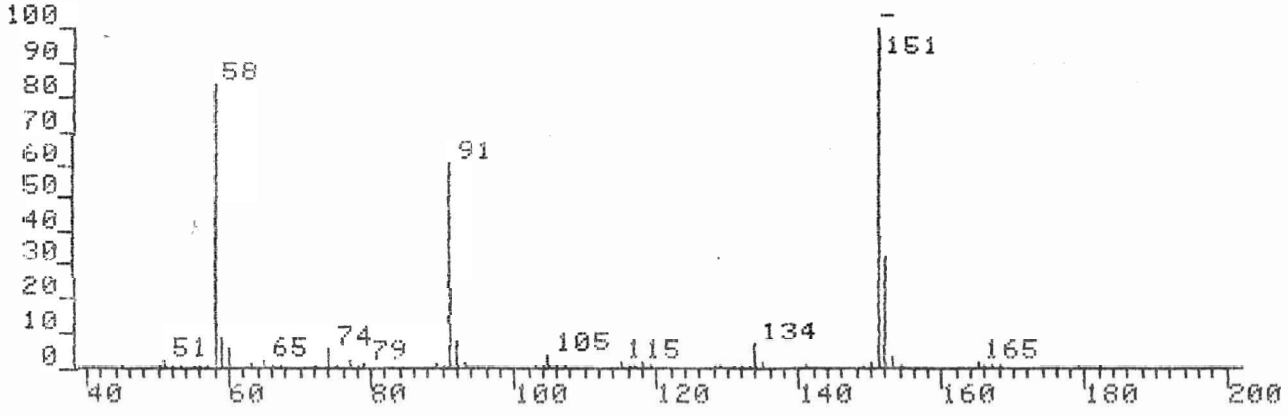

703MD2.1 [TIC=7755008, 100%=58165] EI

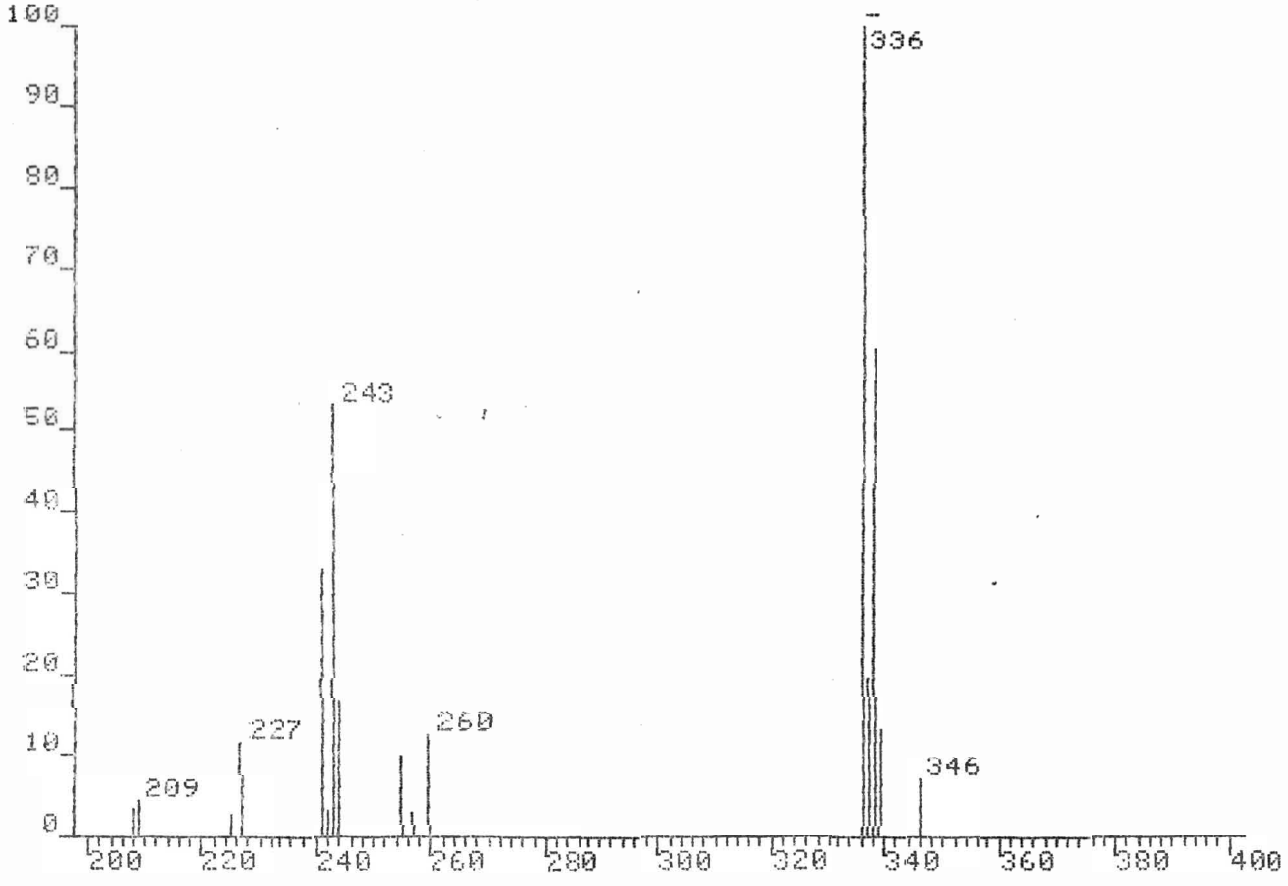

DP1:703MD2.MS BTMAH/Gly/5H_2O
SCAN: 1, 7/ 3/84 17:34

IONISATION: EI
NO. PEAKS: 207
BASE/NREF INT: 1694784./ 1694784.
TIC: 7755008.
MASS RANGE: 45.1512 - 346.4650
RETN TIME/MISC: 0: 0/ 0/ 0/ 0
PAGE 1

PEAK NO.	MEASURED MASS	NO. POINTS	ABSOLUTE INTENSITY	% INT. BASE	% INT. NREF	% TOT. ION
6	338	51	15730.	0.9	0.9	0.2
7	338	51	19206.	1.1	1.1	0.2
8	337	43	11439.	0.7	0.7	0.1
9	336	59	47418.	2.8	2.8	0.6
10	336	59	58165.	3.4	3.4	0.8
19	243	51	13649.	0.8	0.8	0.2
20	243	51	17278.	1.0	1.0	0.2
22	241	43	9494.	0.6	0.6	0.1
23	241	43	9851.	0.6	0.6	0.1
54	165	43	11158.	0.7	0.7	0.1
55	165	51	12928.	0.8	0.8	0.2
62	153	59	20617.	1.2	1.2	0.3
63	153	51	22766.	1.3	1.3	0.3
64	152	71	181348.	10.7	10.7	2.3
65	152	71	166516.	9.8	9.8	2.1
66	152	87	191124.	11.3	11.3	2.5
67	151	207	1462464.	86.3	86.3	18.9^
68	151	239	1694784.	100.0	100.0	21.9^
133	91	103	487680.	28.8	28.8	6.3
134	91	103	537104.	31.7	31.7	6.9
182	58	87	445840.	26.3	26.3	5.7
183	58	103	478032.	28.2	28.2	6.2
184	58	87	498288.	29.4	29.4	6.4

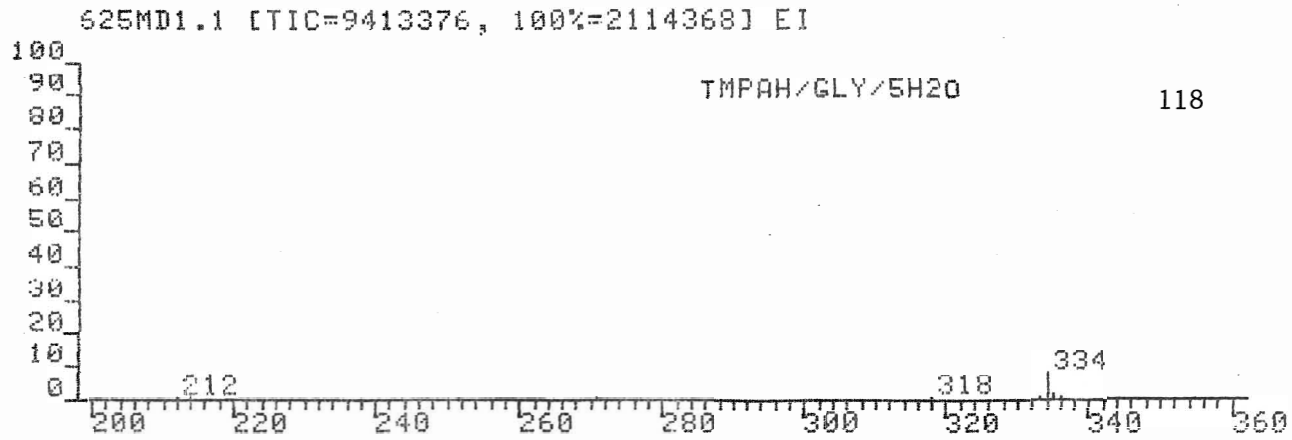
625MD1.1 [TIC=9413376, 100%=2114368] EI
TMPAH/GLY/5H2O
212
318
334

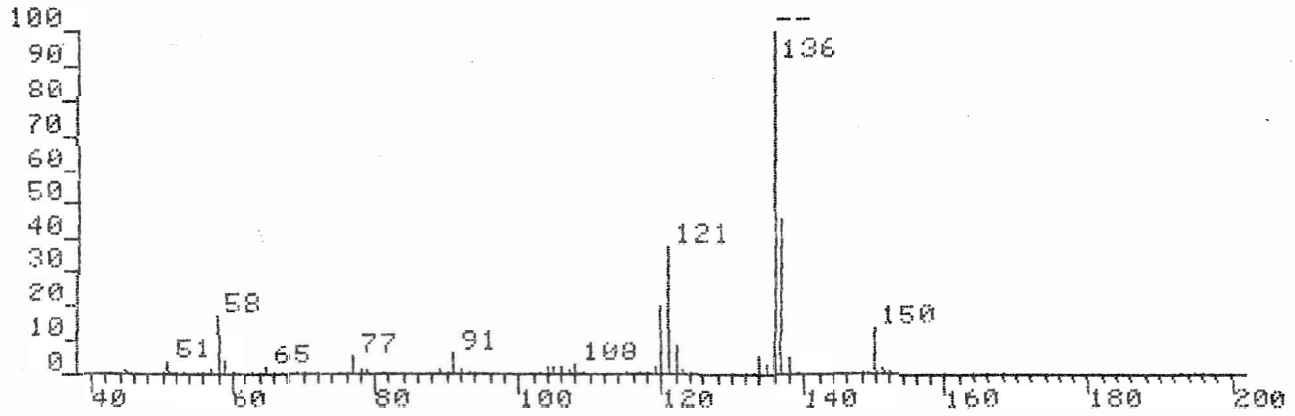
136
121
58
150
51
65
77
91
100

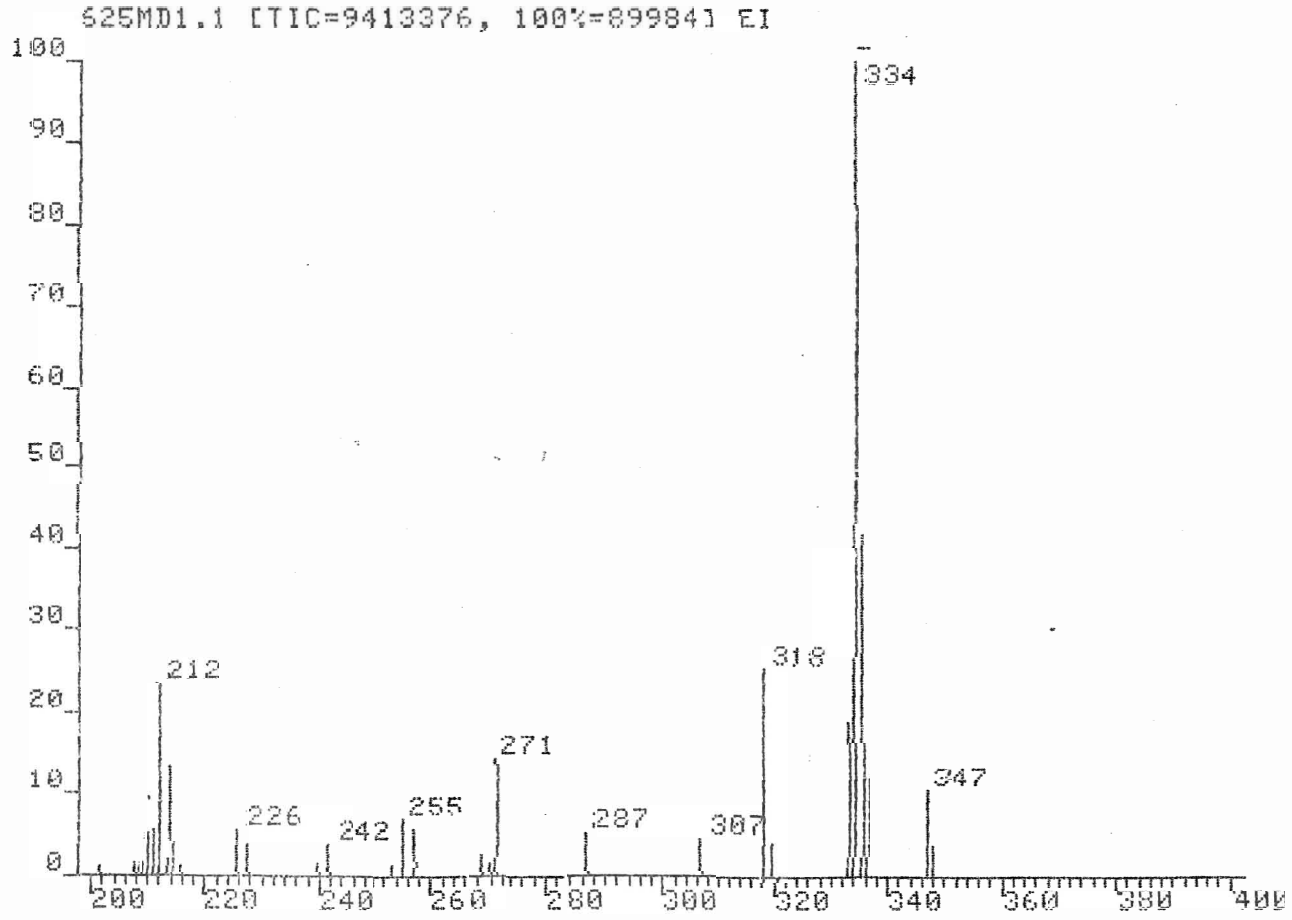
625MD1.1 [TIC=9413376, 100%=899841 EI
334
212
318
271
347
226
242
255
287
307

DP1:625MD1.MS TMPAH/Gly/5H_2O

SCAN: 1. 6/25/84 18:47

IONISATION: EI
NO. PEAKS: 303
BASE/NREF INT: 2114368./ 2114368.
TIC: 9413376.
MASS RANGE: 44.9517 - 348.2356
RETN TIME/MISC: 0: 0/ 0/ 0/ 0
PAGE 1

PEAK NO.	MEASURED MASS	NO. POINTS	ABSOLUTE INTENSITY	% INT. BASE	% INT. NREF	% TOT. ION
1	348	29	1268.	0.1	0.1	0.0
2	348	35	1844.	0.1	0.1	0.0
3	347	29	2154.	0.1	0.1	0.0
4	347	35	3397.	0.2	0.2	0.0
5	347	35	3789.	0.2	0.2	0.0
6	336	35	2880.	0.1	0.1	0.0
7	336	35	4142.	0.2	0.2	0.0
8	336	35	3491.	0.2	0.2	0.0
9	335	51	17984.	0.9	0.9	0.2
10	335	51	19529.	0.9	0.9	0.2
11	334	59	80140.	3.8	3.8	0.9
12	334	87	89984.	4.3	4.3	1.0
13	333	43	8430.	0.4	0.4	0.1
14	333	35	8435.	0.4	0.4	0.1
15	319	29	1461.	0.1	0.1	0.0
16	319	29	1937.	0.1	0.1	0.0
17	318	43	7495.	0.4	0.4	0.1
18	318	43	8106.	0.4	0.4	0.1
19	318	43	7130.	0.3	0.3	0.1
20	307	35	2080.	0.1	0.1	0.0
21	307	29	1991.	0.1	0.1	0.0
25	271	35	4116.	0.2	0.2	0.0
26	271	35	4318.	0.2	0.2	0.0
27	271	35	4572.	0.2	0.2	0.0
29	269	29	2414.	0.1	0.1	0.0
31	257	35	2987.	0.1	0.1	0.0
32	255	35	2963.	0.1	0.1	0.0
33	255	35	3072.	0.1	0.1	0.0
40	226	35	2650.	0.1	0.1	0.0
41	226	35	2310.	0.1	0.1	0.0
43	214	35	3780.	0.2	0.2	0.0
44	214	43	4051.	0.2	0.2	0.0
45	214	35	4370.	0.2	0.2	0.0
47	212	35	6822.	0.3	0.3	0.1
48	212	43	7335.	0.3	0.3	0.1
49	212	43	7176.	0.3	0.3	0.1
50	211	29	2478.	0.1	0.1	0.0
51	211	35	2332.	0.1	0.1	0.0
53	210	35	2762.	0.1	0.1	0.0
129	137	87	302016.	14.3	14.3	3.2
130	137	103	315856.	14.9	14.9	3.4
131	137	87	340320.	16.1	16.1	3.6
133	136	287	2114368.	100.0	100.0	22.5^
134	136	287	2099904.	99.3	99.3	22.3^
163	121	87	390368.	18.5	18.5	4.1
164	121	103	408128.	19.3	19.3	4.3
166	120	119	203148.	7.6	9.6	2.2
167	120	143	223536.	10.6	10.6	2.4
279	58	71	169796.	8.0	8.0	1.8
280	58	71	184564.	8.7	8.7	2.0

709MD2.1 [TIC=4324096, 100%=2085184] EI

TBAH/GLY/5H2O

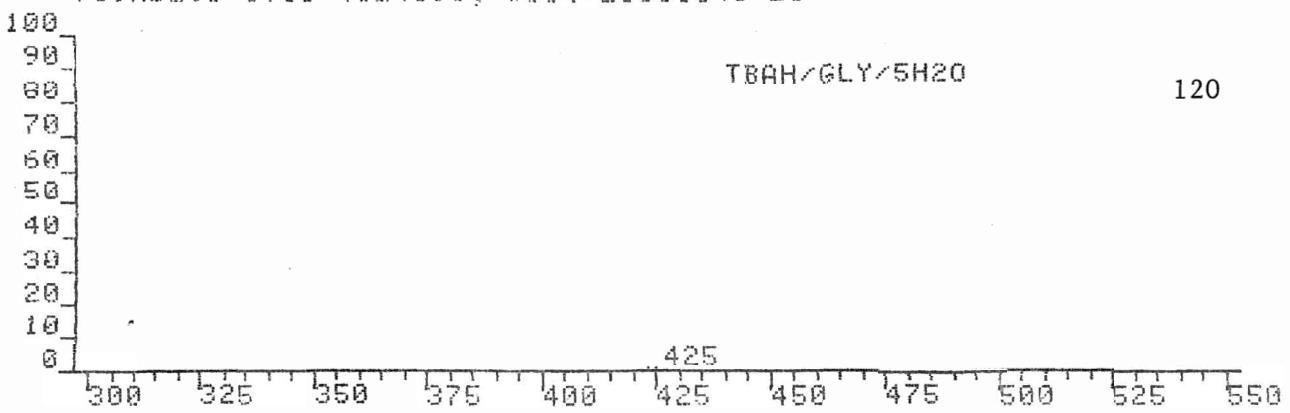

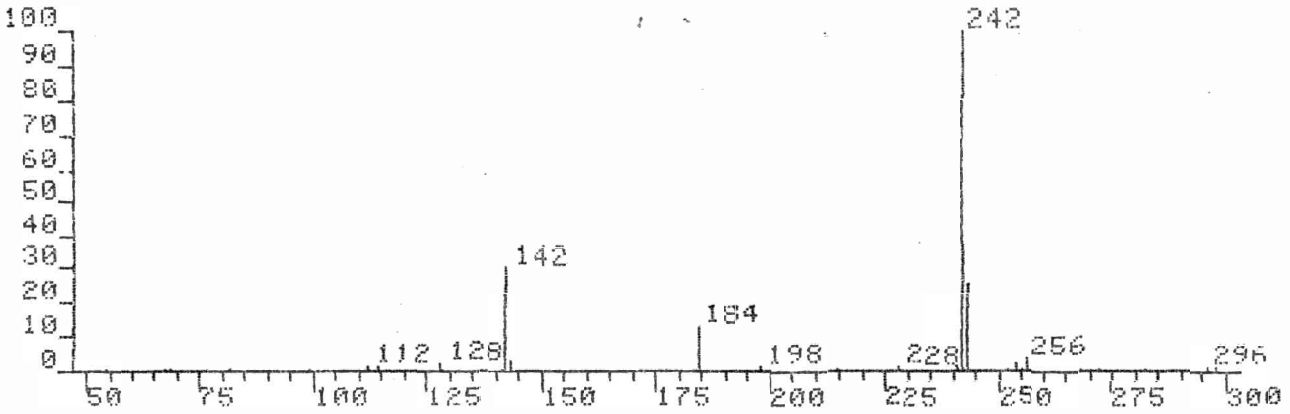

709MD2.1 [TIC=4324096, 100%=24037] EI

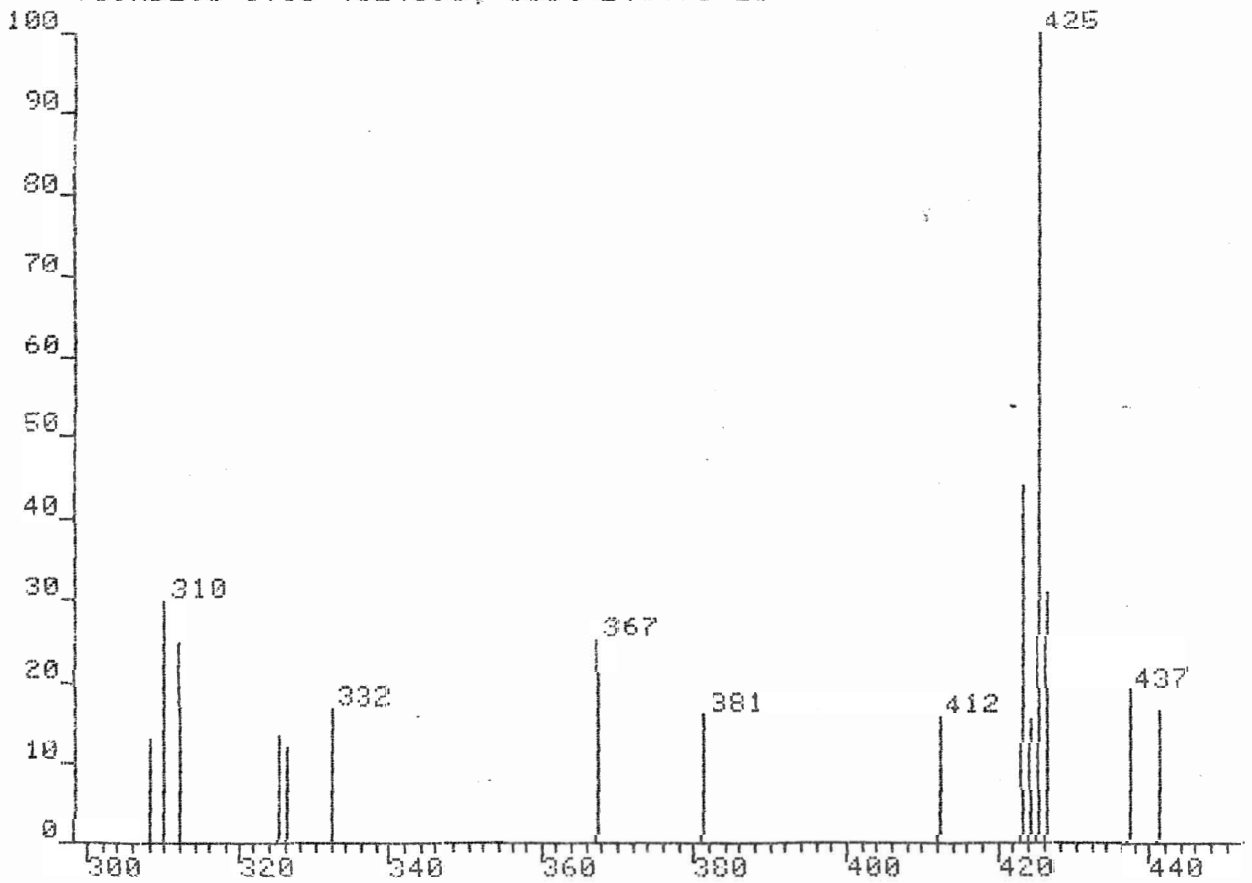

DP1:709MD2.MS TBAH/Gly/5H_2O
SCAN: 1, 7/ 9/84 21: 7

IONISATION: EI
NO. PEAKS: 78
BASE/NREF INT: 2085184./ 2085184.
TIC: 4324096.
MASS RANGE: 54.0516 - 547.6952
RETN TIME/MISC: 0: 0/ 0/ 0/ 0
PAGE 1

PEAK NO.	MEASURED MASS	NO. POINTS	ABSOLUTE INTENSITY	% INT. BASE	% INT. NREF	% TOT. ION
2	547	43	3757.	0.2	0.2	0.1
3	544	29	2457.	0.1	0.1	0.1
5	441	35	2470.	0.1	0.1	0.1
6	437	35	4515.	0.2	0.2	0.1
7	426	35	7433.	0.4	0.4	0.2
8	425	59	24037.	1.2	1.2	0.6
9	424	35	3691.	0.2	0.2	0.1
10	423	43	10551.	0.5	0.5	0.2
11	412	35	3768.	0.2	0.2	0.1
12	381	35	3875.	0.2	0.2	0.1
13	367	35	6045.	0.3	0.3	0.1
14	332	35	4019.	0.2	0.2	0.1
15	326	35	2933.	0.1	0.1	0.1
16	325	35	3243.	0.2	0.2	0.1
17	312	43	5960.	0.3	0.3	0.1
18	310	43	7136.	0.3	0.3	0.2
19	308	29	3178.	0.2	0.2	0.1
20	298	51	22995.	1.1	1.1	0.5
21	297	43	5270.	0.3	0.3	0.1
22	296	51	23219.	1.1	1.1	0.5
23	294	43	5322.	0.3	0.3	0.1
24	286	35	4412.	0.2	0.2	0.1
25	283	29	3078.	0.1	0.1	0.1
26	282	43	9978.	0.5	0.5	0.2
27	273	35	3542.	0.2	0.2	0.1
28	272	51	17054.	0.8	0.8	0.4
29	269	35	2770.	0.1	0.1	0.1
30	268	43	13754.	0.7	0.7	0.3
31	266	35	4390.	0.2	0.2	0.1
33	257	43	12821.	0.6	0.6	0.3
34	256	71	67364.	3.2	3.2	1.6
35	255	51	7076.	0.3	0.3	0.2
36	254	51	39488.	1.9	1.9	0.9
38	252	51	8135.	0.4	0.4	0.2
39	243	175	540704.	25.9	25.9	12.5*
40	242	207	2085184.	100.0	100.0	48.2*^
54	184	119	276208.	13.2	13.2	6.4
63	142	175	640320.	30.7	30.7	14.8

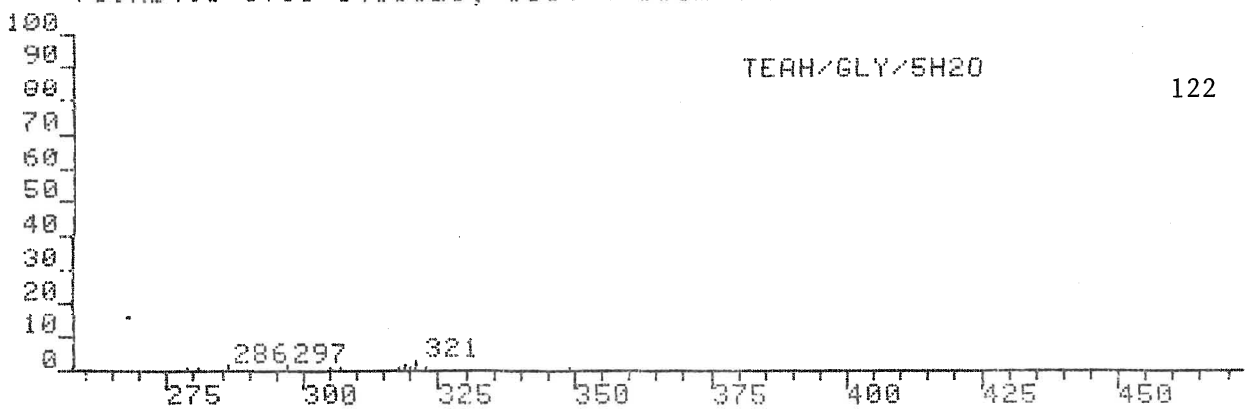
709MD4.1 [TIC=3416320, 100%=11665281 EI
TEAH/GLY/5H2O
286297
321

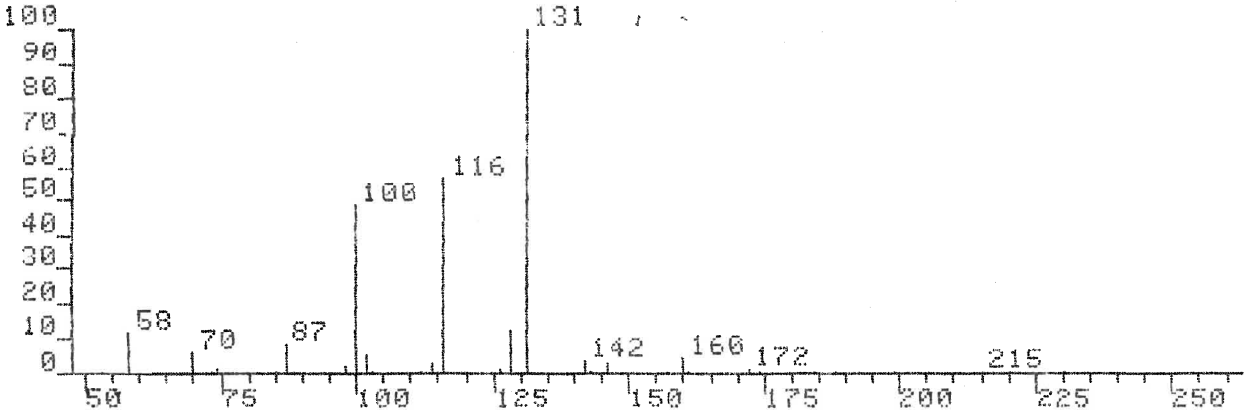
131
116
100
58
70
87
142
160
172
215

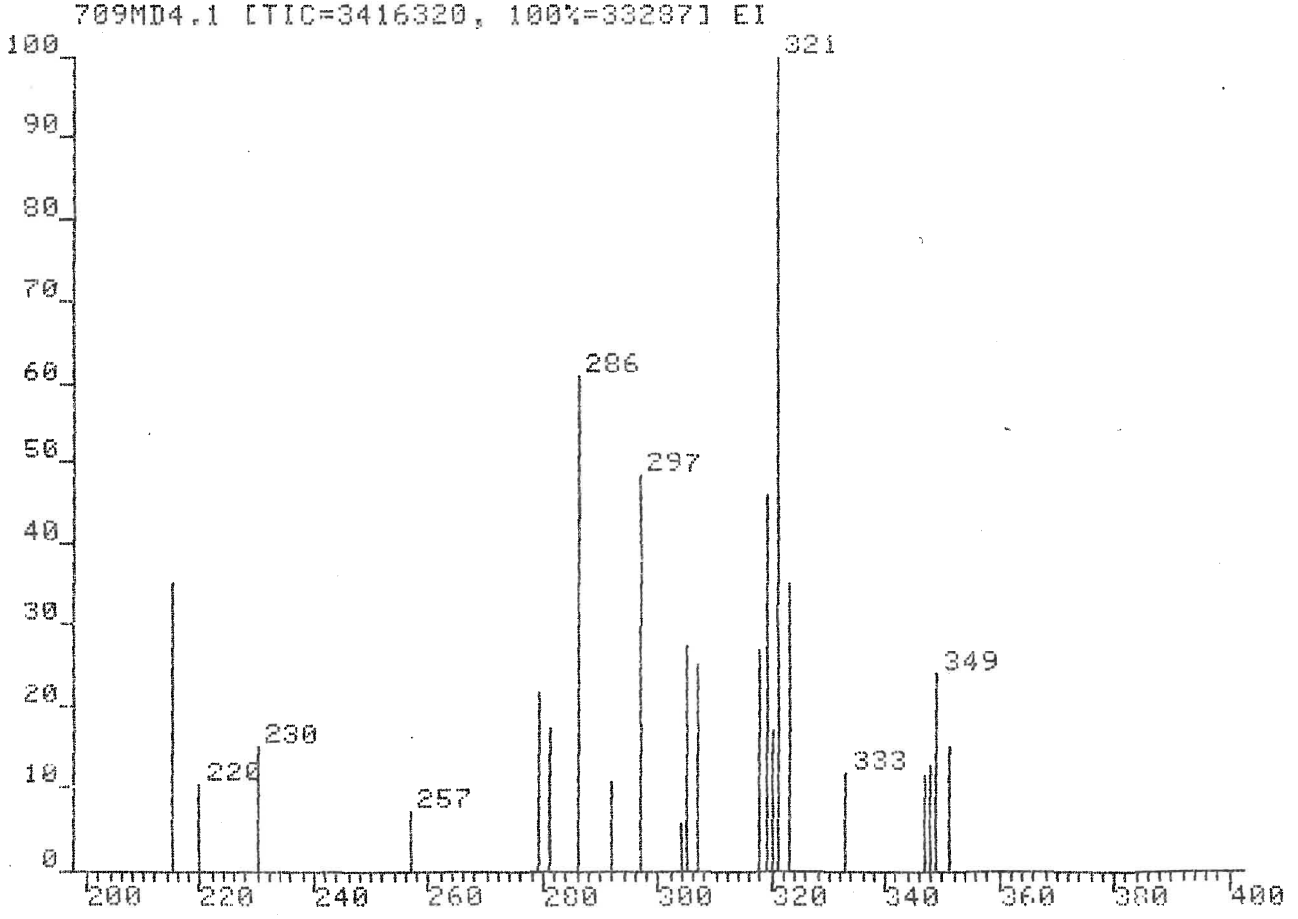
709MD4.1 [TIC=3416320, 100%=33287] EI
321
286
297
349
230
220
257
333

DP1:709MD4.MS TEAH/Gly/5H_2O
SCAN: 1, 7/ 9/84 · 21:13

IONISATION: EI
NO. PEAKS: 56
BASE/NREF INT: 1166528./ 1166528.
TIC: 3416320.
MASS RANGE: 53.0755 - 450.5795
RETN TIME/MISC: 0: 0/ 0/ 0/ 0
PAGE 1

PEAK NO.	MEASURED MASS	NO. POINTS	ABSOLUTE INTENSITY	% INT. BASE	% INT. NREF	% TOT. ION
1	450	35	3667.	0.3	0.3	0.1
2	351	43	5040.	0.4	0.4	0.1
3	349	43	7995.	0.7	0.7	0.2
4	348	43	4237.	0.4	0.4	0.1
5	347	35	3781.	0.3	0.3	0.1
6	333	35	3975.	0.3	0.3	0.1
7	323	43	11682.	1.0	1.0	0.3
8	321	51	33287.	2.9	2.9	1.0
9	320	43	5723.	0.5	0.5	0.2
10	319	43	15480.	1.3	1.3	0.5
11	318	43	8907.	0.8	0.8	0.3
12	307	43	8379.	0.7	0.7	0.2
13	305	43	9191.	0.8	0.8	0.3
14	304	29	1922.	0.2	0.2	0.1
15	297	43	16213.	1.4	1.4	0.5
16	292	35	3527.	0.3	0.3	0.1
17	286	51	20207.	1.7	1.7	0.6
18	281	43	5836.	0.5	0.5	0.2
19	279	43	7221.	0.6	0.6	0.2
20	257	29	2398.	0.2	0.2	0.1
21	230	35	5063.	0.4	0.4	0.1
22	220	35	3469.	0.3	0.3	0.1
23	215	43	11847.	1.0	1.0	0.3
37	131	175	1166528.	100.0	100.0	34.1*
38	128	71	146376.	12.5	12.5	4.3
40	116	87	654816.	56.1	56.1	19.2
45	100	119	564176.	48.4	48.4	16.5
55	58	87	131904.	11.3	11.3	3.9

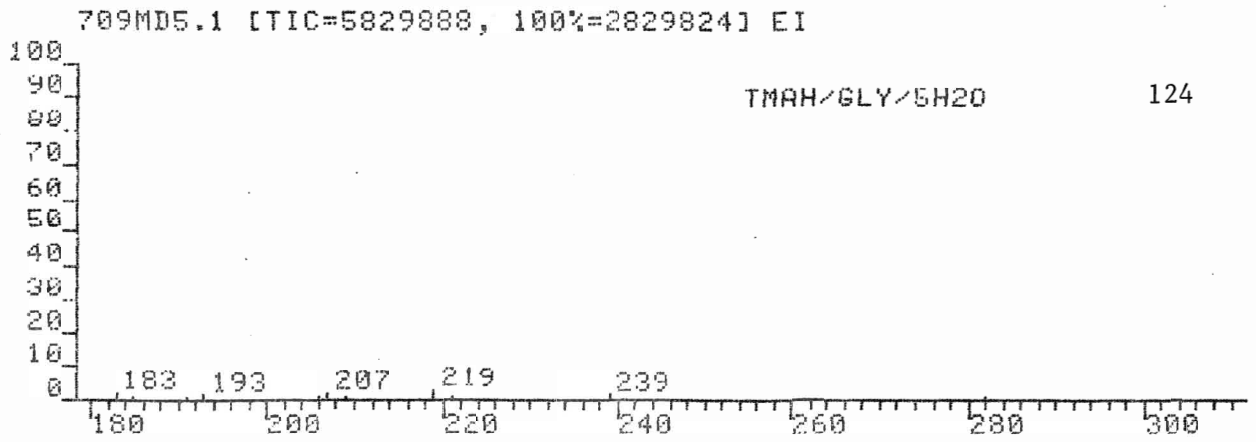
709MD5.1 [TIC=5829888, 100%=2829824] EI
TMAH/GLY/5H2O
124
183
193
207
219
239

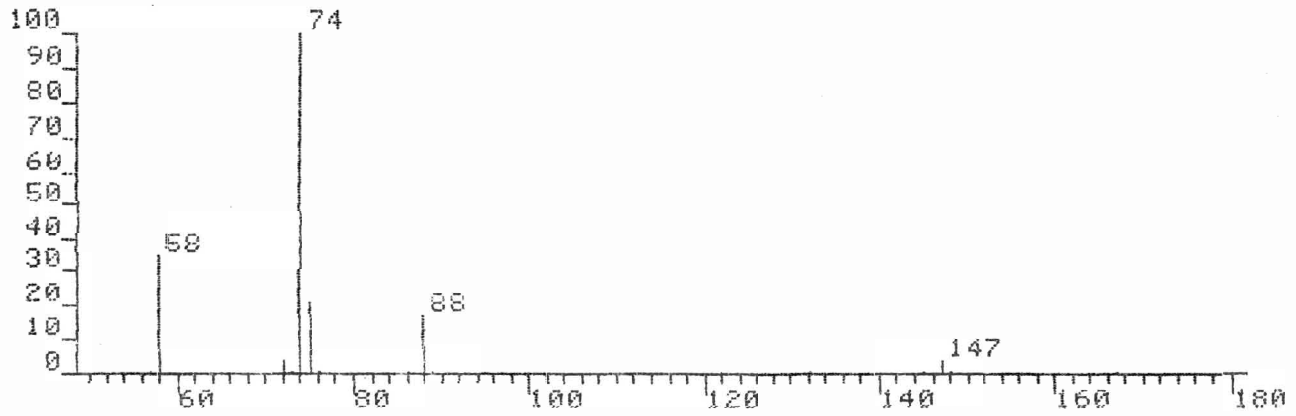
74
58
88
147

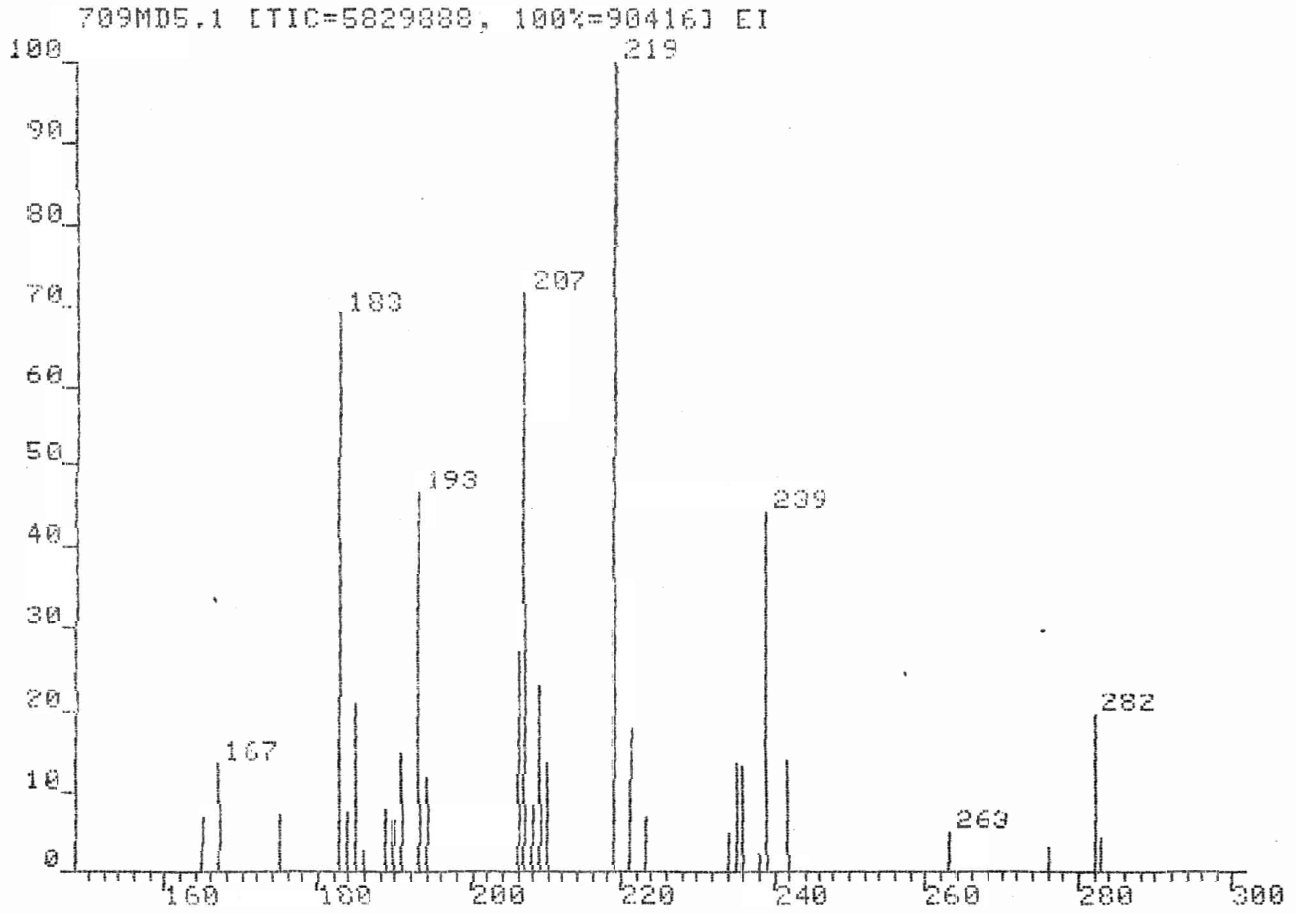
709MD5.1 [TIC=5829888, 100%=90416] EI
219
207
183
193
239
167
282
263

DP1:709MD5.MS TMAH/Gly/5H_2O
SCAN: 1, 7/ 9/84 21:17

IONISATION: EI
NO. PEAKS: 51
BASE/NREF INT: 2829824./ 2829824.
TIC: 5829888.
MASS RANGE: 57.1023 - 308.3528
RETN TIME/MISC: 0: 0/ 0/ 0/ 0
PAGE 1

PEAK NO.	MEASURED MASS	NO. POINTS	ABSOLUTE INTENSITY	% INT. BASE	% INT. NREF	% TOT. ION
1	308	43	4329.	0.2	0.2	0.1
2	283	35	3800.	0.1	0.1	0.1
3	282	51	17880.	0.6	0.6	0.3
4	276	29	2528.	0.1	0.1	0.0
5	263	35	4430.	0.2	0.2	0.1
6	242	35	12708.	0.4	0.4	0.2
7	239	43	40246.	1.4	1.4	0.7
8	238	29	2093.	0.1	0.1	0.0
9	236	43	12072.	0.4	0.4	0.2
10	235	43	12332.	0.4	0.4	0.2
11	234	43	4224.	0.1	0.1	0.1
12	223	35	6183.	0.2	0.2	0.1
13	221	43	16235.	0.6	0.6	0.3
14	219	59	90416.	3.2	3.2	1.6
15	210	43	12330.	0.4	0.4	0.2
16	209	43	21170.	0.7	0.7	0.4
17	208	35	7384.	0.3	0.3	0.1
18	207	51	64815.	2.3	2.3	1.1
19	206	43	24696.	0.9	0.9	0.4
20	194	43	10878.	0.4	0.4	0.2
21	193	43	42080.	1.5	1.5	0.7
22	191	35	13762.	0.5	0.5	0.2
23	190	35	5888.	0.2	0.2	0.1
24	189	43	7109.	0.3	0.3	0.1
25	186	29	2238.	0.1	0.1	0.0
26	185	43	19120.	0.7	0.7	0.3
27	184	29	6557.	0.2	0.2	0.1
28	183	59	62377.	2.2	2.2	1.1
29	175	43	6529.	0.2	0.2	0.1
30	167	35	12374.	0.4	0.4	0.2
31	165	35	6253.	0.2	0.2	0.1
32	148	51	11254.	0.4	0.4	0.2
33	147	71	108096.	3.8	3.8	1.9
34	145	35	10118.	0.4	0.4	0.2
41	88	71	481168.	17.0	17.0	8.3
44	75	87	600544.	21.2	21.2	10.3
45	74	415	2829824.	100.0	100.0	48.5^
50	58	119	987504.	34.9	34.9	16.9

Comparative EI and FAB study for five different types of compounds were done by us, but as the instrument broke down for two months, I could not discuss this in detail in my thesis. However, the percent relative intensities of the tin-containing ions in tabular forms are being included in the appendix.

Some of the important features of this study are summarized below.

1. the ion clusters $(ClC_6H_4)_3.2HMPA$ and $(FC_6H_4)_3Sn.2HMPA$ were quite consistent for all the halogenated compounds, indicating that the presence of extra HMPA-containing species in both tin and lead organometallics (discussed earlier) were not because of the use of HMPA as a matrix. This also reflected that the exchange probably took place within the molecules themselves and not between the sample and the matrix.

2. The intensity of HMPA-containing metal ions varied from 75 to 80% in FAB whereas they were absent in EI.

3. Halogen-transferred species were also observed for these compounds in EI.

Table A-I.

Comparison of the EI and FAB Mass Spectra

of Ph_3SnX (X = Ph, Cl, Br, I) (tin-containing ions)*

Ion^+	X = Ph		X = Cl		X = Br		X = I	
	EI	FAB	EI	FAB	EI	FAB	EI	FAB
$Ph_3Sn.NPOE$	--	3.1	--	3.0	--	4.4	--	8.3
$Ph_2SnX.NPOE$	--	--	--	8.8	--	6.2	--	5.5
PhSn.NPOE	--	--	--	1.1	--	2.9	--	2.7
SnX.NPOE	--	--	--	1.9	--	2.0	--	1.0
Ph_3SnX	--	--	0.4	--	0.5	--	--	--
Ph_2SnX	x	x	50.9	32.1	30.8	27.8	3.4	25.9
PhSnX	x	x	3.4	--	2.6	--	0.08	--
Ph_3Sn	49.8	55.0	2.8	22.8	18.0	24.3	59.7	31.2
Ph_2Sn	11.8	2.5	0.8	--	2.4	--	0.8	--
PhSn	19.2	16.1	11.6	12.6	19.5	10.8	20.9	17.3
SnX	x	x	24.7	8.6	20.0	8.8	4.8	1.0
Sn	20.0	23.2	5.7	9.1	6.3	12.5	10.3	7.6

*percentage of the total absolute intensity of metal-containing ions.

x the ion is present and the intensity has already been mentioned in the table.

NPOE = p-nitrophenyl octyl ether, the FAB matrix liquid

Table A-II.

Comparison of the EI and FAB Mass Spectra

of (4-ClC H) SnX (X = C_6H_4Cl, Cl, Br, I) (tin-containing ions)*

Ion^+	X = C_6H_4Cl		X = Cl		X = Br		X = I	
	EI	FAB	EI	FAB	EI	FAB	EI	FAB
$(ClC_6H_4)_2SnX.NPOE$	--	--	--	9.5	--	--	--	4.7
$(ClC_6H_4)_3Sn.NPOE$	--	10.7	--	--	--	--	--	--
$(ClC_6H_4)Sn.NPOE$	--	4.6	--	--	--	2.7	--	3.4
SnX.NPOE	--	--	--	1.6	--	4.5	--	7.9
$(ClC_6H_4)_3SnX$	--	--	1.6	--	1.1	--	--	--
$(ClC_6H_4)_3Sn$	52.5	43.4	1.8	17.2	4.6	18.1	55.2	27.5
$(ClC_6H_4)_2Sn$	4.8	--	0.3	--	0.4	--	0.2	--
$(ClC_6H_4)Sn$	14.7	13.3	10.5	12.0	13.4	17.8	17.3	20.6
$(ClC_6H_4)_2SnX$	x	x	52.4	30.4	44.3	37.7	6.7	27.0
$(ClC_6H_4)SnX$	x	--	1.7	--	2.2	--	0.1	--
SnX	x	x	29.6	16.2	19.0	9.4	4.9	3.9
Sn	5.2	19.3	2.0	13.1	1.4	3.0	1.5	5.1
$(ClC_6H_4)_2SnCl$	--	--	--	x	4.0	--	2.7	--
SnCl	22.8	8.0	--	x	9.5	6.8	11.3	--

* percentage of the total absolute intensity of the metal-containing ions.

x the ion is present and the intensity has already been mentioned in the table.

NPOE = p-nitrophenyl octyl ether, the FAB matrix liquid.

Table A-III.

Comparison of the EI and FAB Mass Spectra

of $(4\text{-}FC_6H_4)_3SnX$ (X = C_6H_4F, Cl, Br, I) (tin-containing ions)*

Ion^+	X = C_6H_4F		X = Cl		X = Br		X = I	
	EI	FAB	EI	FAB	EI	FAB	EI	FAB
$(FC_6H_4)_3Sn.NPOE$	--	9.5	--	5.3	--	4.8	--	8.6
$(FC_6H_4)_2SnX.NPOE$	--	--	--	11.9	--	11.8	--	5.6
$(FC_6H_4)_2Sn.NPOE$	--	1.0	--	--	--	1.5	--	--
$(FC_6H_4)Sn.NPOE$	--	1.2	--	1.8	--	2.8	--	2.2
$(FC_6H_4)_3SnX$	--	--	0.9	--	1.3	--	--	--
$(FC_6H_4)_2SnX$	x	x	48.7	33.8	39.8	33.4	2.3	25.0
$(FC_6H_4)SnX$	x	--	2.3	--	3.0	--	0.5	--
$(FC_6H_4)_3Sn$	51.0	57.0	4.0	28.6	7.0	22.9	54.4	31.3
$(FC_6H_4)_2Sn$	3.9	--	0.4	--	0.7	--	0.2	--
$(FC_6H_4)Sn$	17.6	17.3	9.8	14.1	14.3	14.8	19.2	18.0
SnX	x	x	23.2	4.4	21.0	6.3	4.1	2.1
Sn	17.2	8.7	4.7	--	5.5	1.5	8.5	7.0
SnF	9.8	5.4	5.7	--	6.9	--	10.4	--
$(FC_6H_4)_2SnF$	--	--	0.2	--	--	--	--	--

* percentage of the total absolute intensity of metal-containing ions.

x the ion is present and the intensity has already been mentioned in the table.

NPOE = p-nitrophenyl octyl ether, the FAB matrix liquid.

Table A-IV.

Comparison of the EI and FAB Mass Spectra

of $(4\text{-}ClC_6H_4)_3SnX.HMPA$ (X = Cl, Br, I) (tin-containing ions)*

Ion^+	X = Cl		X = Br		X = I	
	EI	FAB	EI	FAB	EI	FAB
$(ClC_6H_4)_3Sn.2HMPA$	--	1.7	--	2.4	--	1.9
$(ClC_6H_4)_3Sn.HMPA$	--	52.1	--	64.0	--	62.1
$(ClC_6H_4)_2SnX.HMPA$	--	11.9	--	12.5	--	4.4
$(ClC_6H_4)_2Sn.HMPA$	--	3.0	--	3.5	--	2.6
$(ClC_6H_4)Sn.HMPA$	--	8.5	--	4.8	--	8.0
$(ClC_6H_4)_2SnX.NPOE$	--	6.9	--	--	--	--
$(ClC_6H_4)_3SnX$	1.6	--	0.9	--	--	--
$(ClC_6H_4)_2SnX$	53.4	1.9	51.5	1.5	5.0	1.9
$(ClC_6H_4)SnX$	1.9	--	2.6	--	0.3	--
$(ClC_6H_4)_3Sn$	1.9	6.5	4.7	5.2	55.0	10.9
$(ClC_6H_4)_2Sn$	0.1	--	--	--	--	--
$(ClC_6H_4)Sn$	11.0	3.4	16.7	3.5	16.8	4.9
SnX	29.1	2.2	9.0	--	5.1	--
Sn	0.9	1.5	--	2.6	1.8	2.5
$(ClC_6H_4)_2SnCl$	x	x	5.7	--	2.7	--
SnCl	x	x	9.0	--	13.3	--

* percentage of the total absolute intensity of metal-containing ions

x The ion is present and the intensity has already been mentioned in the table

NPOE = p-nitrophenyl octyl ether, the FAB matrix liquid

Table A-V.

Comparison of EI and FAB Mass Spectra

of $(C\text{-}FC_6H_4)_3SnX.HMPA$ (X = Cl, Br, I) (tin-containing ions)*

Ion^+	X = Cl		X = Br		X = I	
	EI	FAB	EI	FAB	EI	FAB
$(FC_6H_4)_3Sn.2HMPA$	--	1.4	--	1.4	--	0.8
$(FC_6H_4)_3Sn.HMPA$	--	57.6	--	62.3	--	58.0
$(FC_6H_4)_2SnX.HMPA$	--	11.9	0.2	8.9	--	8.7
$(FC_6H_4)_2Sn.HMPA$	--	1.5	--	0.6	--	--
$(FC_6H_4)Sn.HMPA$	--	7.5	--	6.9	--	7.6
$(FC_6H_4)_3SnX$	1.3	--	1.0	--	--	--
$(FC_6H_4)_2SnX$	55.8	4.2	42.4	2.6	8.4	4.1
$(FC_6H_4)SnX$	1.9	--	3.4	--	0.8	--
$(FC_6H_4)_3Sn$	1.7	10.9	7.6	11.1	50.7	10.5
$(FC_6H_4)_2Sn$	--	--	0.4	--	0.1	--
$(FC_6H_4)Sn$	10.2	5.1	14.3	3.1	20.0	4.8
SnX	21.9	--	21.4	--	5.7	--
Sn	3.8	--	4.0	3.0	7.5	5.1
SnF	3.3	--	4.9	--	6.7	--

* percentage of the total absolute intensity of metal-containing ions